

APPENDIX A. TECHNICAL REVIEW COMMITTEE MEMBERSHIP & CHARTER

A.1 Membership

Sheila E. Widnall – Chair

Dr. Sheila Widnall is currently an Institute Professor at the Massachusetts Institute of Technology. Her research activities have included: boundary layer stability, unsteady hydrodynamic loads on fully wetted and supercavitating hydrofoils of finite span, unsteady lifting-surface theory. Teaching activities have included undergraduate dynamics and aerodynamics, graduate level aerodynamics of wings and bodies, aeroelasticity, acoustics and aerodynamic noise, and aerospace vehicle vibration. She recently served as Secretary of the Air Force, where she was responsible for all the affairs of the Department of the Air Force, including formulation of policies and programs, program implementation, supervision and control of the intelligence activities of the Air Force, and presentation of Air Force policies to Congress.

James D. Barnes

Jim Barnes has worked in acoustics and vibration measurement and analysis since 1973. He has worked extensively in the measurement of community noise levels that result from industrial operations. He has gained extensive field experience in outdoor sound measurement, and use of appropriate instrumentation and techniques through management and supervision of hundreds of projects in the energy, transportation, manufacturing, and processing industries. He is a Senior Engineering Consultant at Acentech, Cambridge, MA. He has B.S. and M. Eng. degrees in Mechanical Engineering from Cornell University and is a registered Professional Engineer.

David N. Keast

Dave Keast has worked in acoustics since 1954 when he began work for Bolt Beranek and Newman, Inc. Mr. Keast is also a retired general aviation pilot with over 1,500 hours of flight time, and an avid backcountry hiker. He has worked both as consultant and manager of acoustics activities, including extensive work with instrumentation, and serving as Supervisory Consultant and Manager of the Environmental Technologies Department at BBN. He has been involved in research, consulting, lecturing, writing, serving as expert witness, and project management in issues related primarily to acoustics. He consults now from his home in Carlisle, MA. He holds B.S. and M.S. degrees in Electrical Engineering from MIT and is a registered Professional Engineer.

Robert A. Lee

Mr. Robert Lee is currently the Chief of the Audio Displays and Bioacoustics Branch of the Air Force Research Laboratory at Wright-Patterson Air Force Base, OH. Mr. Lee was the former branch chief of the Noise Effects Branch of the Armstrong Laboratory that coordinated all the research on Environmental Noise Issues for the Air Force. Mr. Lee graduated Magna Cum Laude from the University of Wisconsin-Superior with a major in Physics and Mathematics and began work for the Air Force in 1974. His work has included measurements of aircraft noise and sonic booms, development of noise models and general research in acoustics and its impacts on humans, animals and structures. He is the Air Force expert in the aircraft noise computation programs developed and supported by the Department of Defense.

Kåre Liasjø

Kåre Liasjø has been active in acoustics since 1970 when he received a B. Sc. Degree from the Technical University of Trondheim, Norway. He helped establish an acoustics laboratory for the Oslo City Health Department, where he was active in building acoustics and noise reduction for all types of transportation activities, and where he was responsible for the instrumentation of the laboratory. He worked for 17 years in the Norwegian acoustics research center in Trondheim, where he introduced the INM and later developed a new computer model that is the first airport noise model to include topographical effects on sound propagation. He now works for the Civil Aviation Administration (CAA) of Norway and is responsible for all noise related activities of that agency.

Allan Piersol

Allan Piersol has over 45 years of experience in the field of shock, vibration and acoustic engineering and is an internationally recognized expert in the statistical analysis of all types of environmental data. He has taught graduate courses at the University of Southern California in engineering statistics and random process theory, and has co-authored or contributed to eleven books on the analysis of random signals. He holds a B.S. degree from the University of Illinois, and a M.S. degree in Engineering from the University of California. He is a Fellow of both the Acoustical Society of America the Institute of Environmental Sciences, a life member of the American Society of Mechanical Engineers, and a registered Professional Engineer. He now has his own engineering company, Piersol Engineering Company in Woodland Hills, California.

Clemans A. (Andy) Powell

Andy Powell is currently Senior Scientist for the Aerodynamics, Aerothermodynamics and Acoustics Competency, and Manager of the Community Noise Impact Reduction Project of the Quiet Aircraft Technology Program at NASA Langley Research Center. He has been in acoustics research at NASA since 1971 and has conducted numerous laboratory and field studies of human response to aircraft noise. As Head of the Structural Acoustics Branch for 10 years, he was responsible for NASA's research activities in aircraft interior noise control, acoustic fatigue and aircraft community noise impact. He is a Fellow of the Acoustical Society of America, and holds a D. Sc. in Acoustics from The George Washington University.

Lou Sutherland

Lou Sutherland has nearly 50 years of experience in acoustics related research and consulting. In addition to BS and MS degrees in EE from the University of Washington, he conducted early work there and at the Boeing Company, and worked for 25 years as Deputy Director and Chief Scientist at Wyle Laboratories. He was the principal investigator on a pilot study for a national survey of outdoor noise environments, he has studied the effects of high noise levels from rocket launches on communities, has developed new models for atmospheric absorption. He is a Fellow of the Acoustical Society of America, is Board certified by, and is a past president of the Institute of Noise Control Engineering, and has served on many committees and organizations active in the field of acoustics. He consults from his home in Rancho Palos Verdes, California.

A.2 Charter

Congress has identified resource preservation as the National Park Service's (NPS's) primary responsibility. Among the resources NPS seeks to preserve are natural soundscapes in which visitors have the opportunity to experience solitude or to experience nature in a state unaltered by the effects of civilization. At Grand Canyon National Park, legislation specifies natural quiet (or natural soundscapes) as a resource requiring preservation.

Preservation of natural soundscapes has many aspects, including technical issues related to measuring and quantifying sound, and predicting how various actions may alter the soundscapes. These technical acoustic issues may at times be unusual or significantly complex so that NPS access to individuals with relevant technical expertise is important.

Accordingly, the NPS and the Federal Aviation Administration (FAA) have jointly contracted with Harris Miller Miller & Hanson Inc. (HMMH) to form a group of experts, called the Technical Review Committee (TRC). TRC members are to review and comment on various technical issues that may arise related to the measurement, quantification and analysis of soundscapes. The TRC has been formed using the following general criteria:

A.3 CRITERIA FOR MEMBERSHIP

Many Years Experience in Environmental Acoustics

NPS and FAA are not concerned about the specific areas in which their environmental acoustics expertise lie, but require that the members have a sense for the inherent limitations of measuring and predicting sound levels and sound propagation in outdoor, non-laboratory, and park-like situations. Measurement and analysis of sound in park situations will have to recognize that outdoor sounds are subject to many uncontrollable variables, and that, even if funding were unlimited, these variables cannot be controlled per se but can be managed only through statistics. Membership should include at least one individual experienced in statistical analysis of random data.

Capable of Working as a Team

A high value is placed on expertise and on the ability of the individual member to bring that expertise into a team setting, working cooperatively with the team to find the best, most feasible solutions. The technical quantification and analysis of soundscapes should be as devoid as possible of decisions based on anything other than scientific and feasibility considerations. Members of the TRC need to be able to clearly express their perspectives, but equally able to listen and react objectively to the perspectives of others.

Experienced in Balancing the Scientifically Desirable with the Feasible

Many technical problems can have complex, involved solutions. Members should be experienced in striking the balance that is required by feasibility considerations. Limitations imposed by time, budget, instrumentation capabilities, human capabilities, etc., must be recognized, and feasible solutions found without undue compromise of the technical / scientific concerns.

Relatively Free of Previous Involvement with the Issues

NPS and FAA believe that the best perspectives and recommendations will be produced by individuals who have little or no direct involvement with or stake in current park soundscape issues or the setting of noise standards for the parks.

Stature in their Field of Expertise

Members of the TRC should have reputations in environmental acoustics that will be unchallenged by others who could have also served on the TRC. For effectiveness of the TRC, it will be kept small. The area of environmental acoustics has many competent practitioners who could serve on a third party review group. But, even with the criteria listed, final membership must be somewhat arbitrary, and those not chosen may feel overlooked. It is important, therefore, that those who are selected be of sufficient stature as to be recognized by most observers as highly qualified for the role.

A.4 FIRST ISSUE TO BE ADDRESSED: Modeling Tour Aircraft Sound in the Grand Canyon

Increased numbers of low-flying aircraft over various units of the National Park System have diminished the opportunities for solitude and for experiencing uninterrupted sounds of nature. Consequently, in 1987, Congress passed Public Law 100-91, commonly referred to as the National Parks Overflights Act, which directed the Secretary of the Interior to conduct studies to provide information regarding the effects and values of aircraft overflights of National Park units.

One of the requirements of the law was that a plan be developed that would substantially restore natural quiet at Grand Canyon National Park. By definition, substantial restoration of natural quiet will be achieved when “50% or more of the park is naturally quiet (i.e., no aircraft audible) 75-100% of the day”. “Day” is taken as the average 12-hour daylight period. The plan involved a structuring of the airspace over the Grand Canyon into flight corridors and “flight free zones.” This plan was formalized by the FAA as Special Federal Aviation Regulation (SFAR) 50-2, 14 CFR Part 91.

In the NPS’ “Report to Congress” (1995), through use of both sound monitoring and computer modeling, the park service concluded that implementation of SFAR 50-2 had not brought a substantial restoration of natural quiet to Grand Canyon National Park. Because the goal of substantial restoration of natural quiet was not achieved, NPS and the FAA are currently working on revising the Grand Canyon airspace and use practices so that this goal will be met in the foreseeable future.

As is typical of airspace / noise related planning efforts, computer models are the primary tool for analysis of changes in sound that result from changes in the use of airspace. Several models are available for use, but none have been compared side-by-side with measured sounds produced by air tour operations over National Park settings, over a range of aircraft operating conditions. Consequently, the NPS and FAA jointly decided to conduct a field measurement-based validation of the models.

Aircraft Noise Model Validation Study Objectives

To collect, reduce, analyze, and interpret appropriate field data that will allow the contractor to determine the ability of candidate currently available computer models to accurately predict the audibility of noise produced by air tour aircraft over Grand Canyon National Park.

To make certain that all data, methods, and metrics employed in the study are appropriate to the task and scientifically defensible.

Specific TRC Tasks

TRC members are to advise the government's contractor, HMMH, on issues associated with the field validation of aircraft noise models to be used for modeling noise from air tour operations over the Canyon. Advice may be solicited through meetings of the group, through mailings or by electronic means. For assistance with the model validation study, the TRC will attend a meeting at the Grand Canyon with HMMH. The meeting will also be attended by NPS and FAA staff and by staff from Volpe and from Wyle Labs. For this meeting, the TRC will be provided with a draft Model Validation Study Plan and with background information on associated issues. At the meeting, TRC members will participate in a detailed discussion of the Study Plan and provide comments and suggestions related to:

1. The general approach that is proposed for the model validation study plan;
2. Technical issues that are insufficiently addressed or not addressed by the study plan;
3. Alternative procedures or methods that could be used in the model validation exercise; and
4. Approaches that could be used for comparison analyses of measured and modeled results.

All comments and suggestions should be cognizant of feasibility considerations. Funding is limited, and the primary concern is: does the proposed study plan represent the best use of available resources?

Page Intentionally Blank

APPENDIX B. MEETING AGENDA AND ATTENDEES

B.1 First TRC Meeting

Albright Training Center, Room A

Monday, August 16, 1999

8:00 – 8:20 am: Welcome (Rob Arnberger)
8:20 – 9:00: Introductions (Tom Connor, Tom Hale)
9:00 – 11:00: Orientation to GCNP and scope of problem (Ken Weber)
11:00 – 2:30 p.m.: Field trip and box lunch (provided): Visit Shoshone Point, Hermits Rest, and locations under and to the side of Zuni Point Corridor
2:30 – 2:45: Discuss objectives and procedures for group discussion
2:45 – 5:30: Introduction to and discussion of Proposed Study Plan (HMMH)
5:30 – 7:30: Dinner at El Tovar (Grand Canyon Room overlooking rim – each pays for own meal)
7:30 – 8:00 Adjourn to veranda or rim overlook for wrap-up discussion and objectives for Tuesday

Tuesday, August 17, 1999

8:00 – noon: Discuss study plan
Noon – 1:00: Lunch provided
1:00 – 3:00: Final discussions of plan
3:00 – 5:00: Summarize discussion and revisions to study plan (TRC)

Wednesday, August 18, 1999

8:00 – noon: Site selection discussion
1:00 – 3:00: Public Information Meeting (HMMH)

Attendees:

TRC

Jim Barnes
Dave Keast
Bob Lee
Kåre Liasjø
Allan Piersol
Andy Powell
Lou Sutherland
Sheila Widnall

FAA

Tom Connor

Volpe

Gregg Fleming
David Senzig

Wyle

Ken Plotkin

HMMH

Nick Miller
Chris Menge
Dick Horonjeff
Gene Reindel

NPS

Wes Henry
Rick Ernenwein
Bill Schmidt
Tom Hale
Ken Weber
Dan Spotskey
Tracey Felger
Jennifer Burns

B.2 Public Meeting – Briefing on Noise Model Validation Study Plan

August 18, 1999

Panel

Nicholas Miller	Harris Miller Miller & Hanson Inc.
Richard Ernenwein	National Park Service – Intermountain Region
Howard Nesbitt	Federal Aviation Administration

Participants

Brad Fuqua	Grand Canyon News
Brenda Halvorson	Papillon Helicopters
John Alberti	J.R. Engineering
Pete Harris	Air Grand Canyon
Roberto Andrews	Kenai Helicopters
Patty Brookins	Office of Congressman J.D. Hatworth
Joe Corrao	Helicopter Association International
Paul Joly	Federal Aviation Administration – Las Vegas
Paul Gilbert	National Park Service – Grand Canyon
Jim McCarthy	Sierra Club, Grand Canyon Chapter
Dick Hingson	Sierra Club, Utah Chapter
Fumihiro Honda	Tokyo Broadcasting System
Jake Wachtel	Tokyo Broadcasting System
J.T. Reynolds	National Park Service – Grand Canyon
Bill Schmidt	National Park Service – Washington DC
Wes Henry	National Park Service – Washington DC
Bob Karotko	National Park Service – Albright Training Center
Tom Pittenger	National Park Service – Grand Canyon
Maureen Oltrogge	National Park Service – Grand Canyon
Mike Ebersole	National Park Service – Grand Canyon

B.3 Second TRC Meeting

Agenda for 29 March 2001 TRC Meeting

Goal: Define the various possible paths for providing the most accurate and precise means for modeling the audibility of air tours over the Grand Canyon.

Objectives:

1. Review model validation plan process to-date.
2. Understand the analyses of measured percent time audible – identify additional analyses needed and reasons therefore.
3. Understand comparisons of modeled and measured results.
4. Discuss alternative paths to accurate modeling of air tours over Grand Canyon.
5. List Action Items.

8:30 – 8:45 Introduction
8:45 – 10:00 Review Model Validation Process
 Overview
 Measurement Process
 Data Reduction Process
 Model Inputs
 Tracks
 Operations
 Source levels
 Ambients
 Measured Results
 Modeling – four models overview
10:00 – 10:15 Break
10:15 – 12:00 Examine Relations of Measured Data with Other Parameters
12:00 – 13:00 Lunch Break (sandwiches in meeting room)
13:00 – 14:30 Examine Comparisons of Modeled and Measured Results
14:30 – 14:45 Break
14:45 – 16:00 Continue Comparison of Modeled and Measured Results
16:00 – 17:00 Define Alternative Paths To Accurate Modeling Of Air Tours Over Grand Canyon
17:00 – 17:30 Review Action Items

Note: HMMH will lead the meeting and provide initial “seed ideas” for discussion. Modelers should be prepared to answer questions about how their models work (but not why their models gave the results they did when compared with measurements). Everyone should be prepared to think and ask questions.

Attendees:

TRC

Jim Barnes
Dave Keast
Bob Lee
Kåre Liasjø
Allan Piersol
Andy Powell
Sheila Widnall

FAA

Barry Brayer
Tom Connor
Howard Nesbitt
Jon Pietrak

Volpe

Gregg Fleming
Chris Roof
David Senzig

Wyle

Ken Plotkin

HMMH

Nick Miller
Chris Menge
Dick Horonjeff
Grant Anderson

NPS

Rick Ernenwein
Tracey Felger
Bill Schmidt
Ken Weber

Senzig Engineering

David Senzig

Page Intentionally Blank

APPENDIX C. AUDIBILITY AND AMBIENT LEVELS

C.1 Introduction

This appendix provides background information about audibility and the associated detection theory as applied in this study. Congress tasked NPS and FAA with developing a plan for tour aircraft use of Grand Canyon airspace that will succeed in “substantially restoring the natural quiet in the park”⁷² and NPS defined substantial restoration of natural quiet as occurring when “50% or more of the park achieve[s] ‘natural quiet’ (i.e., no aircraft audible) for 75 – 100 percent of the day.”⁷³ Hence, determination of success in substantial restoration of natural quiet must address tour aircraft audibility.

C.2 Audibility and Detection Theory

C.2.1 Concept

In its simplest form, audibility occurs when an attentive person of normal hearing acuity listens and can hear a tour aircraft. Detection occurs because humans have the ability to distinguish changes in sound level in narrow frequency regions. These narrow regions correspond approximately to 1/3-octave bands, where an octave is a doubling of frequency. Hence, when the sound level in one or two 1/3-octave bands starts to increase above previous levels, human hearing is capable of identifying this increase and identifying the source, if it is a familiar one. This listening approach was used during the logging at the audibility sites.

However, in order to calculate when an aircraft is likely to be heard, algorithms that use measurable sound quantities are required. There exist well-developed mathematical relationships that reliably predict when human hearing can identify a “target” source in the presence of background “noise”.⁷⁴ These relationships are based on the results of the testing of human subjects, and use frequency information of both the source to be detected and of the noise that covers or “masks” that source.

C.2.2 Calculation

These auditory signal detection calculations compare the *source sound levels* with the *background or ambient sound levels* and with the human threshold of hearing by frequency in 1/3-octave bands. The metric of audibility is called d' (“dee prime”), and the metric used in this study is the Detectability Level, abbreviated D’L computed as $10 \log(d')$. In essence, d' is the root-mean-square sum of the signal to noise ratios across all 1/3-octave bands, each adjusted for bandwidth and for frequency-specific human hearing characteristics, see Eq. 7 below. More generally, d' is a ratio of the sound intensity of the source to the sound intensity of the background, and $10 \log(d')$ is a decibel representation of that ratio. Generally, sounds become audible in a laboratory setting when $10 \log(d')$ is between 1 and 3 dB. In a park setting, early research showed that listeners were hearing tour

⁷² Public Law 100-91, August 18, 1987, § 3. (b) (3) (A).

⁷³ U.S. DOI, National Park Service, “Report on Effects of Aircraft Overflights on the National Park System,” Report to Congress, July 1995, Section 9.2.1, p. 182.

⁷⁴ See for example, Green, David M. and J. A. Swets, “Signal Detection Theory and Psychophysics,” Peninsula Publishing, 1988.

aircraft on average when $10 \log (d')$ equaled approximately 7 dB,⁷⁵ and this value was used in the spectral models (spectral INM, NODSS and NMSIM) to compute when aircraft were audible.⁷⁶

The basic d' equation for a single frequency band is:

$$d' = \eta \times \frac{S}{N} \sqrt{BW} \quad (7)$$

Where:

η is frequency dependent and is a measure of human hearing sensitivity with respect to an ideal detector, but is approximately 0.4 for most frequencies,
 BW is the bandwidth at the 1/3-octave band frequency in question,
 S is the signal energy in the 1/3-octave band, and
 N is the noise energy in the 1/3-octave band.

C.2.3 Special Considerations Regarding Background Sound Levels

As part of the sound level analysis of the recorded data tapes, a detailed analysis of the sound levels measured when aircraft were not present revealed that, for some periods and locations in the Canyon, natural ambient sound levels are significantly below the threshold at which a human with normal hearing could detect a sound. Hence, to apply the detection calculations simply to the measured aircraft sound levels and the measured ambient sound levels would, in these quiet periods / locations, falsely indicate when the aircraft would be audible. In determining the measured ambient levels to be used for modeling, these quiet period ambients were therefore adjusted upward by adding to the measured levels an estimate of the human “auditory system noise” derived from an international standard threshold of hearing (ISO 389-7:1996). The next section describes this addition with an example, then tabulates the measured ambients as used in modeling.

C.3 Determining the Measured Ambient Sound Levels

C.3.1 Introduction

Tape recordings made during all audibility logging at 17 sites (1A, 2A, 2D, 3A, 3B, 3D, 4A, 5A, 5B, 6A, 7A, 7C, 8A, 8D, 9A, 9C, 9D, see Figure 22) were used to determine the ambient sound levels during measurements at these sites. One second, 1/3-octave band levels were used to develop the median values (L_{50}) by 1/3-octave band, during morning and afternoon measurement periods. These L_{50} values were adjusted, by frequency, for instrumentation noise and windscreen effects, and then added to the derived auditory system noise. The resulting spectra provided the “measured ambient” for each hour of data collected and modeled at each of the 17 sites.

C.3.2 Reduction of Taped Sound Levels

⁷⁵ Fidell, Sanford, et al., “Evaluation of the effectiveness of SFAR 50-2 in restoring natural quiet to Grand Canyon National Park.” NPOA Report No. 93-1, June 23, 1994, p. 55.

⁷⁶ In order to provide additional diagnostic information, the audibility logs and the tape recorded sound levels were used to estimate the Detectability Levels, $10 \log (d')$ at which the measurement personnel were operating during data collection. Section C.4 describes the estimation process and presents the resulting empirical values.

Each tape of recorded data (about four hours in length) was processed using a Larson-Davis Model 2900 1/3-octave band analyzer. The frequency range analyzed was 0.8 to 10,000 Hz, and the sound level resolution of the LD-2900 is approximately 1/40th of a decibel. One-second linear averages were obtained every second for the duration of each DAT tape. Each tape's 1/3-octave band time history was stored in a separate file. Using the observer logs for sound source identification, the 1/3-octave band files were analyzed to produce sound level histograms with bin widths of 0.1 dB for each band for sound segments identified as "natural"; that is, for all periods when no human produced sounds were audible. These histograms provided L_{50} values for each 1/3-octave band, for each DAT tape. Note that these L_{50} values apply to the entire tape, so that the derived measured ambients apply to all hours of audibility data collected during that taped period.

C.3.3 Accounting for Instrumentation Noise

Resulting L_{50} sample sizes for "natural" sounds from the nominal 4-hour DAT tapes ranged from 6,000 to 10,000 spectra. The plots of spectral L_{50} values of these spectra are smooth and orderly. Figure 66 shows the relationships of a measured L_{50} spectra, the instrumentation noise floor, and the measured levels corrected for the noise floor. It also shows for reference the ISO threshold of hearing. At the higher frequencies the spectral content is dictated by instrumentation noise (more high-frequency bands are affected when using the 1/2-inch electret microphones than when using the 1-inch low-noise condenser microphones). In general, bands above 1,000 Hz are affected with the 1/2-inch system, and above 5,000 Hz with the 1-inch system. Using the constant-slope of the high-frequency sound levels vs. frequency band as a guide, the instrumentation noise curve was extrapolated to lower frequencies and used to correct the mid-frequency bands by energy subtracting the extrapolated L_{50} instrument noise from the measured L_{50} sound levels, as shown in Figure 14. This energy subtraction was not done when the difference between the measured and extrapolated instrument noise became less than 0.5 dB; in those cases, the adjusted ambient was set to a large negative number. In most cases, the sound levels adjusted for instrumentation noise were near the ISO threshold of hearing over some of the range of interest.

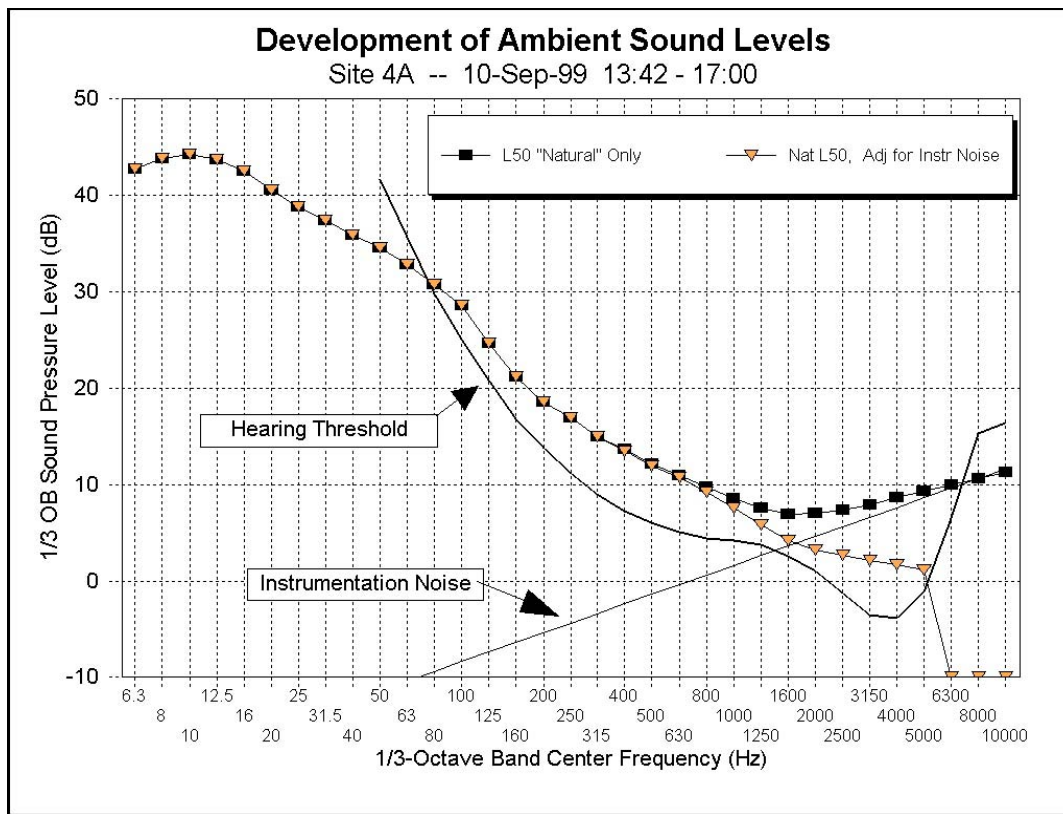


Figure 66. Effect of Instrument Noise Floor Adjustment to Ambient L50

C.3.4 Accounting for Auditory System Noise

Because the adjusted natural L_{50} spectra were often close to or below the ISO human threshold of hearing, an adjustment of the "natural" spectra was required. Without this adjustment, computations of signal to noise level ($10 \log(d')$) could indicate aircraft audibility even when a person with normal hearing would not have detected the aircraft sound.

The assumption was made that the phenomenon controlling the human hearing threshold was a Gaussian masking noise spectrum internal to the human auditory system. This mathematical construct assumes that the reason people can not hear sound levels any lower in level than the threshold of hearing is because there is masking noise in the combined auditory system and brain. Whether this is in fact the case is not important. The important point is that this construct provides a way to mathematically combine the signal (aircraft sound), ambient noise, and hearing threshold, and it does so in a way that yields common sense results under a variety of conditions.

Equation 7 was solved for the 1/3-octave band equivalent auditory system noise, N , using the assumption that S is the ISO pure tone sound level at the threshold of hearing and that d' is about 1.5 in the laboratory conditions in which the ISO threshold was determined.

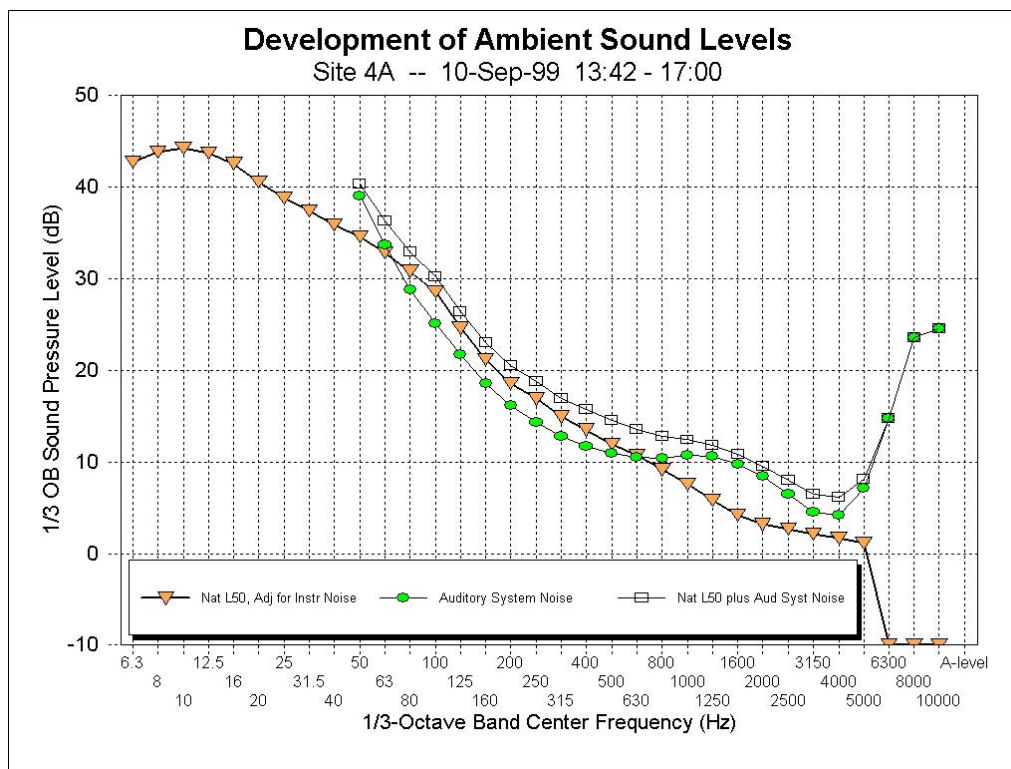


Figure 67. Adjustment of Natural L50 for Auditory System Noise

Figure 67 shows the effect of adding the instrumentation noise adjusted natural L_{50} spectrum energy to the derived auditory system noise energy spectrum. Additional small adjustments were made for microphone / windscreen frequency response. The resulting adjusted summations were used for the “measured ambient” in the modeling. In general, at the lower frequencies the total was controlled by the measured ambient, and at higher frequencies the total was controlled by the equivalent auditory system noise. It should be noted that, in detection of tour aircraft, the important energy generally lies somewhere between 100 Hz and 300 Hz, and hence, these are the frequency bands in which the ambient levels are most important; the exact levels in the higher bands are not significant in computing detectability of current rotor or propeller powered tour aircraft. (Section C.4, below, provides an example of the relationship between aircraft spectrum, ambient spectrum and 10 log (d’).)

Additionally, a second set of spectra were provided for modeling, referred to as the “ambient plus 10 dB.” These spectra were derived by increasing the auditory system noise 10 dB and then recalculating the energy sum again using the instrument noise adjusted natural L_{50} spectra. This second ambient was used to assess the sensitivity of the models to assumptions about background sound levels.

C.3.5 Resulting Ambient Levels for Modeling

The tables on the following pages give the measured ambient L_{50} spectra (adjusted for instrumentation noise and auditory system noise) for each of the audibility sites where DAT recordings were made. The columns identify the site, the date of the measurement, the time at which the measurement began, and the L_{50} sound pressure levels in each listed 1/3-octave band. The last two columns provide first the A-weighted value for the instrumentation noise (and microphone/windscreen) adjusted spectrum, and second the A-weighted value for the instrumentation and

auditory system noise adjusted spectrum. Because auditory system noise would likely control the A-weighted level due to the high levels above about 4,000 Hz, see Figure 67, these last A-weighted values are based on the 1/3-octave band levels up to 3,150 Hz only.

Site	Date	Start Time	1/3- Octave Band Center Frequency >>>							
------	------	------------	---	--	--	--	--	--	--	--

Site	Date	Start Time	1/3- Octave Band Center Frequency >>&					
------	------	------------	---	--	--	--	--	--

C.4 Empirically Determined Values of Detectability Level

C.4.1 Introduction

As part of the information provided here for diagnostic purposes, this section presents the Detectability Levels at which the measurement staff operated during data collection. The following sections describe the method used to calculate the Detectability Levels, $10 \log(d')$, for each tour aircraft event heard, and present the resulting distributions of $10 \log(d')$.

C.4.2 Method

In order to compute $10 \log(d')$, two matched spectra are needed: the spectrum of the tour aircraft and the spectrum of the non-tour aircraft background at the times when the tour aircraft was first heard (onset) and last heard (offset). By matching the continuous one-second spectra obtained from the DAT recordings, see Section C.3.2, with periods when tour aircraft were logged by the observers, these spectra could be estimated.

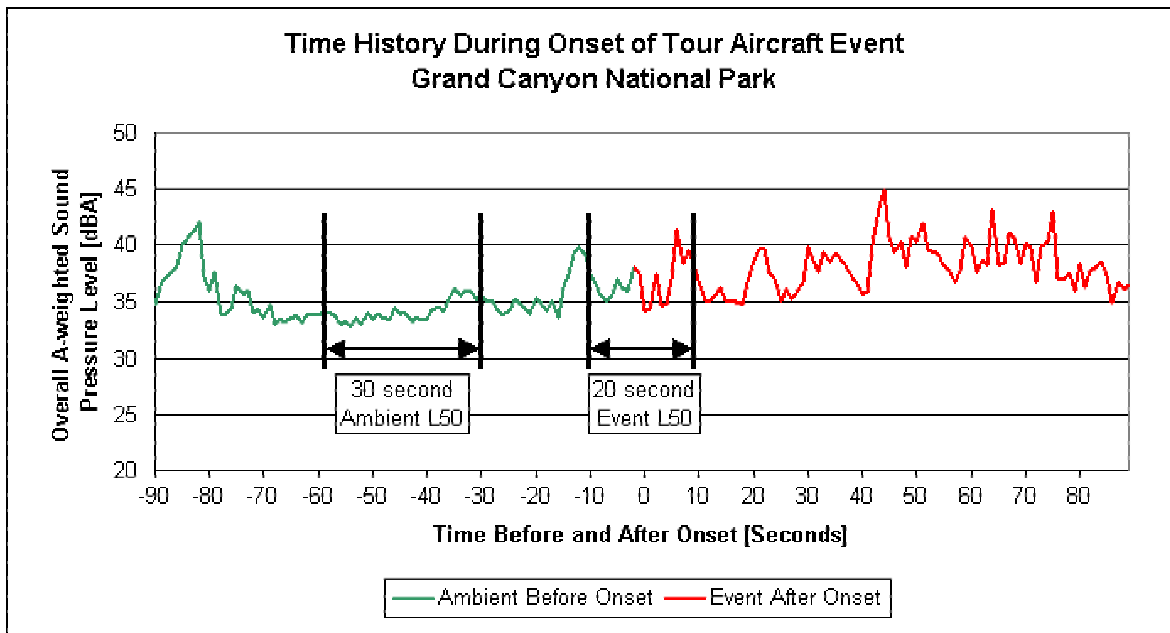


Figure 68. Example of Derivation of Aircraft and Non-Aircraft Spectra for $10 \log(d')$ Calculations

Figure 68 shows how these spectra were obtained. To estimate the non-aircraft background spectrum, a 30 second sample of the 1/3-octave band time history was extracted from 60 seconds to 30 seconds before the event onset was logged. The background spectrum used was the median sound pressure level, L_{50} , in each 1/3-octave band during this 30-second sample. The aircraft spectrum was similarly obtained from the 20-second time history starting 10 seconds before the event onset and ending 10 seconds after onset. The ambient spectrum was then energy summed with the auditory system noise, as described in Section C.3.4, and $10 \log(d')$ computed. Spectra for the offset (end of the event) were similarly determined by sampling 10 seconds before to 10 seconds after offset for the aircraft spectrum, and 30 seconds to 60 seconds after offset for the background spectrum.

Figure 69 provides an example of the relationship of the various spectra for an identified tour aircraft. The ambient spectrum is energy summed with the auditory system noise, and the result then compared

with the aircraft spectrum to yield $10 \log (d')$ of 9 dB. In this example, the frequency of maximum Detection is 100 Hz.

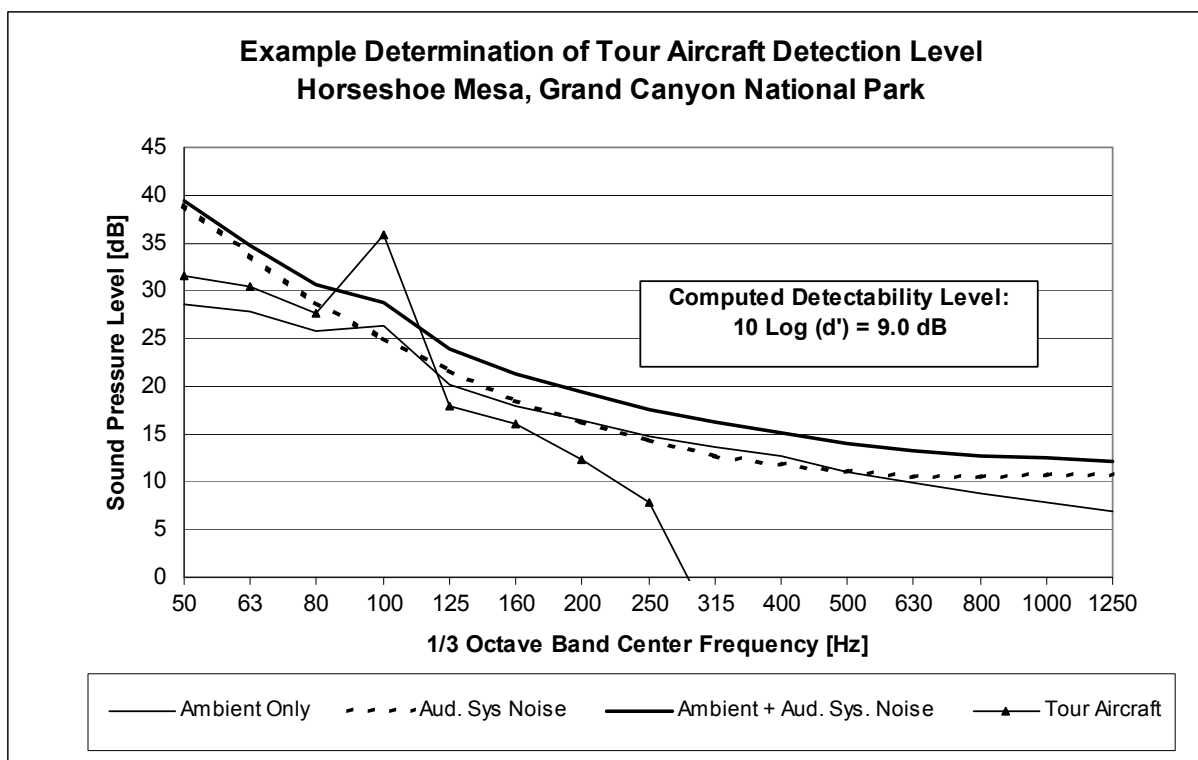


Figure 69. Example of Relationships Between Tour Aircraft and Adjusted Ambient Spectra and the Resultant Detectability Level, $10 \log (d')$

C.4.3 Results

Table 35 summarizes the numbers of events available for analysis by the frequency of maximum detection, as determined by the method described above. Because it is very unlikely that any tour aircraft detection frequencies exceeded about 300 Hz, events with maximum detection frequencies at or above 500 Hz were excluded from the $10 \log (d')$ computations. It is possible that the method did not always capture the appropriate spectra, with the result that the frequency of maximum detection is unrealistic, and the $10 \log (d')$ computations would be suspect.

Table 35. Number of Events by Frequency of Maximum Detection

Number of Observations of 1/3-Octave Band Center Frequencies of Maximum Detection														
1/3-Octave Band, Hz	63	80	100	125	160	200	250	315	400	500	630	800	1000	1250
Number of Observations	3	8	38	59	44	17	24	23	14	13	9	12	13	16

Table 36 summarizes the computed results, while the following figures present the specific results in various formats. Figure 70 shows how the results varied by day, and Figure 71 gives the computed detectability levels by audibility site, from sites closest to the tour aircraft corridor to the sites most distant from the corridor, see Table 15. Finally, Figure 72 shows the distribution of detectability levels by frequency of maximum detection, and Figure 73 presents the results by observer.

Table 36. Summary of Empirical 10 log (d') Results

	Event Onset	Event Offset
Number of Events	129	101
Average 10 log (d')	5.7	4.26
Standard Deviation	5.95	5.93

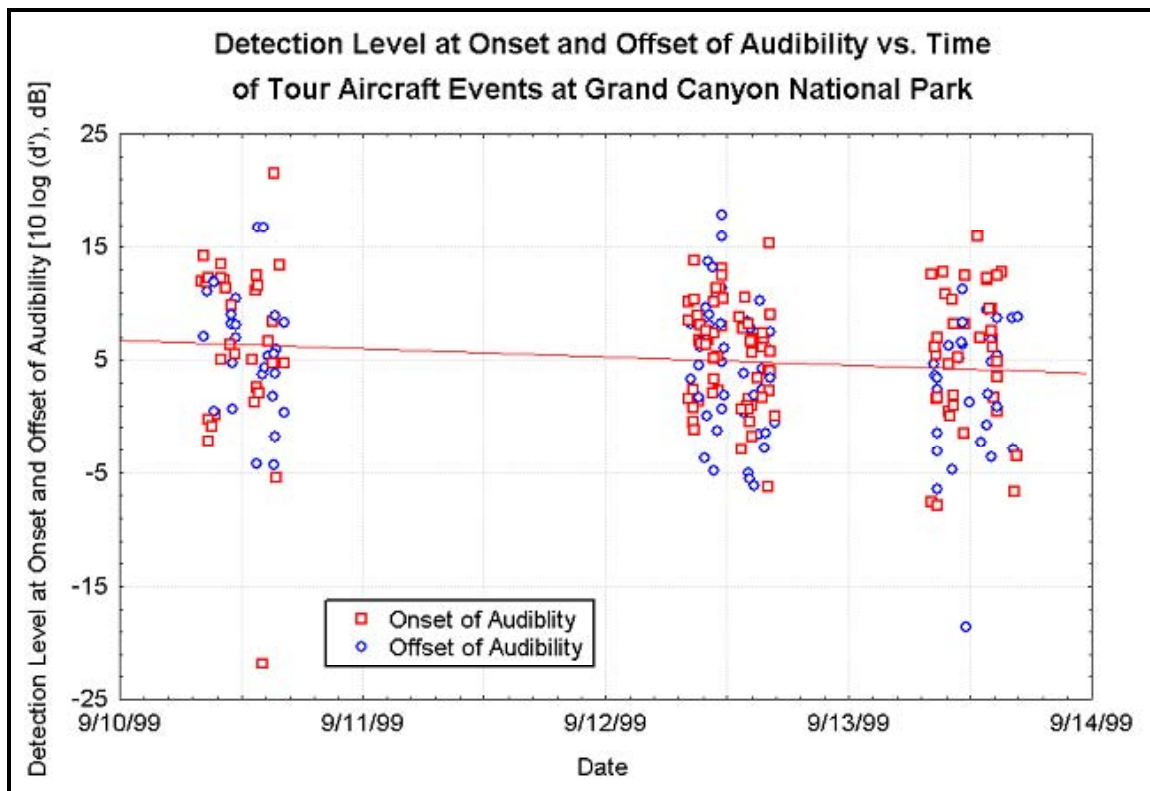


Figure 70. Computed Detectability Levels by Day

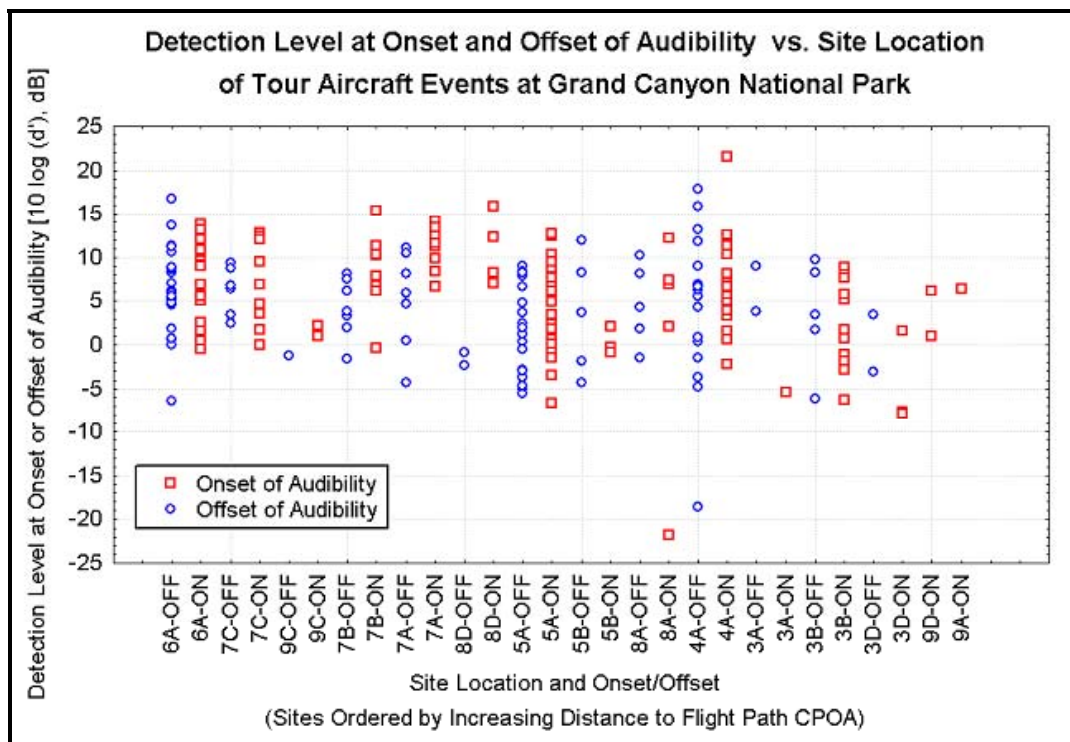


Figure 71. Computed Detectability Levels by Site, Nearest to Most Distant from Tour Corridor

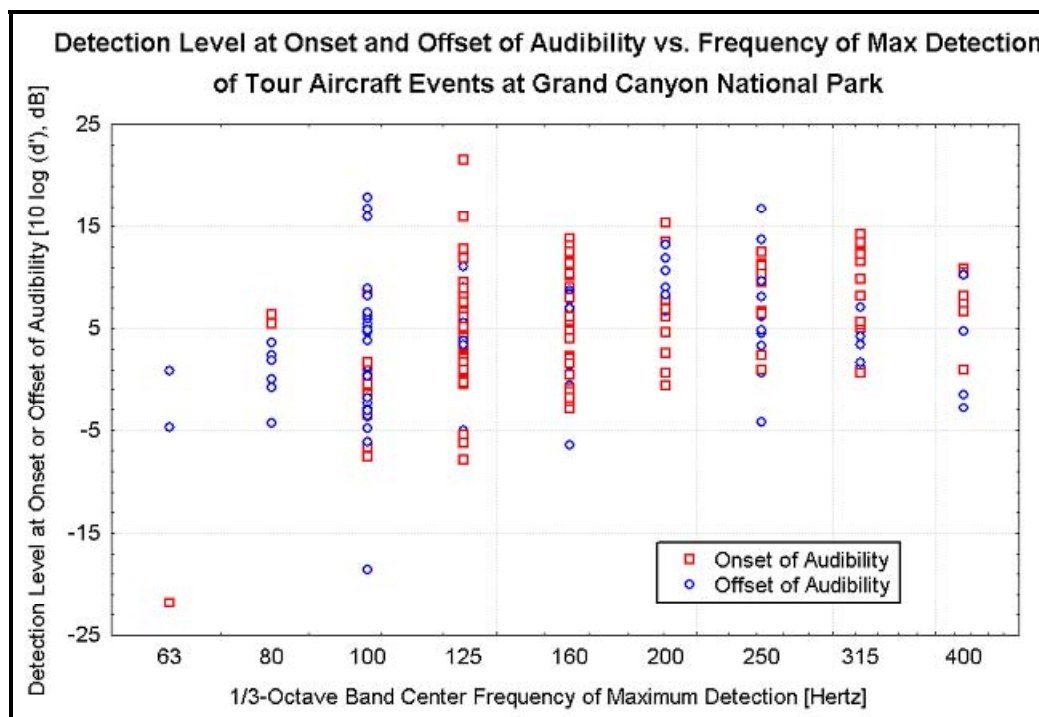


Figure 72. Computed Detectability Level by Frequency of Maximum Detection

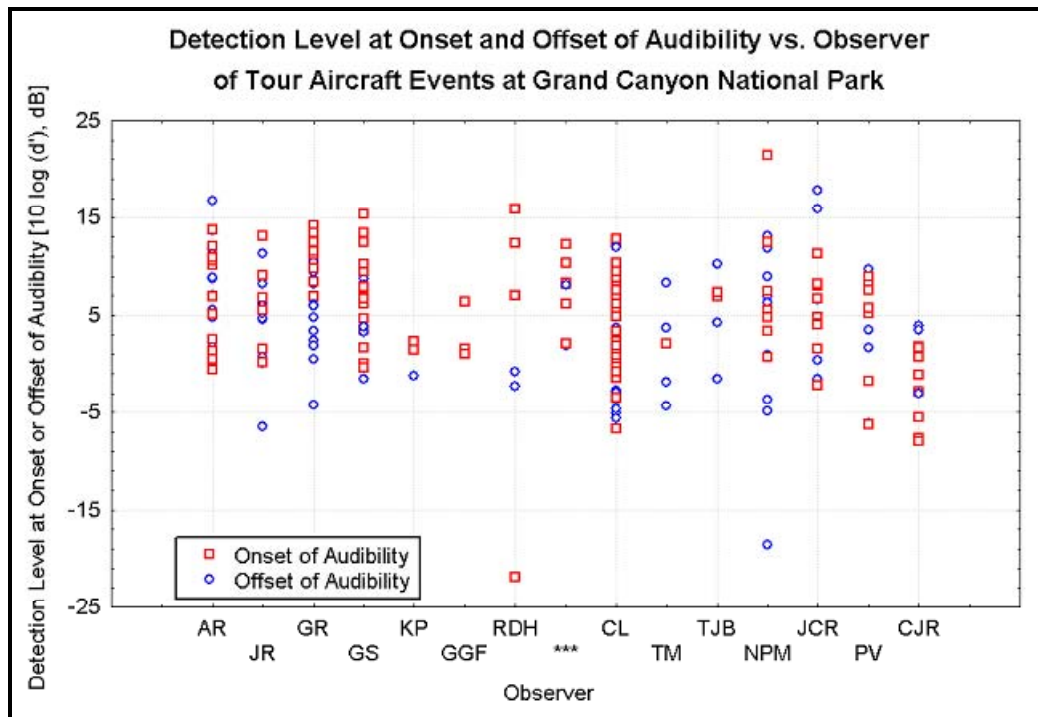


Figure 73. Computed Detectability Levels by Observer

Page Intentionally Blank

APPENDIX D. FIGURES SHOWING DATA COLLECTION SITES

The figures in this appendix show the specific locations of each data acquisition site.

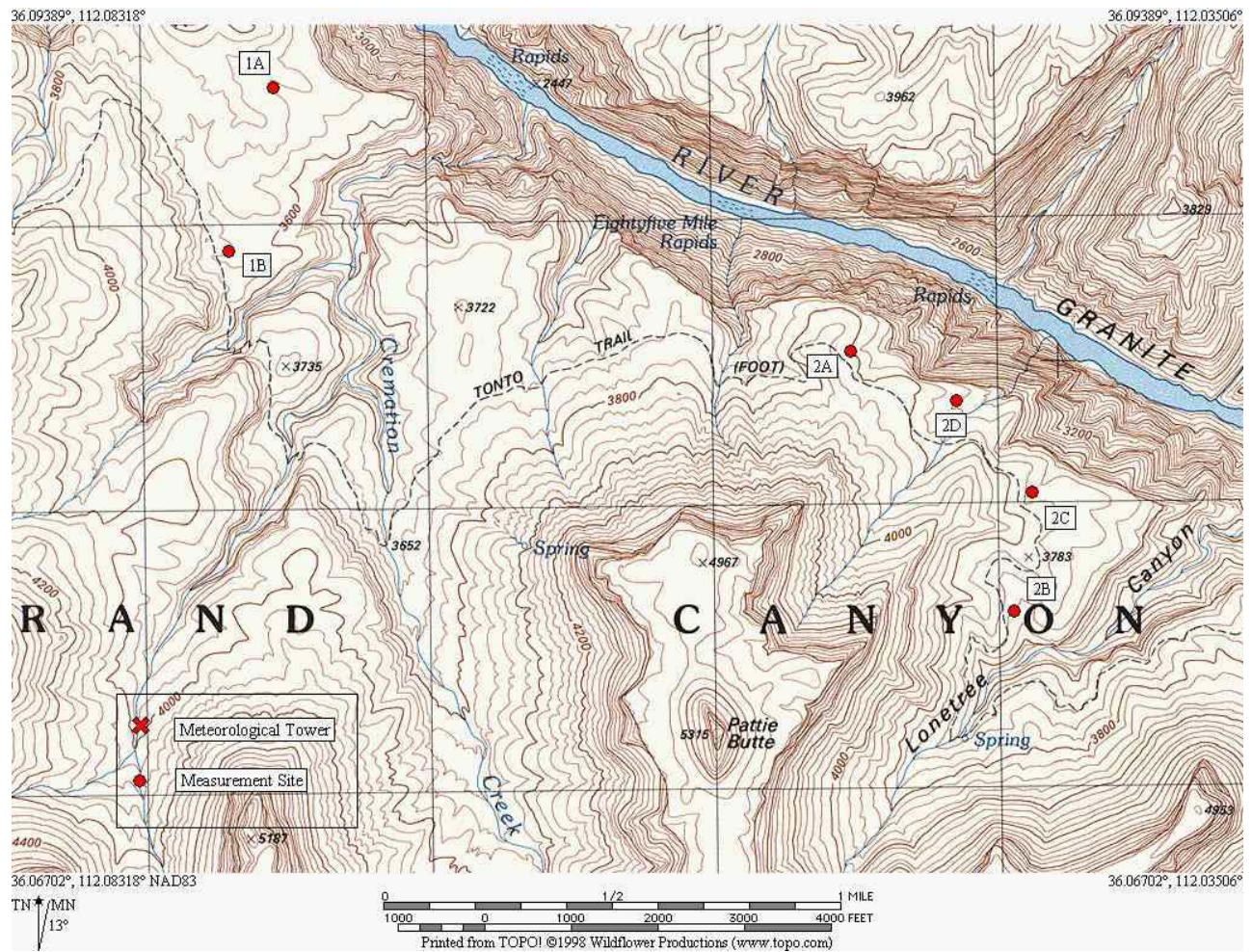


Figure 74. Sites 1 and 2 Locations

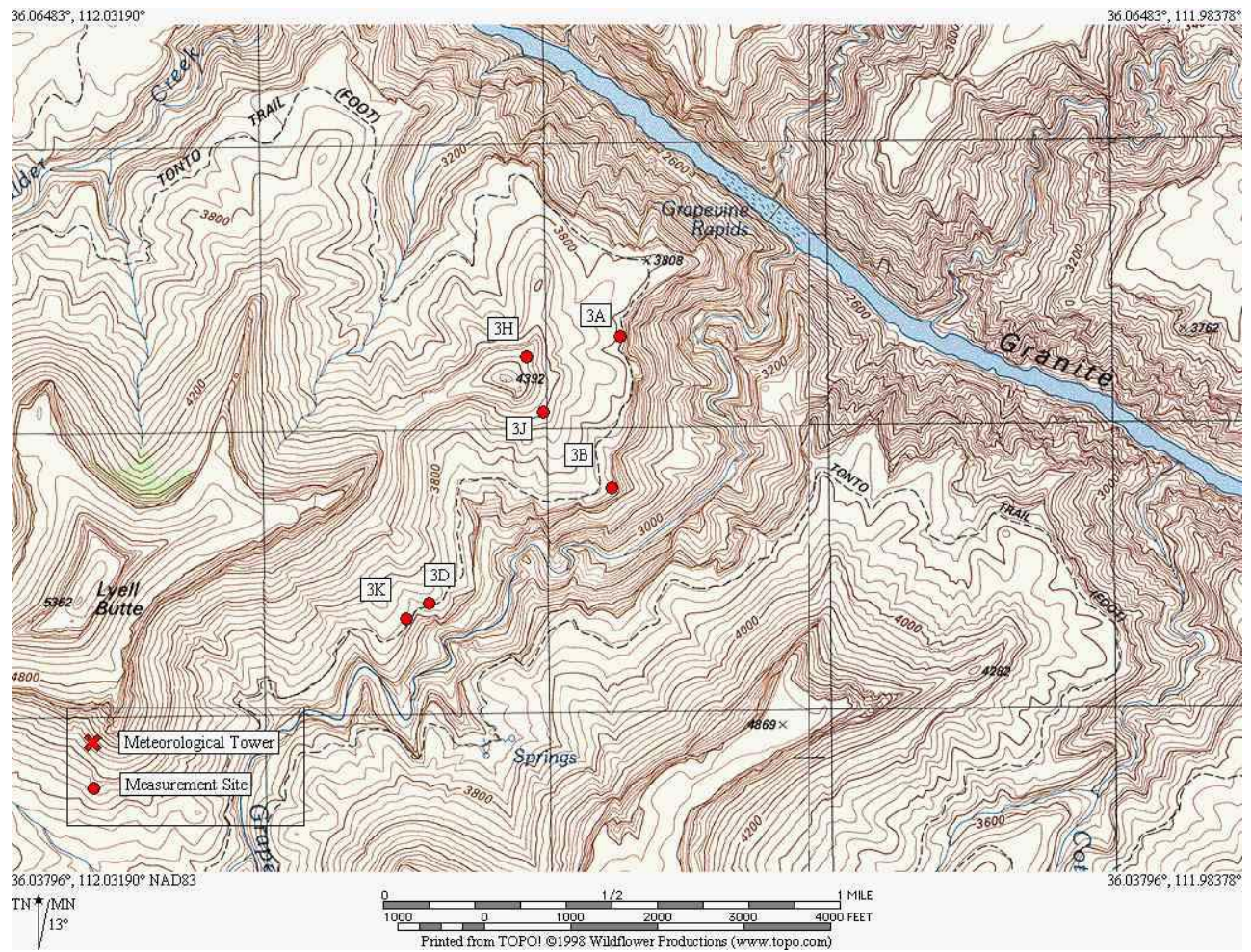


Figure 75. Site 3 Locations

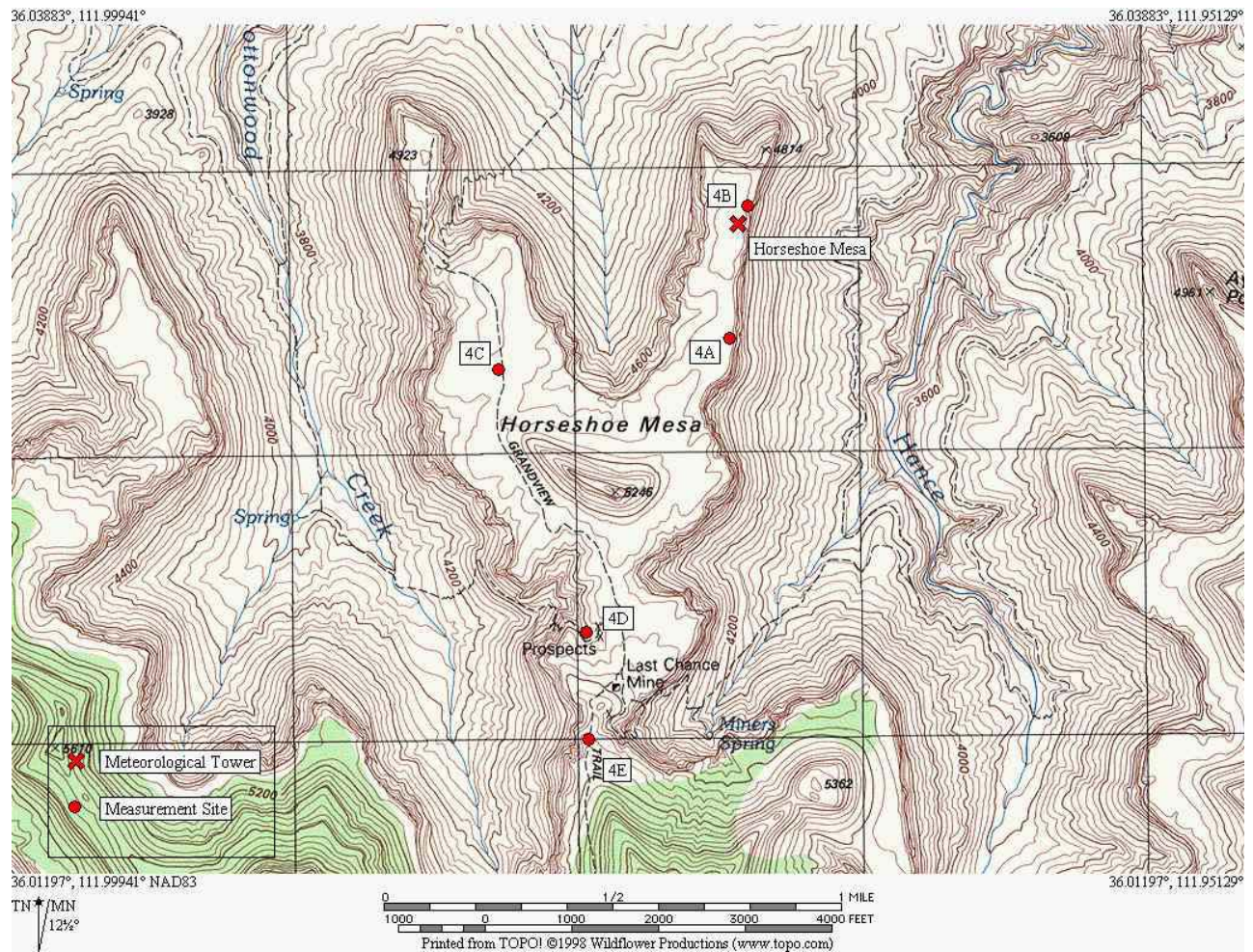


Figure 76. Site 4 Locations

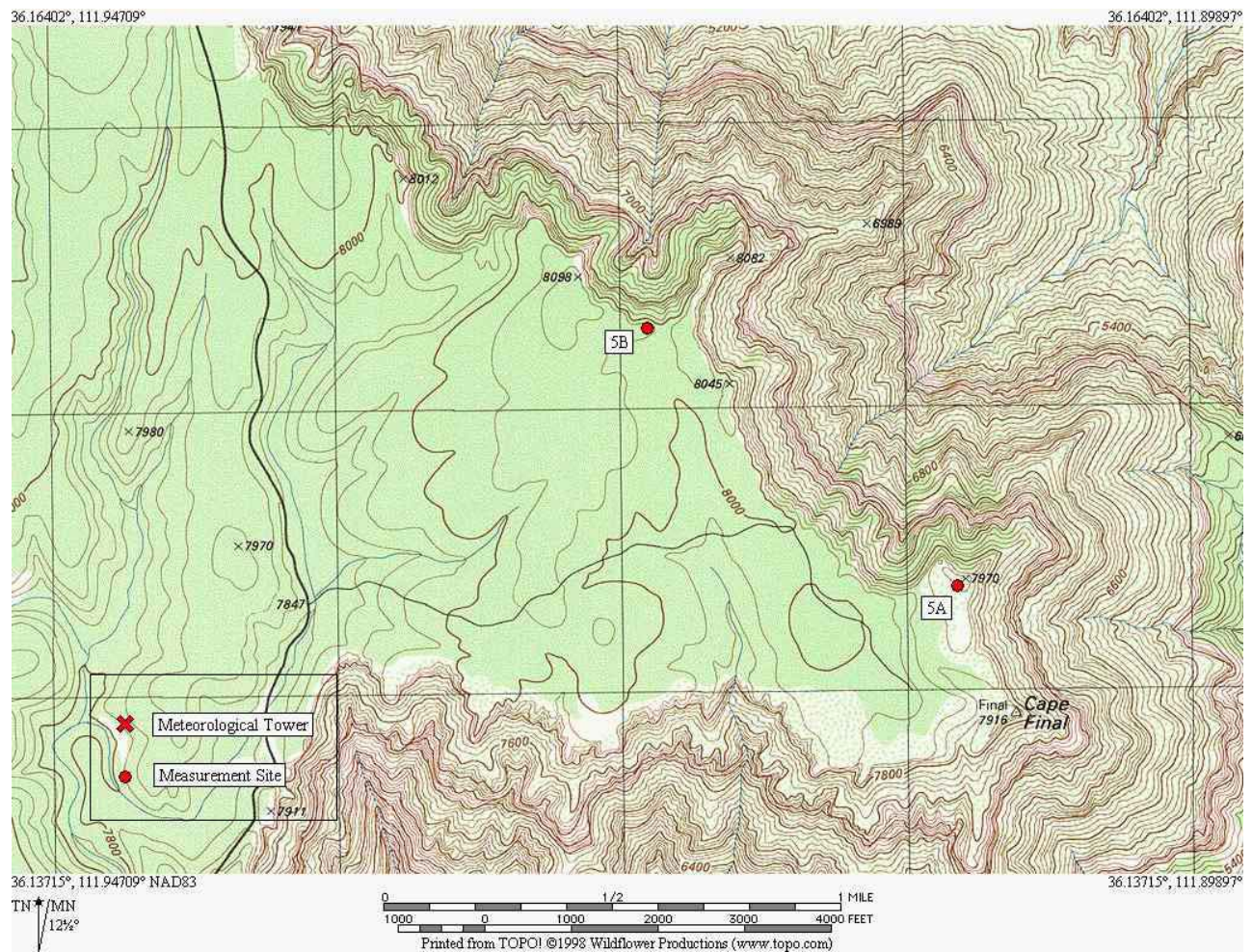


Figure 77. Site 5 Locations

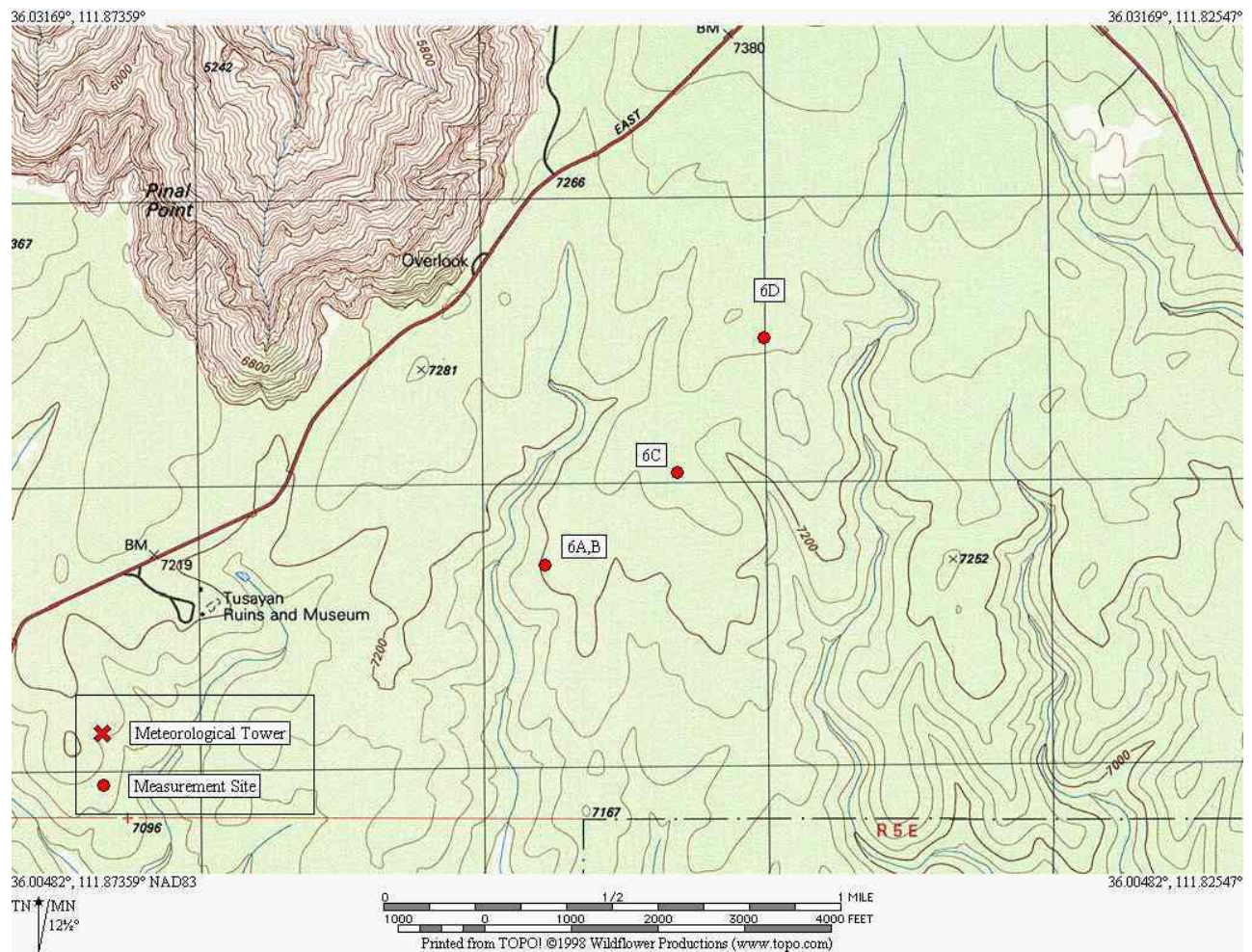


Figure 78. Site 6 Locations

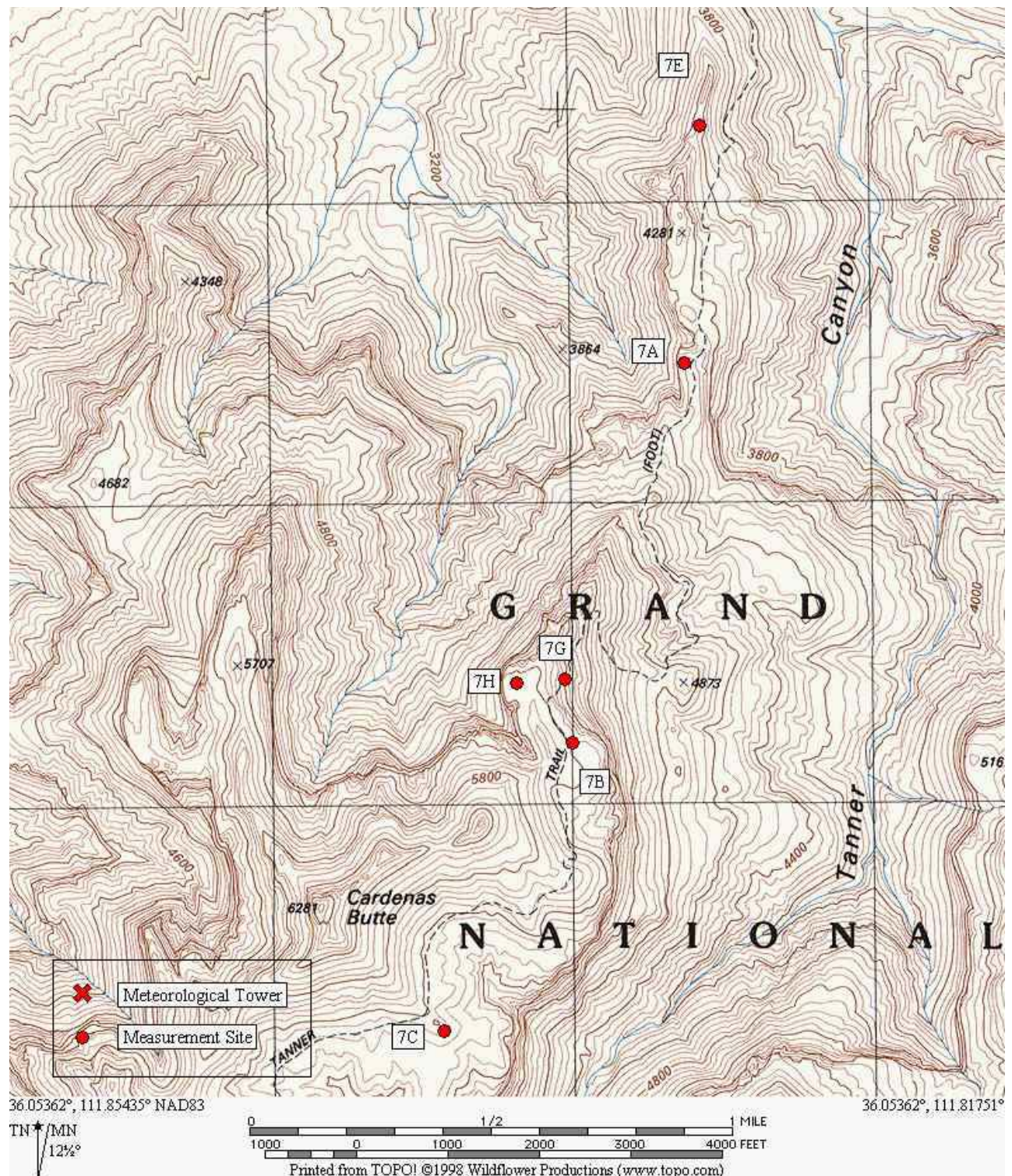


Figure 79. Site 7 Locations

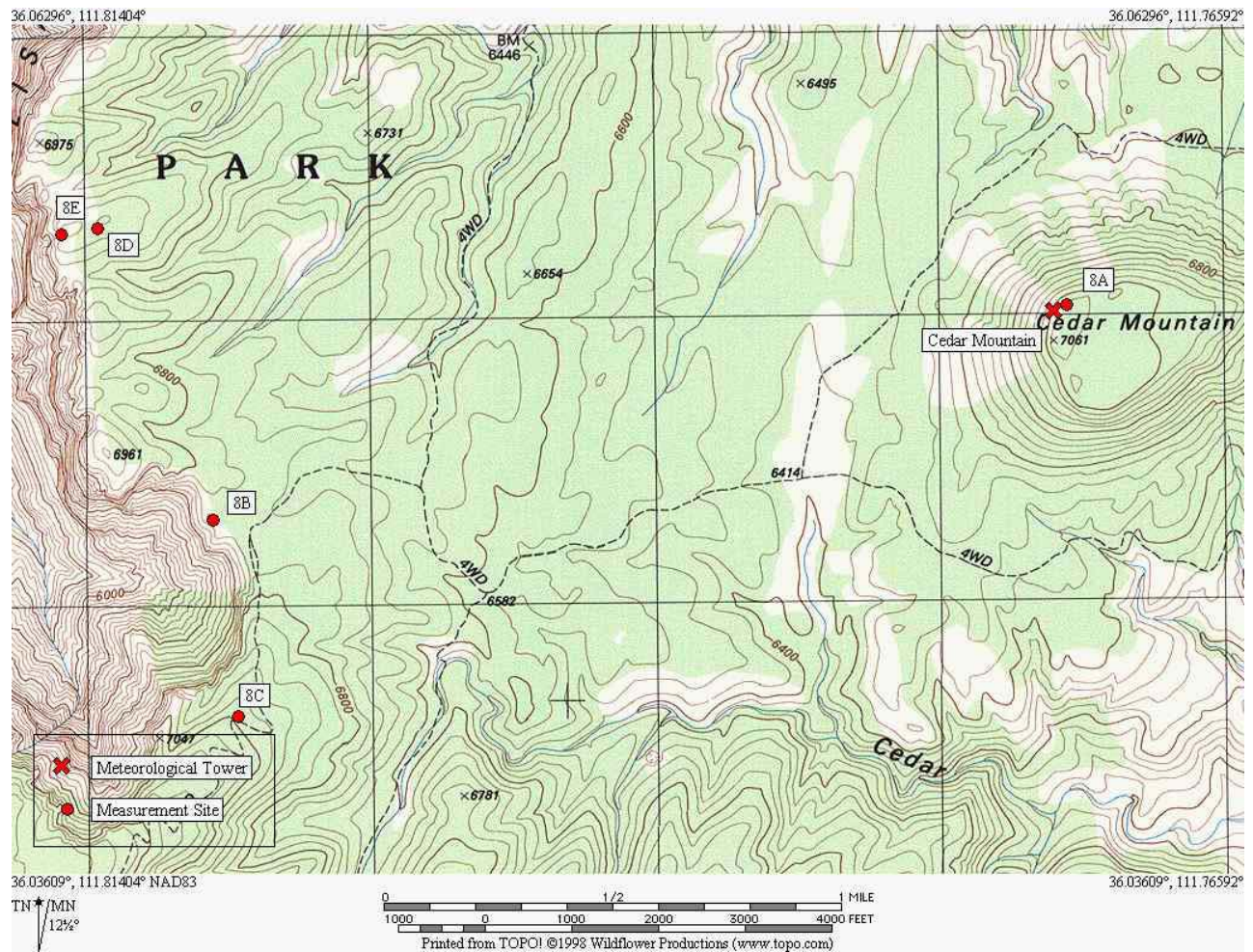


Figure 80. Site 8 Locations

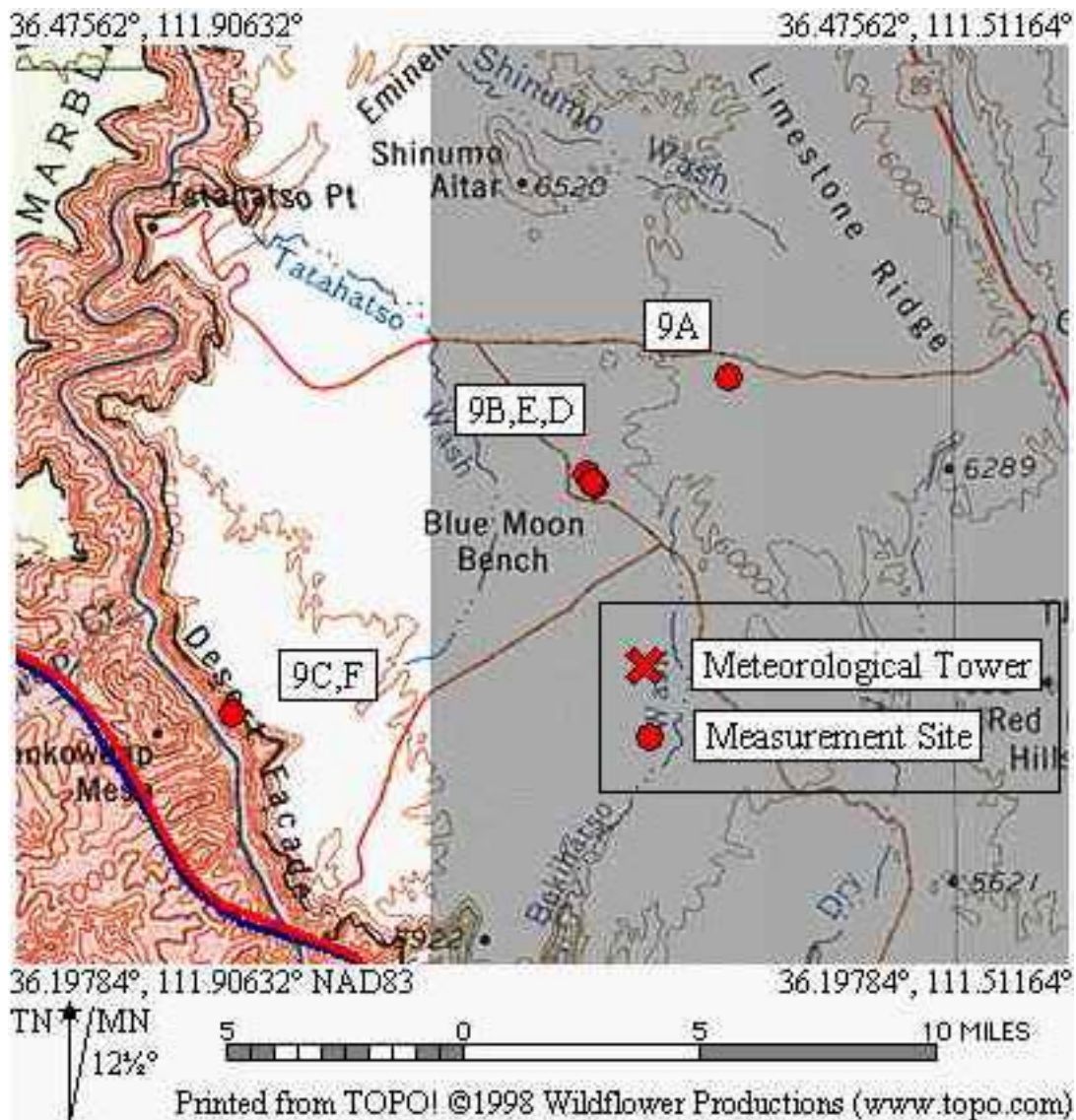


Figure 81. Site 9 Locations

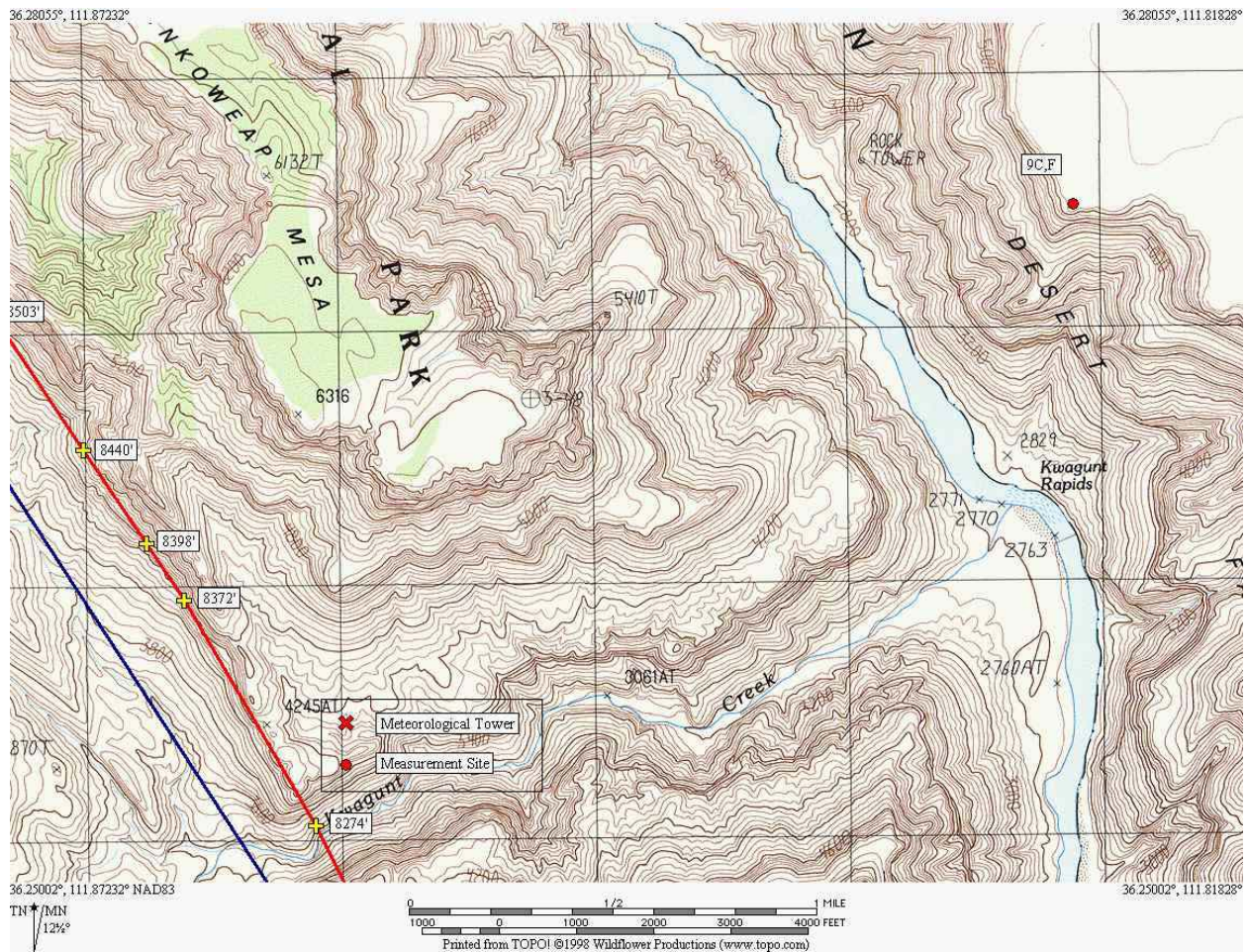


Figure 82. Site 9C, F Locations

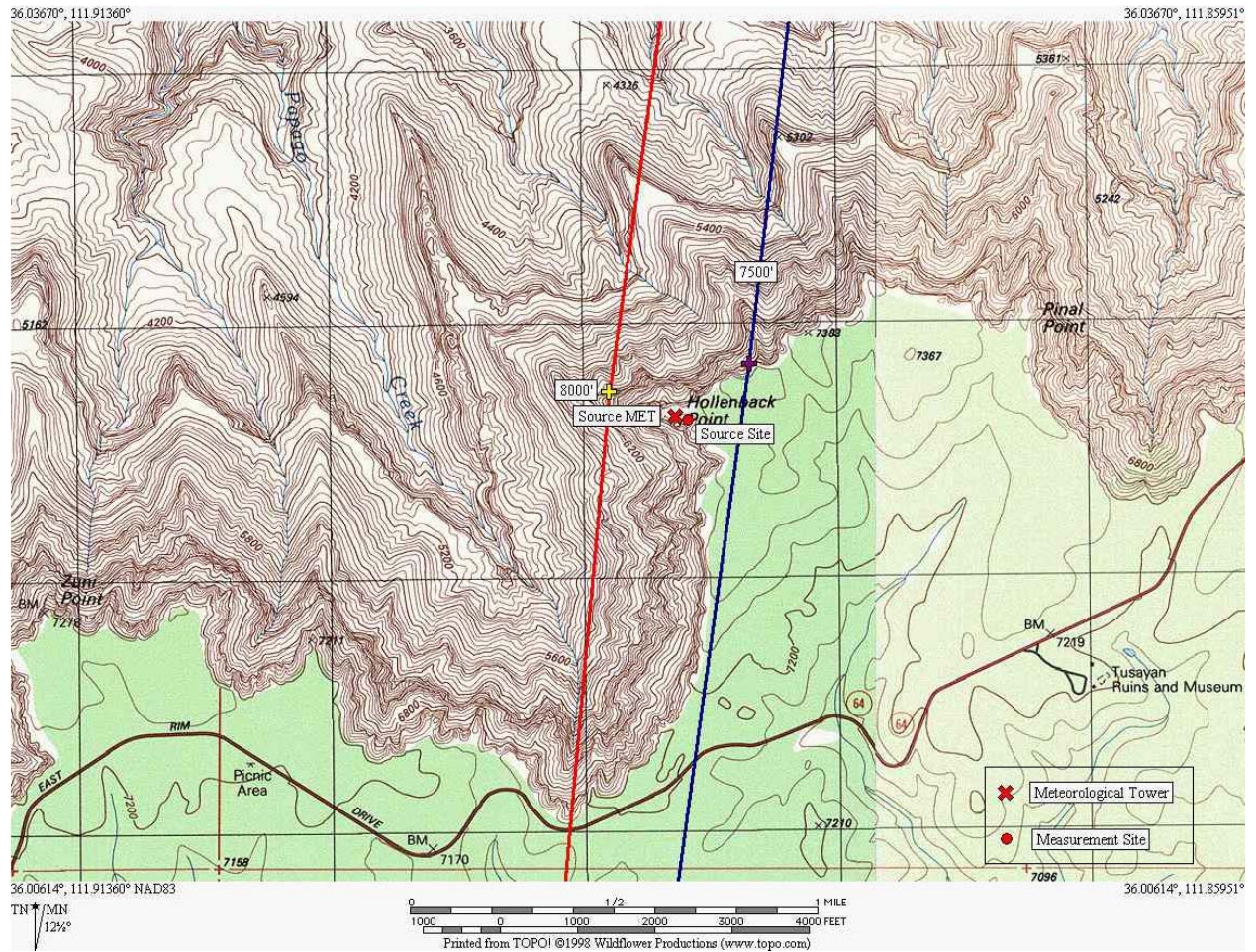


Figure 83. Source Site Location

APPENDIX E. INSTRUCTIONS FOR SOURCE LOGGING

The REAL-TIME logging of sound sources is one of the primary objectives of this field study.

The protocol described below has been found to work well. The ability to match this log with the recordings on Digital Audio Tape and with air traffic logs maintained at other sites is critical to the success of the project. The goal is to be able to perform the matches to within one second during the data analysis phase of the project. .

E.1 Setting the Palmtop Date and Time

Press the "&..." key to display the menu screen.

Using the arrow keys move the cursor to the "C:\DOS" icon

Press enter.

At the DOS prompt type "date<enter>"

The current date will be displayed.

If the date is correct, simply press enter

If the date is incorrect, enter the correct date (mm/dd/yy<enter>)

At the DOS prompt type "time<enter>"

The current time will be displayed to the nearest second.

If the time is correct to the nearest second, simply press enter.

If the time is not correct to the nearest second, enter a time 10 to 20 seconds hence, wait for that time to appear on the reference clock, then press <enter>.

E.2 Starting the Logging Spreadsheet

The log will be maintained on the palmtop computer in a spreadsheet form using the built-in Lotus 1-2-3 Version 2.3.

Press the "1-2-3" key to start Lotus

Press "/F(ile)R(etrieve)"

Use the arrow keys to highlight "GCMV_LOG.WK1"

Press <enter>

On the second line down from the top, above the column labels, the spreadsheet will prompt you for your site (e.g., 1A, 1B, 2A, etc.)

Site #:

Type the 2 character site code; then press <enter>.

The spreadsheet will display the site and date in the header as shown below, and the cursor will appear directly below the "Time" heading.

NATIONAL PARK SERVICE - GRAND CANYON MODEL VALIDATION STUDY
Site: 1A - Tipoff/Cremation - unshield 06-Sep-99

Time	Acoustic State	A/C Type	A/C Oper	Backgnd Descrip	Comments
-----	-----	-----	-----	-----	-----

E.3 Save the Spreadsheet Using Site and Date Naming Convention

It is important not to overwrite the "GCMV_LOG.WK1" file. Therefore, immediately save the spreadsheet using the naming convention described below.

Press "/F(ile)S(ave)

At the File Name prompt Type "ssmmdd<enter>"

Where "ss" = 2 character site identification

"mm" = 2 character month

"dd" = 2 character day of the month

Example: "1A0915" for site 1A on September 15.

The spreadsheet is now saved under this file name, and all subsequent saves will be to this file.

The spreadsheet contains 26 different macros (one for each letter of the alphabet) that perform the logging functions. The template on the palmtop keyboard shows the functions. Pressing the <ALT> key followed by the desired function activates a macro.

Creating a new entry in the log is done with a 2-step process:

1. Enter a time stamp
2. Enter the new acoustic status

E.4 Time Stamping

Whenever a new entry is made, the first thing to do is to enter a time stamp. This is done with the <alt>TIME macro (<alt>Q), which places the current system clock reading in the Time column. The result is shown below. This macro takes about 2 seconds to execute, but the time displayed is that when the key is pressed, not when it appears in the spreadsheet.

NATIONAL PARK SERVICE - GRAND CANYON MODEL VALIDATION STUDY
Site: 1A - Tipoff/Cremation - unshield 06-Sep-99

Time	Acoustic State	A/C Type	A/C Oper	Backgnd Descrip	Comments
-----	-----	-----	-----	-----	-----
11:56:31					

E.5 Adjusting the Time Stamp

If you need to adjust a time stamp backwards or forwards in time a few seconds, use the <alt>ChgT macro (<alt>A). At the prompt shown below, enter a + or - sign followed by the number of seconds you want to add or subtract from the time stamp followed by <enter>.

New Time:

E.6 Beginning a Logging Session

There are two steps to beginning a logging session.

1. The Begin Log entry

After performing the time stamp, press <alt>B/E
Enter your initials at the prompt, followed by <enter>.
The result is shown below.

```
NATIONAL PARK SERVICE - GRAND CANYON MODEL VALIDATION STUDY
Site: 1A - Tipoff/Cremation - unshield 06-Sep-99
```

Time	Acoustic State	A/C Type	A/C Oper	Backgnd Descrip	Comments
11:56:31	Beg Log	***	***	***	Observer: RDH

The “B/E” key toggles back and forth between “Begin Log” and “End Log”. If for some reason the entry in the acoustic state column is incorrect, simply press <alt>B/E again.

2. The Time Check entry

The purpose of this entry is to compare the palmtop system clock with your personal wristwatch, which has already been set to the correct time. When your wristwatch changes to an even minute, <alt>TIME. Then <alt>TimeChk. At the prompt, enter the time on your wristwatch (hhmmss). Just 6 digits, no colons required. The log form should then look as follows.

```
NATIONAL PARK SERVICE - GRAND CANYON MODEL VALIDATION STUDY
Site: 1A - Tipoff/Cremation - unshield 06-Sep-99
```

Time	Acoustic State	A/C Type	A/C Oper	Backgnd Descrip	Comments
11:56:31	Beg Log	***	***	***	Observer: RDH
11:56:59	Time Chk			11:57:00

E.7 Acoustic State Documentation

For the purposes of this study the acoustic environment will be divided into 4 states:

- Tour Aircraft
- Other Aircraft
- Non-Aircraft - Human (human related sounds)
- Non-Aircraft - Natural (park-indigenous sounds)

The function of the log is to document the acoustic state at any instant in time. Because of the difficulty in keeping track of multiple sound sources that may all be audible at the same time, a source hierarchy has been developed to simplify the procedure. That hierarchy is shown above. Within each hierarchy are different categories of sounds. These are shown in the table below, and a key on the palmtop represents each. In most cases, placing a new entry in the log requires only two keystroke sequences, <alt>Time followed by <alt>source.

Aircraft (Orange)

- Prop - propeller aircraft
- Helo - Helicopter
- Pr/He - propeller and/or helicopter (if both are audible or you can't tell which it is)
- Jet - high altitude jet aircraft

Aircraft Operator (Yellow)

- Tour - tour aircraft for sure
- Other - commercial jet, general aviation, tour maybe, can't tell for sure, etc.

Non-Aircraft - Human (Green)

- Veh - vehicles such as cars, trucks, buses, etc.
- Voice - human voices or conversation
- Mules - sounds of pack animals
- Spare - available for site-specific source (change cell xx-yy)
- Other - other human-related source (identify in Comment column if there's time)

Non-Aircraft - Natural (Blue)

- Thndr - thunder. Try to identify each occurrence if possible
- Birds - bird chatter
- Insct - insects such as crickets, etc.
- Mam - mammals (try to identify in Comment column if there's time)
- Water - running water, such as rapids
- Drzzl - light drizzle precipitation
- Rain - steady rainfall
- WndF - wind noise created by wind interacting with foliage
- WndE - wind noise created by wind interacting with your ear. This category should be used only when there is NO other identifiable source present.
- Other - other indigenous source (identify in Comment column if there's time)

Within each of the three primary categories, a sound higher on the above list takes precedence over one lower on the list. For example, if no aircraft or human sounds are present, and you hear running water and insects, the correct entry is insects. If you have the time, add the running water as a comment.

E.8 Sample Sequence of Log Entries

No aircraft or human-related sounds audible, only wind in the foliage:

NATIONAL PARK SERVICE - GRAND CANYON MODEL VALIDATION STUDY
Site: 1A - Tipoff/Cremation - unshield 06-Sep-99

Time	Acoustic State	A/C Type	A/C Oper	Backgnd Descrip	Comments
11:56:31	Beg Log	***	***	***	Observer: RDH
11:57:38	Time Chk			11:57:40
11:58:42	Natural	***	***	Wind/Fol	

At 11:59:30 the sound of a propeller aircraft becomes audible:

NATIONAL PARK SERVICE - GRAND CANYON MODEL VALIDATION STUDY
Site: 1A - Tipoff/Cremation - unshield 06-Sep-99

Time	Acoustic State	A/C Type	A/C Oper	Backgnd Descrip	Comments
11:56:31	Beg Log	***	***	***	Observer: RDH
11:57:38	Time Chk			11:57:40
11:58:42	Natural	***	***	Wind/Fol	
11:59:30	Aircraft Prop			***	

You subsequently determine that it is a tour aircraft:

NATIONAL PARK SERVICE - GRAND CANYON MODEL VALIDATION STUDY
Site: 1A - Tipoff/Cremation - unshield 06-Sep-99

Time	Acoustic State	A/C Type	A/C Oper	Backgnd Descrip	Comments
11:56:31	Beg Log	***	***	***	Observer: RDH
11:57:38	Time Chk			11:57:40
11:58:42	Natural	***	***	Wind/Fol	
11:59:30	Aircraft Prop		Tour	***	

Aircraft is no longer audible, but human voices can be heard:

NATIONAL PARK SERVICE - GRAND CANYON MODEL VALIDATION STUDY
Site: 1A - Tipoff/Cremation - unshield 06-Sep-99

Time	Acoustic State	A/C Type	A/C Oper	Backgnd Descrip	Comments
11:56:31	Beg Log	***	***	***	Observer: RDH
11:57:38	Time Chk	11:57:40
11:58:42	Natural	***	***	Wind/Fol	
11:59:30	Aircraft	Prop	Tour	***	
12:01:22	Human	***	***	Voices	

E.9 Commonly encountered situations

1. You think you hear something new but you're not sure.

This is a commonly encountered situation. The rule is: When in doubt, <alt>Time. When you can properly classify the sound, then press the appropriate key(s). If it turns out that nothing really changed enter nothing further on this line. The data analysis software will ignore time stamps with nothing following on that line.

2. You change your mind about an entry already made.

Simply press a new <alt>key sequence. The old entry (but not the time stamp) will be overwritten.

3. You change your mind about a past entry (i.e. not the most recent one) already made.

Simply use the arrow keys to move the cursor to the line where an entry is to be changed (doesn't matter which column on that line the cursor is on). Then pres the new <alt> key sequence. The old entry (but not the time stamp) will be overwritten.

E.10 Periodic File Saving

The general rule is "Save early, and save often." A simple "/F(ile)S(ave)Y(es)" does the job.

E.11 Ending a Logging Session

There are two steps to ending a logging session.

1. The Time Check entry

Computer clocks have a habit of drifting. The purpose of this entry is to compare the palmtop system clock with your personal wristwatch, which has already been set to the correct time. When your wristwatch changes to an even minute (an even half-minute will do), <alt>TIME. Then <alt>TimeChk. At the prompt, enter the time on your wristwatch (hhmmss) when you pressed TIME. Just 6 digits, no colons required. The log form should look as follows:

NATIONAL PARK SERVICE - GRAND CANYON MODEL VALIDATION STUDY
Site: 1A - Tipoff/Cremation - unshield 06-Sep-99

Time	Acoustic State	A/C Type	A/C Oper	Backgnd Descrip	Comments
14:02:28	Time Chk			14:02:30

2. The End Log entry

After performing the time stamp, press <alt>B/E
Enter your initials at the prompt, followed by <enter>.
The result is shown below.

NATIONAL PARK SERVICE - GRAND CANYON MODEL VALIDATION STUDY
Site: 1A - Tipoff/Cremation - unshield 06-Sep-99

Time	Acoustic State	A/C Type	A/C Oper	Backgnd Descrip	Comments
14:02:41	End Log	***	***	***	Observer: RDH

If observers are switched within a logging session, do an “End Log” and “Begin Log” sequence so that the correct observer shows in the Comment column.

E.11.1 Stopping Lotus 1-2-3

Be sure to end the logging session as described above.
Save the current spreadsheet file.
Press “/Q(uit)Y(es)” to terminate Lotus 1-2-3.

E.11.2 To Resume Logging With a Previously Saved File

If you have stopped Lotus (as above) and wish to resume logging at the same site (and on the same day), start Lotus as described at the beginning of this tutorial, and select the previously saved file instead of “GCMV_LOG.WK1.” You will NOT be prompted for a site and date since this information will have already been entered in the spreadsheet, and it is also inherent in the file name and date.

Page Intentionally Blank

APPENDIX F. DEVELOPMENT OF GENERALIZED AMBIENTS FOR MODELING OF ENTIRE CANYON

F.1 Ambient Data Development

This appendix presents the derivation of generalized ambient sound levels that are intended for use when modeling tour aircraft audibility for the entire Canyon. The “measured ambients” used in the study apply to the specific sites. These generalized ambients are intended to apply throughout the Canyon and are to be applied by vegetation zone.

The noise data presented in this appendix were derived from the Digital Audio Tape (DAT) recordings made at many of the audibility sites during September 1999. For this analysis, the “ambient” sound conditions for the Grand Canyon are defined as those periods of time when the observer logged that only “natural” sounds were present. The observer logs were kept at each site second-by-second during all tape recording sessions.

All DAT recordings obtained at all sites were played back through a parallel filters spectrum analyzer to obtain one-second L_{eq} values for each 1/3 octave band as well as for the A-weighted sound level. These data sets were then processed by computer along with the source-identification logs to compute the L_{50} and L_{90} values for each 1/3 octave band and for the A-weighted sound level for each approximately 4-hour tape for two conditions. The first condition included all sounds, and the second condition included only natural sounds, based on the source-identification logs.

F.2 Separation of Sites into different Vegetation Zones

The measurement sites were separated into the same classifications of Vegetation Zones as were identified for the earlier EA (see Footnote 37, page 49). These included Desert Scrub, Pinyon Juniper Woodland, and Sparse Coniferous Forest. Although water sites had been identified in the prior studies, none of the sites in the September 1999 measurement program had significant influence from river sounds. The site classifications were as follows:

Table 37. Assignment of Audibility Sites to Vegetation Zones

Vegetation Zone	Audibility Site
Desert Scrub	1A, 2A, 2D, 3A, 3B, 3D, 4A, 7A, 7C, 9A, 9C, 9D*
Pinyon Juniper Woodland	8A, 8D
Sparse Coniferous Forest	5A, 5B

*Note that these assignments are based not only on the zones used in the EA, but also on observations during measurements and discussions with NPS staff. These observations caused some sites (2A, 2D, 3A, 3B, 9C) to be reclassified for this ambient determination from the EA categories of Water / Rapids to desert scrub.

Site 6 was not used for ambient characterization, since road traffic noise was audible almost all of the time.

F.3 Instrument Noise Floor

Two different types of sound measurement instrumentation were used at the measurement sites. One was a system using a standard microphone and having a noise floor of approximately 20 dBA. This system was used at Sites 3, 4, and 7. The other type of system used a “low-noise” microphone system, had a noise floor of approximately 0 dBA, and was used at Sites 1, 2, 5, 8 and 9. Initially, the data from both

measurement systems were assembled together for the Desert Scrub vegetation zone. However, upon inspection, it became clear that the L_{50} and L_{90} natural sound levels for the frequency bands above about 400 Hz data were higher when collected with the standard instrumentation than those metrics from the low-noise system. It was thought preferable to exclude these standard system data rather than adjust them for their instrument noise floors and, because there was no noticeable difference in the standard and low-noise system sound levels at the frequencies below about 400 Hz, it was concluded that the low-noise data from Sites 1, 2 and 9 adequately represented the Desert Scrub environment.

F.4 Measured Natural Ambient in Vegetation Zones

Figure 84, page 203, presents all of the L_{50} spectra of natural sounds only from the 11 four-hour tapes obtained in the desert scrub environment, at Sites 1A, 2A, 2D, 9A, 9C, and 9D. Note that the range of sound levels at most frequencies is only 10 to 15 dB from the quietest to the loudest periods. Also, the sound levels are very low. For example in the 500 Hz 1/3-octave band, the 4-hour L_{50} s range from about 7 to 19 dB over all sites.

Figure 85, page 204, presents the four L_{50} spectra of natural sounds obtained from the four-hour tapes at the two sites in pinyon juniper woodland (PJW), 8A and 8D. Note that three of the spectra are nearly identical, while the other is significantly higher. Site logs show that the measurement period at 8A on the first afternoon (designated 8A pm1) had significant wind, while during the other three measurement periods winds were calm or very light.

Figure 86 presents the six L_{50} spectra of natural sounds collected at the two sites in the sparse coniferous forest (SCF) environment, 5A and 5B. Here as well, the three lowest spectra are very similar, and the other three L_{50} spectra are significantly higher. As with the PJW sites, windy conditions caused the ambient levels to increase.

The type effect of wind evident in Figure 85 or Figure 86 does not appear in any of the Figure 84 data. Since some of the Figure 84 data (notably 9A pm1) were collected during a range of wind conditions similar to those present for the Figure 85 and Figure 86 data, it is evident how little wind affects ambient levels in the desert scrub (DS) environment, as compared with the forested areas. This result may be due to the fact that wind speeds are generally lowest at ground level, and what vegetation exists in desert scrub areas is primarily close to the ground.

F.5 Average Spectra by Vegetation Zone and Windiness

Figure 87 shows L_{50} spectra that are the arithmetic averages of the spectrum values shown in Figure 84 through Figure 86 separately for each vegetation zone. In the PJW and SCF environments, only the data for the time periods where the wind was calm or light are included. Note that the average spectra for the different environments are quite similar, if winds are calm or not able to generate much noise. The A-weighted sound level computed from each spectrum is shown at the right on the figure, and ranges from 16.7 to 20.4 dBA.

Figure 88 presents the same averaged spectra as does Figure 87, but for the L_{90} s rather than for the L_{50} s. The trends are very similar to those in Figure 87 except levels are about 5 dB lower. Calm conditions in the SCF environment generated the lowest levels, where L_{90} s are less than 0 dB at frequencies above 500 Hz. The average A-weighted L_{90} spectra range from 12.8 to 16.8 dBA.

Figure 89 presents the average spectra for the four site-periods affected by wind. These include data from both the PJW and SCF environments. The averages of both L_{50} and L_{90} values are shown in Figure 89.

Note the broad peak centered around 500 Hz, characteristic of wind in conifer trees. The average A-weighted L_{50} is 30.2 dBA, and the L_{90} is 24.3 dBA.

F.6 Effect of Auditory System Noise on Audibility

Where the background sound levels are so low as to be below the threshold of hearing, the audibility of a signal or event is predicated upon the threshold of human hearing rather than the masking of the background sound. A model for detectability of a signal in low noise environments must account for both the hearing threshold and the background sound level to determine an effective threshold for signal detection. An appropriate method of accounting for both of these factors is to use the energy sum of the human “auditory system noise” and the background level in 1/3-octave bands. Appendix C.3.4 presents a technical discussion of this approach. An example of such addition is shown in Figure 90. Note that both the background and auditory system noise contribute to the overall threshold of detection in the low and mid frequencies from 80 Hz to 1000 Hz. For signals above 1000 Hz, the auditory system noise controls the audibility with the Desert Scrub average L_{50} as the background sound level.

F.7 Average Measured Data with Auditory System Noise Added

Figure 91 presents the average L_{50} spectra with auditory system noise (ASN) added, to show spectra representing the effective thresholds for signal detection in the different environments. Note that with ASN added, the spectra for the three different vegetation zones without wind influence are very similar, within about 3 dB of each other throughout the frequency range. Only the average for the wind-affected sites is significantly different. A-levels are not shown because they have little meaning in the context of signal detection.

Figure 92 presents the same information as Figure 91, except it shows the average L_{90} spectra instead of L_{50} . For average L_{90} s, the vegetation zones not affected by wind are within about 2 dB of each other. The wind-affected average at the middle frequencies is up to about 8 dB higher than the averages not affected by wind.

Because of the similarity of the sound levels for the vegetation zones not affected by wind, they have been combined into an arithmetic average of all site-measurement periods where wind did not affect the sound levels materially. Table 38 below presents the overall average values recommended for characterizing the effective threshold for audibility of aircraft in the Grand Canyon. There are four spectra, L_{50} and L_{90} for wind-affected and not wind-affected sites.

Table 38. Average Grand Canyon Measured Spectral Sound Levels Recommended for Use in Modeling Natural Ambient Levels at Non-water Affected Sites

One-Third Octave Band Center Frequency (Hz)	Auditory System Noise (dB)	Average Measured Sound Levels with Auditory System Noise Added (dB)			
		Wind-Affected Sites		Sites not Affected by Wind	
		L50	L90	L50	L90
50	39.0	39.4	39.1	39.3	39.1
63	33.7	34.7	34.1	34.4	33.9
80	28.8	30.7	29.5	30.6	29.4
100	25.1	27.9	26.2	27.7	26.0
125	21.7	25.0	23.0	24.6	22.8
160	18.5	22.8	20.4	21.6	19.8
200	16.2	22.3	19.3	19.5	17.7
250	14.3	22.7	19.1	17.7	15.8
315	12.8	23.5	19.2	15.9	14.2
400	11.7	24.2	19.6	14.9	13.2
500	11.0	24.6	19.5	14.0	12.4
630	10.5	24.2	18.4	13.1	11.6
800	10.4	23.1	17.0	12.6	11.4
1000	10.7	21.4	15.4	12.4	11.5
1250	10.6	18.3	13.4	11.8	11.2
1600	9.7	15.2	11.4	10.6	10.1
2000	8.4	12.3	9.5	9.0	8.7
2500	6.5	9.8	7.5	7.0	6.7
3150	6.5	8.6	7.1	6.8	6.6
4000	4.2	6.2	4.8	4.6	4.4
5000	7.1	7.7	7.3	7.2	7.2

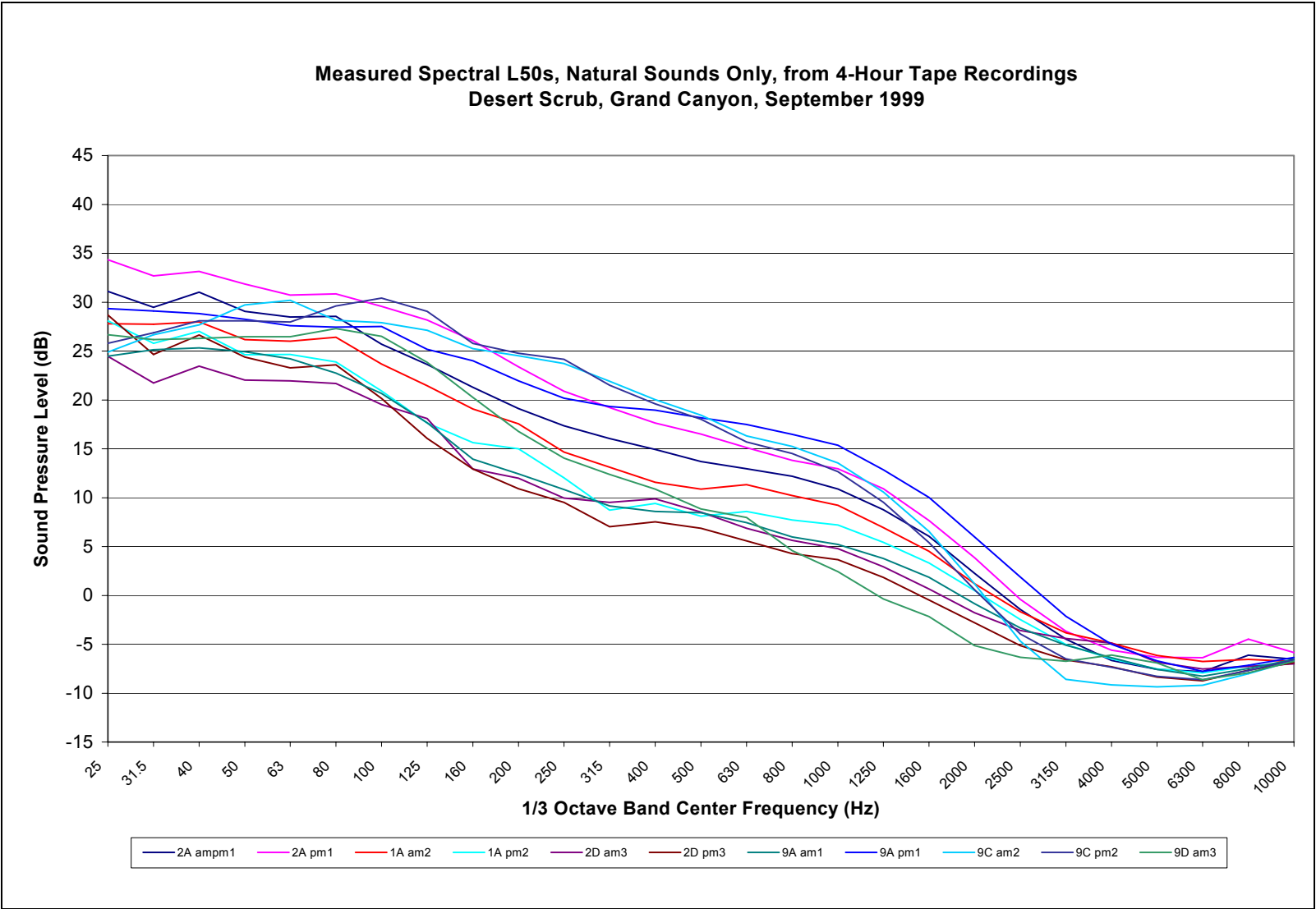


Figure 84. Desert Scrub Spectral L50's

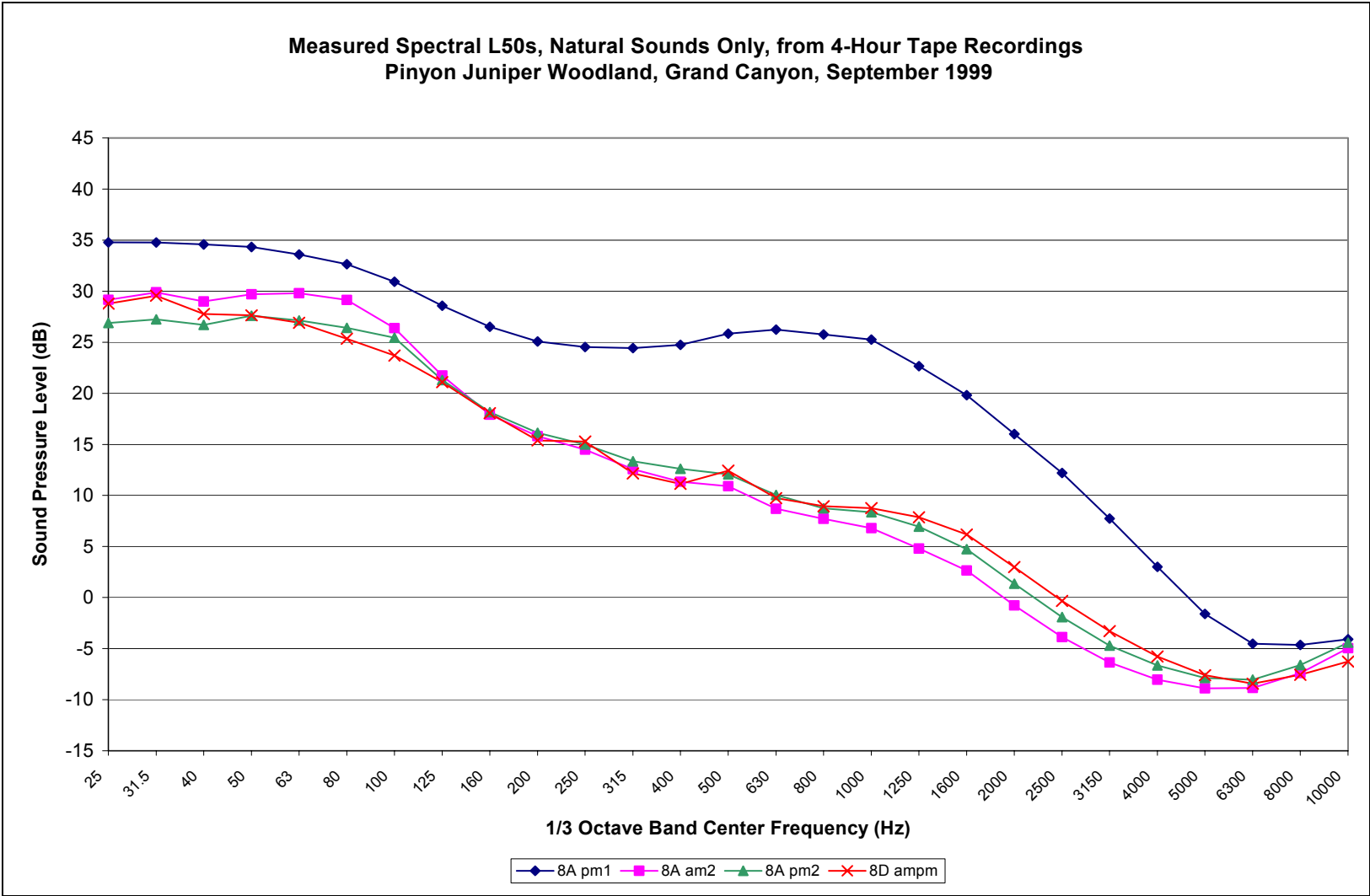


Figure 85. Pinyon Juniper Woodland Spectral L50's

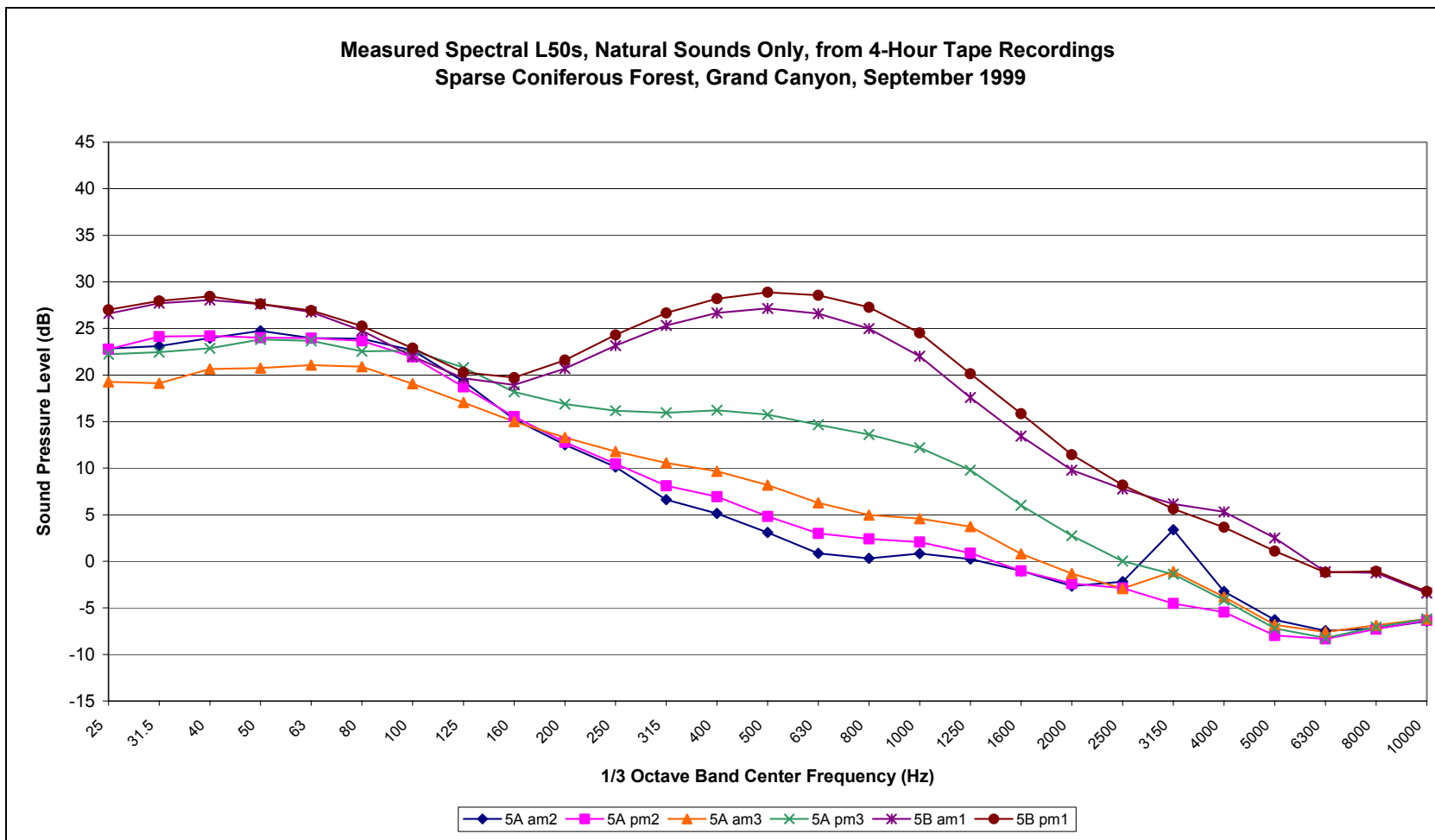


Figure 86. Sparse Coniferous Forest Spectral L50's

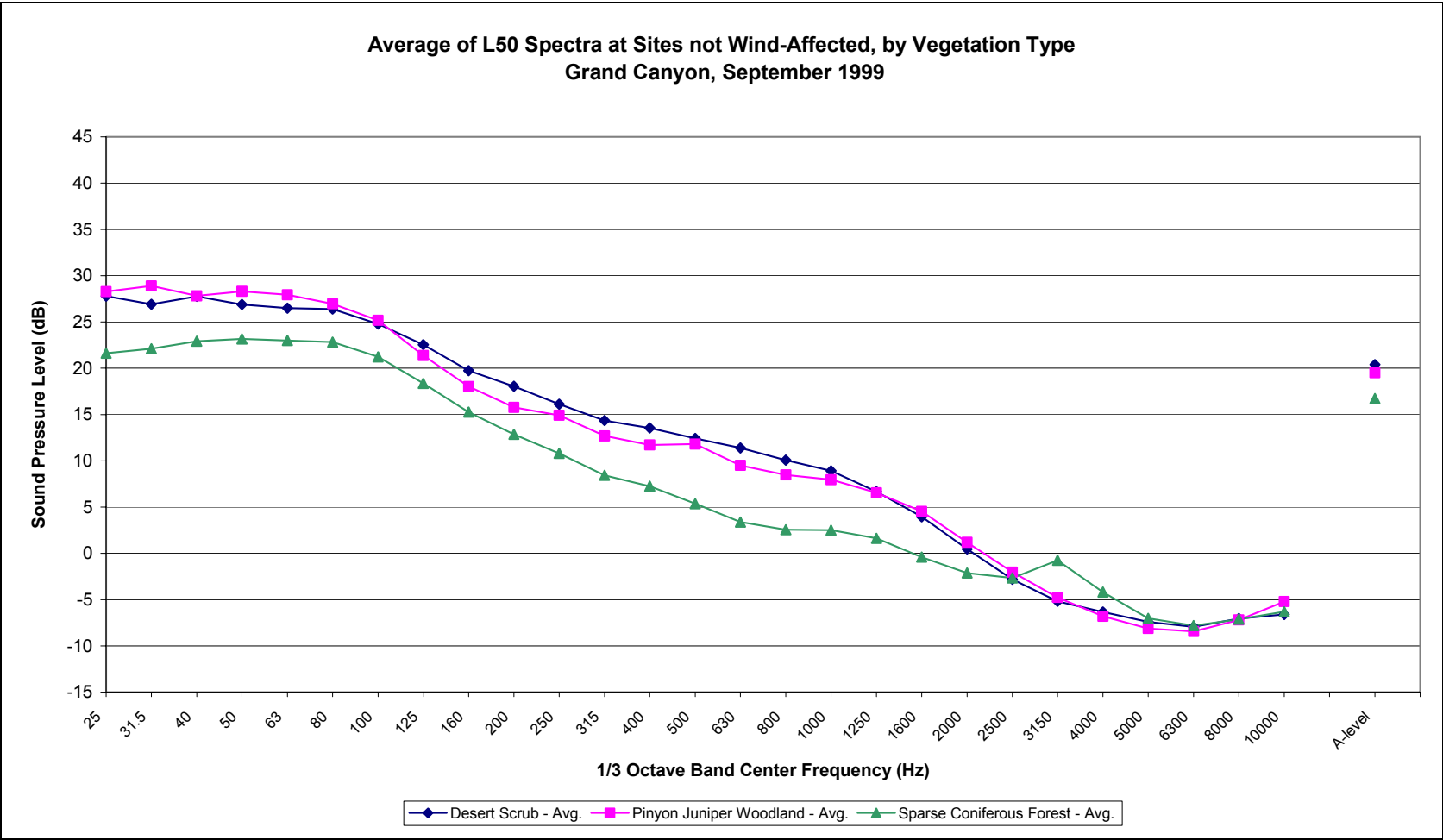


Figure 87. Average L50 Spectra, Sites Not Wind Affected

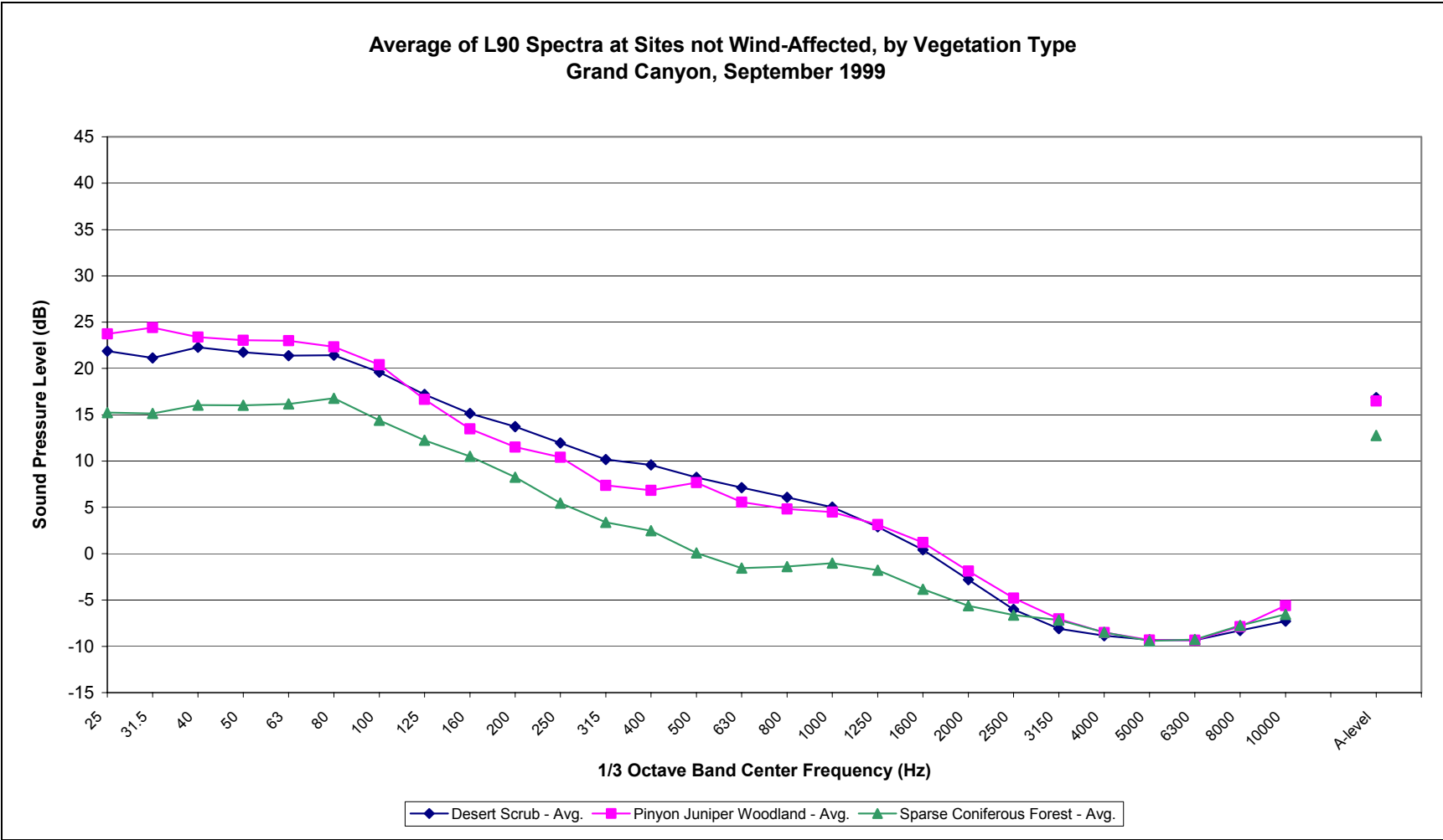


Figure 88. Average L90 Spectra, Sites Not Wind Affected

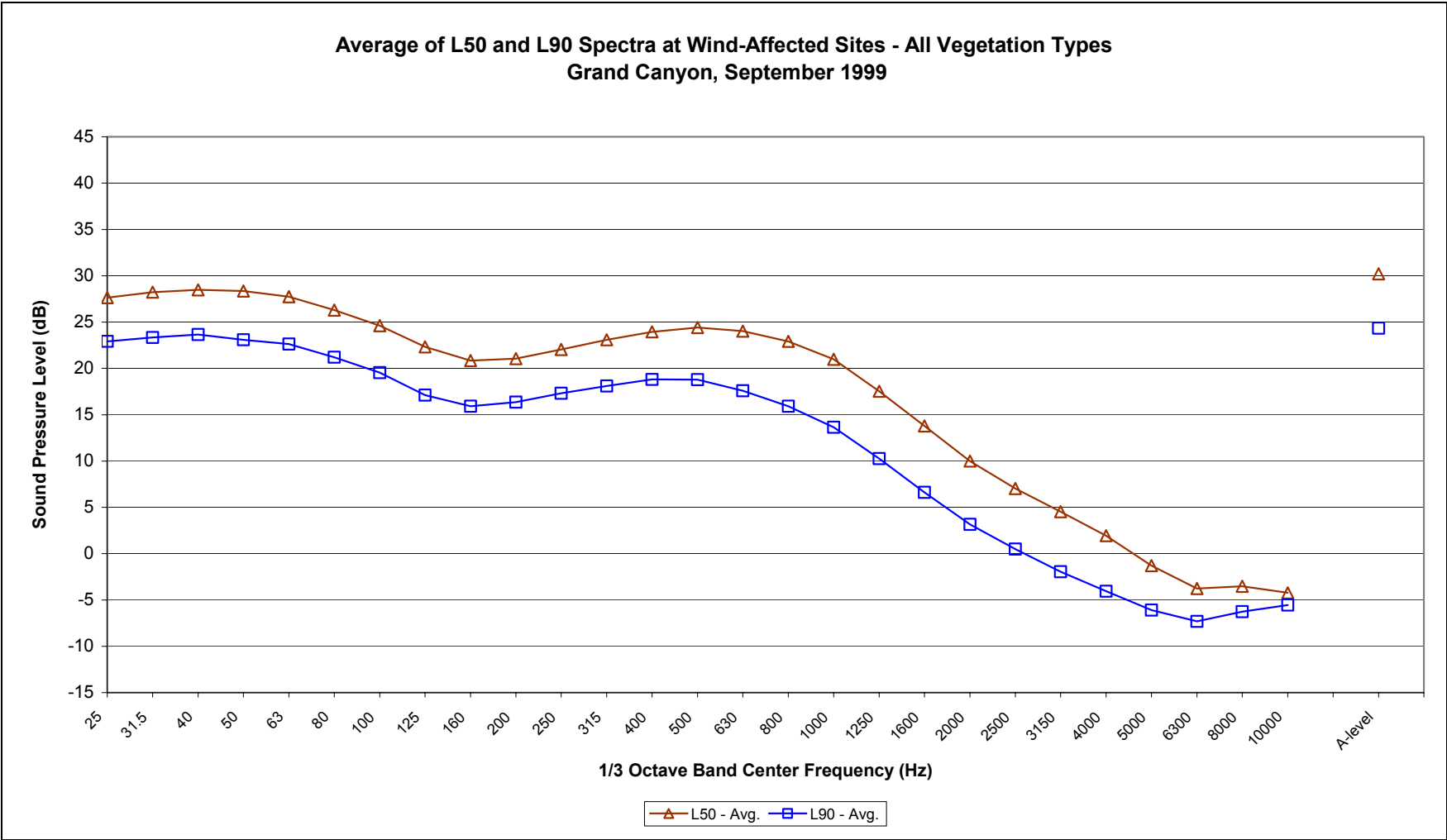


Figure 89, Average L50 and L90 Spectra at Wind Affected Sites

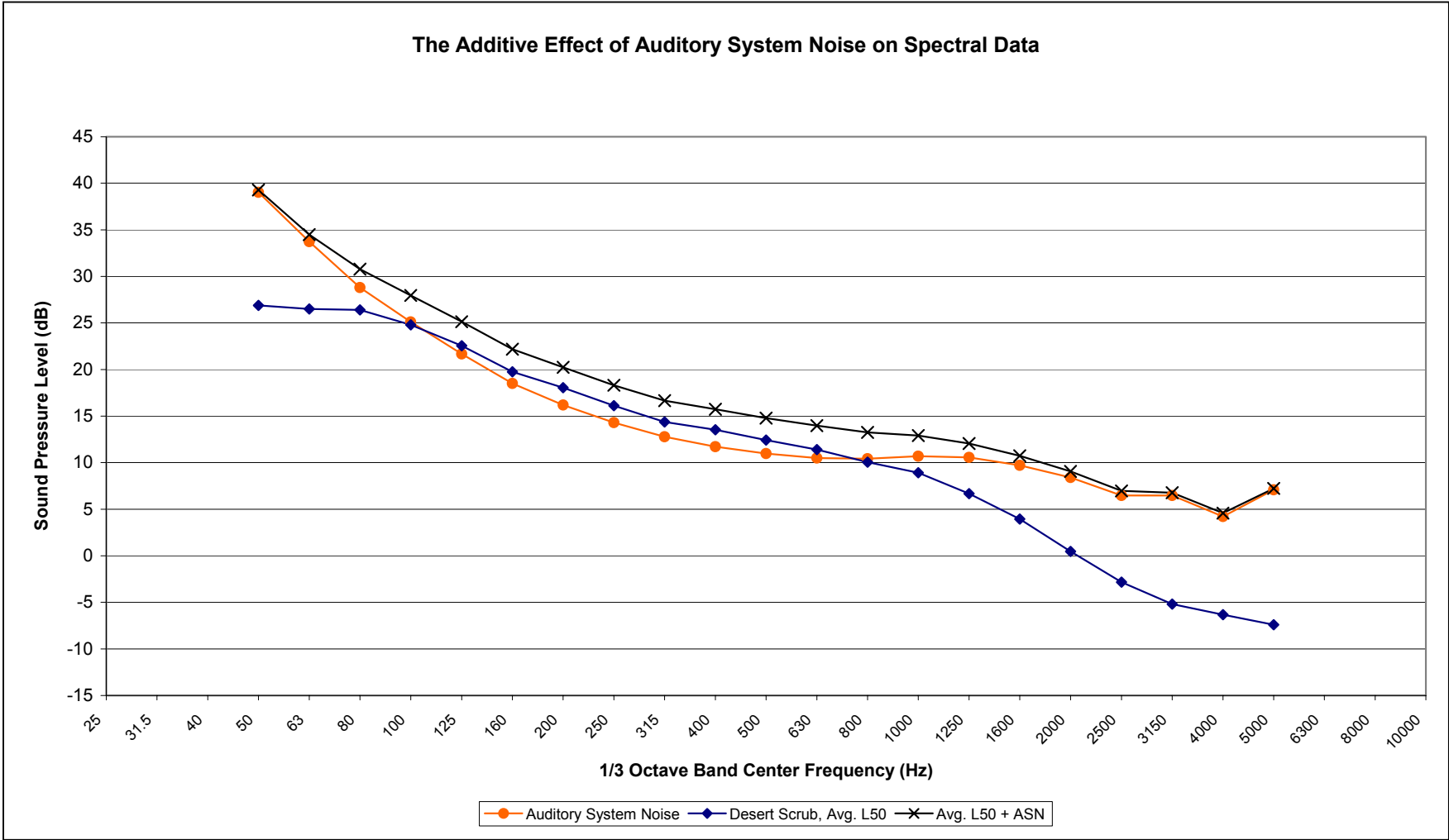


Figure 90. Additive Effect of Auditory System Noise

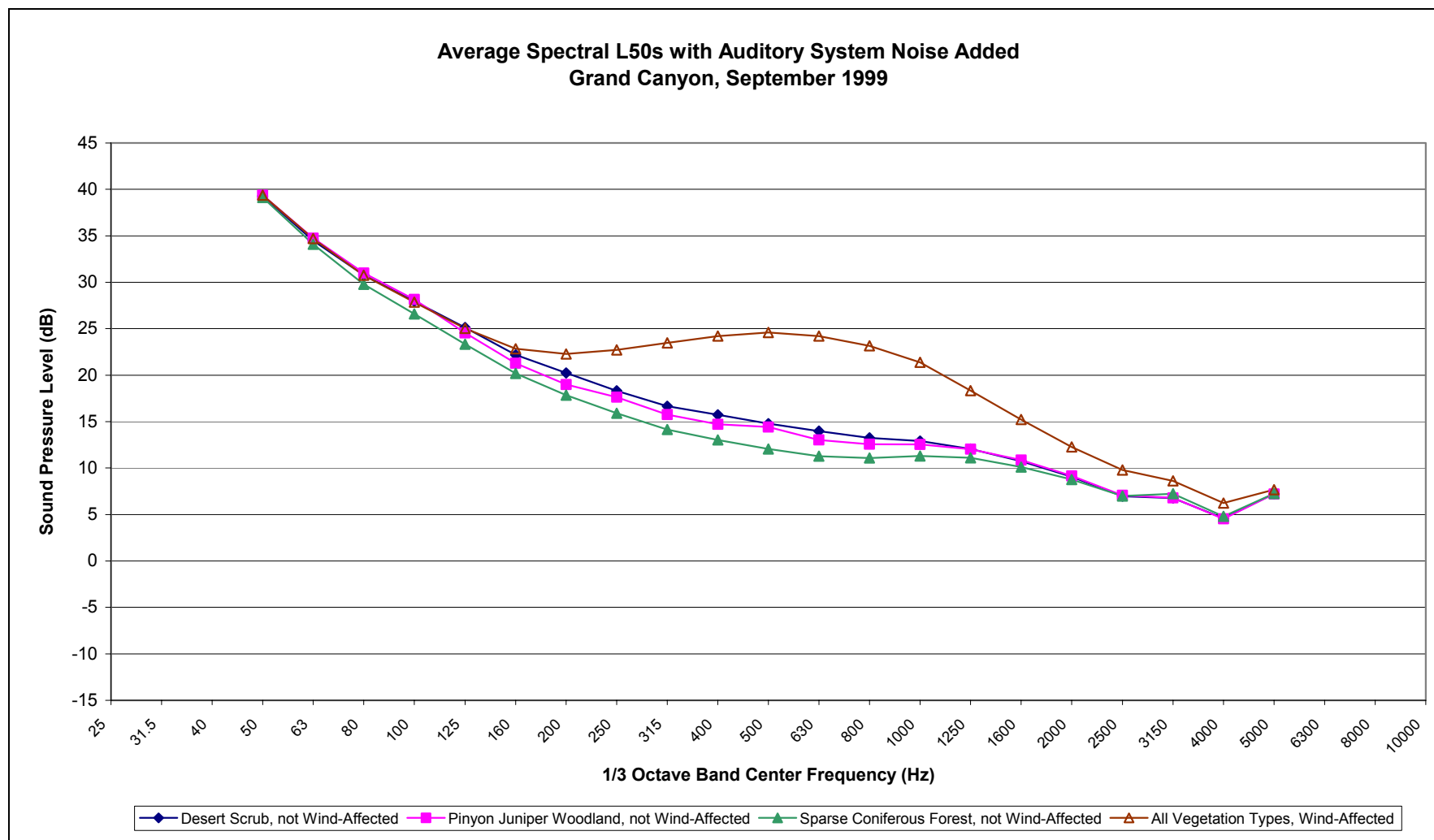


Figure 91. Average L50;s with Auditory System Noise Added

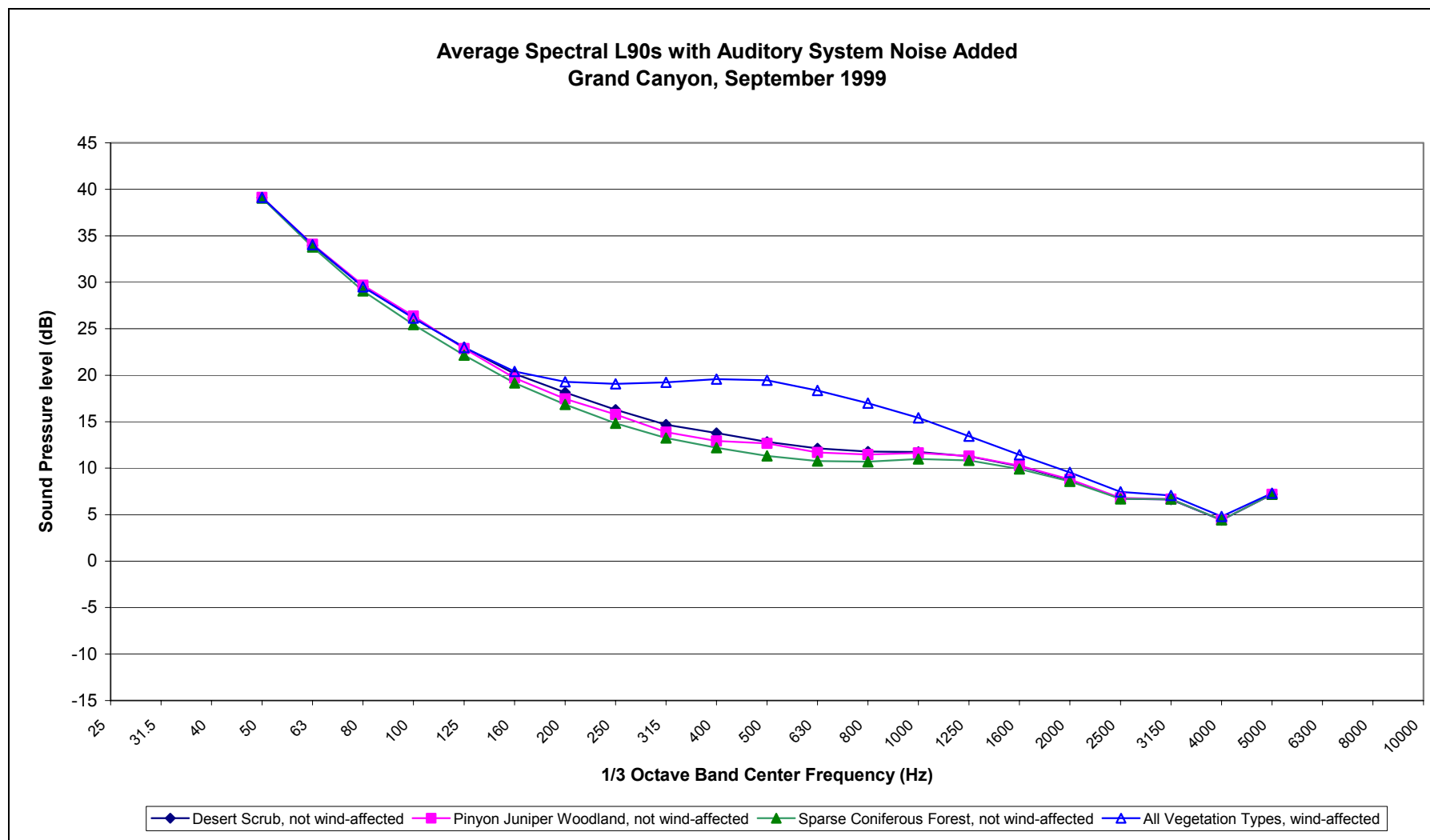


Figure 92. Average Spectral L90s with Auditory System Noise Added

Page Intentionally Blank

APPENDIX G. MEMORANDUM PROVIDING MODELING INPUTS

The following information was provided to document the inputs used by all models. Omitted from this appendix are Figure 1 which depicts the corridor flight tracks (see Figure 22, page 54 of the main report), the referenced 3-½ inch floppy, and the printouts of the comma delimited files on that floppy that provided the data in machine-readable form to the models. Some terminology has been changed to be consistent with the main body of the report. Figure and table numbering is consistent with the original memorandum, rather than with this overall report.

MEMORANDUM

To: Gregg Fleming (Volpe National Transportation Systems Center)
Ken Plotkin (Wyle Laboratories)
Dan Spotskey (National Park Service)
From: Dick Horonjeff
Date: 12 September 2000
Subject: Transmittal of Modeling Data, Grand Canyon Model Validation Study

References: 1) A Reference Source Data for GCNP Noise Model Validation Study, @ DTS-34_FA065-LR2, May 2000.
(2) GC_REF.XLS, 5/30/00, 8:05am
(3) HMMH Job No. 295860.14

Acknowledgments

Many people and organizations contributed to the production of this document. Special thanks go out to Dan Spotskey, Tracey Felger and Mike Ebersole at the National Park Service, to Gregg Fleming and Dave Senzig at Volpe, and to Ken Plotkin at Wyle Laboratories. Their steadfast attention to detail has resulted in a quality product.

1. Objective

This memorandum transmits data needed by the various parties to complete the first round of modeling for the Grand Canyon model validation study. Accompanying this memo is a 3-1/2 inch floppy disk containing the data in machine-readable (IBM-PC) form.

Figure 1 provides an overview of the measurement sites and tour aircraft flight tracks. Sites 9A, 9B, 9D and 9E lie outside the graphic's upper right-hand corner and are not shown.

When geographic locations are provided they are reported in two coordinate systems,

- X-Y coordinates in meters using the Universal Transverse Mercator (UTM) Zone 12, NAD 1927 datum,
- Longitude and Latitude in decimal degrees using the NAD 1983 datum.

All of the data sets described in the following subsections are included on an accompanying floppy disk as comma-separated text files. The first line of these files identifies the data contained therein. At the end of this line "[1]" appears. This is the file version number. It will be incremented in the event that any of these files need to be reissued.

Commas separate both numeric and alpha fields. Since no alpha fields contain commas, quotation marks are not used to enclose the text.

Six aircraft types are to be modeled. They are identified in Table 1.

Table 1. Modeled Aircraft Types

Abbreviation	Aircraft Type
AS350	Aerostar 350
B206B	Bell 206B
B206L	Bell 206 Long Ranger
C182	Cessna 182 Skylane
C207	Cessna 207
DHC6 (Vistaliner)	DeHaviland Twin Otter *

- Note: Vistaliner equipped with McCauley Quiet Propeller

[Figure 1 follows in original memorandum.]

2. Flight Tracks

Two 3-dimensional flight tracks have been carefully prepared, one for fixed-wing aircraft, and one for rotary-wing. Although the tracks closely parallel one another, there are important differences between them in both lateral separation and altitude profiles. They are included as comma-delimited text files (TRAK_FW1.CSV and TRAK_RW1.CSV, for fixed and rotary wing respectively) on the accompanying floppy disk. Each file contains a series of coordinates that define the end points of concatenated straight-line segments. A listing of both files is attached at the end of this memo. The file format is described below:

- Line 1 is a text description of the file contents.
- Line 2 provides the number of coordinate points (N) in the file.
- Line 3 identifies the data fields in the file.
- Line 4 identifies the units for each data field.
- Succeeding Lines tabulate the coordinates of each point.

Field 1 contains a sequential coordinate number beginning with "1" and ending with N.
Fields 2 & 3 contain integer X (Easting) and Y (Northing) coordinates in meters (Universal Transverse Mercator, UTM, NAD 1927).

Fields 4 & 5 contain the Longitude and Latitude in decimal degrees, re: North American Datum (NAD) 1983. Six decimal places provide resolution to the nearest foot.

Field 6 contains the aircraft altitude in feet, re: Mean Sea Level (MSL)

The tracks start near (but not at) the Grand Canyon Airport in Tusayan, initially heading in a northeasterly direction. They then turn north and proceed past the source site on the South Rim (the coordinates of the source site are provided in Table 2). The tracks head north through the Zuni Point Corridor up to the North Rim, proceed westerly across the North Rim, and eventually turn south through the Dragon Corridor.

Table 2. Source Site Coordinates

UTM Easting (meters) NAD 27	UTM Northing (meters) NAD 27	West Longitude (degrees) NAD 83	North Latitude (degrees) NAD 83	Elevation above Mean Sea Level (feet)
420,533	3,986,733	111.88266	36.02366	7,360

3. Traffic Counts

Aircraft audibility calculations will be performed by the models for one-hour periods on the 3 days of data collection at the Grand Canyon. The dates were:

Friday, 10 September 1999
Sunday, 12 September 1999
Monday, 13 September 1999

Inclement weather precluded data collection on Saturday, 11 September. There were 8 nominal 1-hour periods of data collection each day:

Morning	Afternoon
08:00 - 09:00	13:00 - 14:00
09:00 - 10:00	14:00 - 15:00
10:00 - 11:00	15:00 - 16:00
11:00 - 12:00	16:00 - 17:00

Throughout these periods Volpe personnel maintained a detailed aircraft activity log of all tour aircraft transiting the Zuni Point Corridor as they passed northbound over the source site on the south rim. The log identified the date, time, and aircraft type of each flight. That data is tabulated in the comma-delimited text file (AC_LOG1.CSV) on the accompanying floppy disk. A listing of the file is attached at the end of this memo. The file format is described below:

- Line 1 is a text description of the file contents.
- Line 2 provides the number of flights (193) in the file.
- Line 3 identifies the data fields in the file.
- Line 4 identifies the units for each data field.
- Succeeding Lines tabulate the individual aircraft passbys.
 - Field 1 contains a sequence number beginning with 1 for the first record and ending with 193 for the last.
 - Fields 2, 3 & 4 contain the date in month, day, and year, respectively.
 - Fields 5, 6 & 7 contain the time in hours, minutes and seconds.
 - Field 8 contains the aircraft type (one of the six shown in Table 1).

The above aircraft activity log was distilled down into hourly traffic counts for the above dates and time periods. These hourly traffic counts are reported in Table 3. They are also tabulated in a comma-delimited text file (TRAFcnt1.CSV) on the accompanying floppy disk. A listing of that file is attached at the end of this memo. The file format is described below:

- Line 1 is a text description of the file contents.
- Line 2 provides the number of 1-hour periods (24) in the file.
- Line 3 identifies the data fields in the file.
- Line 4 identifies the units for each data field.
- Succeeding Lines tabulate the hourly traffic counts by aircraft type.
 - Field 1 contains the date in MM/DD/YY format.
 - Fields 2 & 3 contain the beginning and ending times for the period in HH:MM format.
 - Fields 4 thru 9 contain the traffic counts for each of the aircraft types identified in the third line of the file.

Field 10 contains the sum of the individual aircraft counts. This number should always equal the arithmetic sum of the individual aircraft.

Table 3. Hourly Traffic counts by Aircraft Type

Date	Time	Rotary-Wing			Fixed-Wing			Total
		AS350	B206B	B206L	C182	C207	DHC6	
10-Sept	08:00 - 09:00	0	0	3	0	3	0	6
	09:00 - 10:00	0	0	2	1	6	0	9
	10:00 - 11:00	0	0	6	0	1	2	9
	11:00 - 12:00	1	0	3	0	4	3	11
	13:00 - 14:00	1	0	5	0	0	1	7
	14:00 - 15:00	2	0	2	0	2	2	8
	15:00 - 16:00	1	0	2	0	2	3	8
	16:00 - 17:00	0	0	3	0	1	3	7
12-Sept	08:00 - 09:00	1	0	6	1	1	1	10
	09:00 - 10:00	3	0	4	0	5	2	14
	10:00 - 11:00	1	0	2	0	3	2	8
	11:00 - 12:00	2	0	6	0	3	2	13
	13:00 - 14:00	1	0	1	0	1	1	4
	14:00 - 15:00	1	2	2	0	4	1	10
	15:00 - 16:00	0	1	1	0	0	0	2
	16:00 - 17:00	0	0	0	0	4	2	6
13-Sept	08:00 - 09:00	1	1	1	1	3	2	9
	09:00 - 10:00	3	3	1	0	4	3	14
	10:00 - 11:00	1	0	4	0	0	2	7
	11:00 - 12:00	2	1	3	0	4	1	11
	13:00 - 14:00	1	1	1	0	1	0	4
	14:00 - 15:00	0	1	0	1	2	1	5
	15:00 - 16:00	0	0	2	0	0	2	4
	16:00 - 17:00	0	2	1	0	1	2	6

4. Audibility Logging Site Locations.

Audibility logging took place at 39 different locations over the 3-day data acquisition period. Logging teams were deployed to 9 different geographic areas around the canyon, and several locations were selected within each area as listening sites. The sites were identified by a single digit number (1-9) for the general geographic area followed by a single letter (A, B, C, etc.) to denote the position within that area. The sites and their coordinates are tabulated in Table 4. The table identifies the X (Easting) and Y (Northing) coordinates in UTM meters (NAD 1927, Zone 12), the Longitude and Latitude in decimal degrees (NAD 1983) where the five decimal places provide resolution to the nearest meter, and the elevation above mean sea level in feet.

Latitudes and longitudes were determined in the field using Global Position System (GPS) receivers. The Selective Availability (SA) option of the GPS system was still in force during the data acquisition period so positional accuracies of better than + or - 150 feet were not expected from the GPS readings. While this accuracy provides better than needed precision for modeling distance relationships between listening sites and aircraft flight trajectories, it may not be sufficient for correctly positioning the site with respect to local, rapidly changing topographic features that might affect the models= acoustic shielding calculations.

To fine tune the GPS-determined positions, each reading was located on a United States Geological Survey (USGS) topographic map and submitted to the personnel staffing the sites for their interpretation. If, for example, a GPS-determined location showed the site as being slightly over the rim of the canyon, but the observer was in fact slightly back from the rim, the GPS-determined position was adjusted accordingly based on topographic features of the map and the verbally-reported position of the observer. The data presented in Table 4 include any such adjustments. The positions in longitude and latitude were then converted to UTM coordinates using the US Army Corps of Engineers= CORPSCON Version 5.11 coordinate transformation software.

Elevations reported in Table 4 were read from USGS topographic maps by visually interpolating between the 40-foot contour intervals. As a quality control precaution, please check the elevations reported by your digital elevation models against these figures and report discrepancies of more than 20 feet to HMMH before proceeding with the acoustic modeling.

The data in Table 4 are included in SITELOC1.CSV on the accompanying floppy disk. A listing of the file is attached at the end of this memo. The file format is as follows:

- Line 1 is a text description of the file contents.
- Line 2 provides the number of sites (39) in the file.
- Line 3 identifies the data fields in the file.
- Line 4 identifies the units for each data field.
- Succeeding Lines tabulate the coordinates of each site.
 - Field 1 contains the 2-character site designator (e.g. A1A@).
 - Fields 2 & 3 contain integer X (Easting) and Y (Northing) coordinates in UTM meters.
 - Fields 4 & 5 contain the Longitude and Latitude in decimal degrees, re: North American Datum (NAD) 1983. Five decimal places provide resolution to the nearest meter.
 - Field 6 contains the site elevation in feet, re: Mean Sea Level (MSL)

Table 4. Audibility Logging Site Coordinates

Site	UTM Easting (meters) NAD 27	UTM Northing (meters) NAD 27	Longitude (degrees) NAD 83	Latitude (degrees) NAD 83	Elevation (feet MSL)
1A	403,461	3,994,482	112.07306	36.09196	3680
1B	403,305	3,993,908	112.07472	36.08677	3640
2A	405,478	3,993,533	112.05055	36.08361	3810
2B	406,056	3,992,609	112.04402	36.07533	3660
2C	406,121	3,993,025	112.04334	36.07909	3750
2D	405,860	3,993,351	112.04628	36.08200	3720
3A	409,266	3,990,315	112.00811	36.05496	3650
3B	409,229	3,989,784	112.00846	36.05017	3560
3D	408,585	3,989,371	112.01556	36.04639	3580
3H	408,933	3,990,248	112.01180	36.05432	4110
3J	408,989	3,990,051	112.01115	36.05255	4010
3K	408,503	3,989,330	112.01647	36.04601	3630
4A	412,543	3,987,394	111.97141	36.02893	4870
4B	412,611	3,987,859	111.97070	36.03313	4890
4C	411,730	3,987,293	111.98042	36.02794	4900
4D	412,120	3,986,368	111.97598	36.01964	4820
4E	412,035	3,985,992	111.97689	36.01624	5140
5A	418,184	4,000,364	111.91015	36.14634	7960
5B	417,102	4,001,271	111.92227	36.15443	8040
6A	423,217	3,985,705	111.85278	36.01460	7210
6C	423,670	3,986,022	111.84778	36.01750	7240
6D	423,994	3,986,498	111.84423	36.02181	7290
7A	425,378	3,992,466	111.82944	36.07572	4270
7B	424,998	3,991,199	111.83354	36.06427	5570
7C	424,564	3,990,242	111.83826	36.05561	5530

Site	UTM Easting (meters) NAD 27	UTM Northing (meters) NAD 27	Longitude (degrees) NAD 83	Latitude (degrees) NAD 83	Elevation (feet MSL)
7E	425,438	3,993,249	111.82885	36.08279	3970
7G	424,977	3,991,407	111.83379	36.06615	5370
7H	424,814	3,991,399	111.83560	36.06606	5620
8A	430,435	3,990,033	111.77306	36.05417	7010
8B	427,442	3,989,297	111.80622	36.04731	6760
8C	427,504	3,988,609	111.80547	36.04111	7010
8D	426,923	3,990,308	111.81208	36.05639	6940
8E	427,033	3,990,326	111.81086	36.05656	6940
9A	442,595	4,025,625	111.64067	36.37583	6060
9B	437,893	4,022,348	111.69283	36.34600	6060
9C	425,875	4,014,475	111.82600	36.27417	6010
9D	438,144	4,021,995	111.69000	36.34283	6060
9E	438,085	4,022,106	111.69067	36.34383	6060
9F	425,875	4,014,475	111.82600	36.27417	6010

5. Aircraft Sound Levels

Aircraft sound level measurements performed by Volpe during the September 1999 measurement period will form the basis for aircraft source level model input. A detailed investigation of the one-third octave band sound level analyses of these data revealed a spectral dependence on the aircraft's elevation angle above the horizon. A joint decision was made by Volpe, Wyle Laboratories, and HMMH to use the subset of these data that most closely matched the elevation angles at which tour aircraft were viewed from the observer locations.

Using the flight track trajectories reported in Section 2 and the observer locations reported in Section 4, the elevation angles of tour aircraft at their closest point of approach to the observer sites were determined. The results are shown in Table 5.

Table 5. Tour Aircraft Elevation Angles as Viewed From Observer Sites

Site	Distance to Track (feet)	Site Elev (feet)	Elevation Angle (deg)		Site	Distance to Track (feet)	Site Elev (feet)	Elevation Angle (deg)	
			Fixed-Wing	Rotary-Wing				Fixed-Wing	Rotary-Wing
1A	59,434	3680	4.2	3.7	6A	8,943	7210	5.0	1.9
1B	59,697	3640	4.2	3.7	6C	10,239	7240	4.2	1.5
2A	52,491	3810	4.6	4.0	6D	11,349	7290	3.6	1.1
2B	50,176	3660	4.9	4.4	7A	12,597	4270	16.5	14.4
2C	49,564	3750	4.9	4.3	7B	12,088	5570	11.4	9.1
2D	51,092	3720	4.8	4.2	7C	10,989	5530	12.7	10.2
3A	38,272	3650	6.5	5.7	7E	11,170	3970	19.8	17.5
3B	38,696	3560	6.5	5.8	7G	11,307	5370	13.1	10.7
3D	40,353	3580	6.3	5.5	7H	11,329	5620	11.9	9.4
3H	39,707	4110	5.6	4.9	8A	30,209	7010	1.9	0.9
3J	39,460	4010	5.8	5.1	8B	20,860	6760	3.4	2.0
3K	40,693	3630	6.1	5.4	8C	21,401	7010	2.6	1.3
4A	26,365	4870	6.8	5.7	8D	18,675	6940	3.2	1.7
4B	26,470	4890	6.7	5.6	8E	19,024	6940	3.2	1.7
4C	28,881	4900	6.1	5.1	9A	78,248	6930	0.8	0.4
4D	27,688	4820	6.6	5.5	9B	59,341	6920	1.0	0.6
4E	27,252	5140	6.0	4.9	9C	12,297	6910	5.1	2.7
5A	19,663	7960	0.1	-1.3	9D	59,341	6920	1.0	0.6
5B	24,334	8040	-0.1	-1.3	9E	59,341	6920	1.0	0.6
					9	12,	6910	5.1	2.7

The angles in Table 5 range from -1 to +20 degrees. Sites 5A and 5B on the North Rim were slightly higher in elevation than the tour aircraft; hence observers at those sites looked down on the aircraft at the closest point of approach. In contrast, only sites 7A through 7H exhibited viewing angles between +9 and +20 degrees. The remaining sites had viewing angles of 0 to +7 degrees.

Acoustic data acquired at the source site covered a broad range of elevation angles. A detailed analysis of these data revealed an elevation angle dependence on spectral content and A-weighted sound level. One cluster of the data was acquired at elevation angles of 12 degrees and below. In light of the information shown in Table 5, this subset was used in developing the data sets reported in the remainder of this section. The specific aircraft measurement event numbers that met the 12 degree criteria are reported in Table 6, below.

Table 6. Measured Aircraft Sound Level Event Numbers Forming Basis of Model Input

Aircraft Abbreviation	Event Numbers
AS350	E34, E59, E62, W62
B206B	C86
B206L	C7, C28, C54, C79, C85, W28, W54, W79
C182	C9, C72, E9
C207	E10, E46, C45, C97
DHC6	E26, E44, E60

Note: C = Center Microphone, E = East Microphone, W = West Microphone

5.1 NODSS Spectral Data

NODSS requires a one-third-octave band spectrum for each aircraft at a reference distance of 1,000 feet. The required band center frequencies are 40 to 10,000 Hz, inclusive. Table 7 provides the one-third octave band sound pressure levels in decibels (dB), re: 20 microPascals (μPa). The tabled values are averages over a number of flights measured at the Grand Canyon on 10-13 September 1999. The measured data were adjusted from the measured closest point of approach distance to a reference distance of 1,000 feet and the average temperature and relative humidity conditions of the period (71 degrees Fahrenheit, 38 percent relative humidity).

These data are also provided in the file SNDSPCT1.CSV on the accompanying floppy disk. A listing of the file is attached at the end of this memo. The file format is as follows:

- Line 1 is a text description of the file contents.
- Line 2 provides the number of aircraft (6) in the file.
- Line 3 identifies the data fields in the file.
- Line 4 identifies the units for each data field.
- Succeeding Lines tabulate the one-third octave band sound levels.
 - Field 1 contains the aircraft designator (e.g. AAS350@).
 - Fields 2 thru 26 contain one-third octave band sound levels, in dB, for the 40 through 10,000 Hz bands, inclusive.

Table 7. Aircraft One-Third Octave Band Sound Levels for NODSS

1/3 OB Center Frequency (Hz)	Rotary-Wing			Fixed-Wing		
	AS350	B206B	B206L	C182	C207	DHC6
40	54.2	60.9	62.8	28.6	37.4	48.3
50	60.6	57.5	61.6	42.0	42.9	48.2
63	66.9	54.1	60.5	55.4	48.4	48.1
80	65.0	51.9	67.3	72.7	48.8	51.8
100	56.1	53.7	63.5	58.8	57.7	69.0
125	60.3	49.8	55.3	69.1	70.9	61.4
160	63.4	60.4	58.5	58.7	53.3	47.9
200	62.0	59.9	55.3	54.0	54.3	46.4
250	62.9	54.3	55.2	58.2	61.7	49.6
315	63.8	59.9	57.0	63.9	58.5	53.8
400	63.2	56.7	58.4	58.1	64.9	55.5
500	62.3	56.6	60.1	59.7	61.1	54.8
630	62.9	55.2	59.9	58.2	54.1	54.3
800	61.9	55.5	58.6	56.5	53.9	56.6
1,000	59.8	54.8	58.8	55.8	51.8	57.8
1,250	58.7	53.1	57.6	53.2	48.3	54.4
1,600	59.6	51.8	55.4	50.6	48.2	53.3
2,000	53.8	48.8	52.0	48.6	45.7	52.0
2,500	50.4	45.5	47.3	43.8	42.0	52.8
3,150	46.9	42.0	41.7	40.0	35.0	45.9
4,000	41.3	36.0	35.5	33.0	28.0	38.9
5,000	35.9	30.2	29.2	26.0	21.0	31.9
6,300	28.2	21.7	21.9	19.0	14.0	24.9
8,000	21.3	10.4	14.7	12.0	7.0	17.9
10,000	13.3	-4.7	7.7	5.0	-0.0	10.9

Note: Sound levels in decibels re: 20 μ Pa at 1,000-foot reference distance.

5.2 NMSIM Spectral Data

Spectral time histories provided to Wyle Laboratories by Volpe. Wyle will use original time history data to develop directivity patterns for the six aircraft types to be modeled. The data runs to be used are identified in Table 6, above.

5.3 INM Version 5.1 A-level Data

NPD curves were developed by Volpe using the one-third octave band spectral data acquired at the source site. Air absorption computations were performed using the average temperature and humidity conditions during the measurements, 71.4 degrees Fahrenheit and 38.1 percent relative humidity, respectively. For each aircraft type the sound exposure level (L_{AE}) and maximum A-weighted sound level (L_{ASmx}) were computed at ten distances ranging from 200 to 25,000 feet. These computed sound levels are listed in Table 8. They may also be found in file NPD_AL1.CSV on floppy disk. A listing of the file is attached at the end of this memo. The file format is as follows:

- Line 1 is a text description of the file contents.
 - Line 2 provides the number of aircraft (6) in the file.
 - Line 3 identifies the data fields in the file.
 - Line 4 identifies the units for each data field.
 - Succeeding Pairs of Lines tabulate the sound levels as a function of distance for each aircraft.
- The sound exposure levels (SEL) are on the first line, and the maximum A-weighted sound levels (Amax) are on the second.

Field 1 contains the aircraft designator (e.g. "AS350").

Field 2 identifies the metric tabulated in the remaining fields on the line (SEL or Amax).

Fields 3 thru 12 contain the sound levels, in dB, at closest point of approach slant distances of 200, 400, 630, 1000, 2000, 4000, 6300, 10000, 16000, and 25000 feet.

Table 8. Noise-Power-Distance Curves for Integrated Noise Model

Slant Dist (feet)	Rotary-Wing						Fixed-Wing					
	AS350		B206B		B206L		C182		C207		DHC6	
	L_{AE}	L_{ASmx}	L_{AE}	L_{ASmx}	L_{AE}	L_{ASmx}	L_{AE}	L_{ASmx}	L_{AE}	L_{ASmx}	L_{AE}	L_{ASmx}
200	85.2	85.1	82.5	78.8	81.5	82.1	78.7	80.7	76.8	80.0	79.4	79.9
400	81.8	78.7	79.1	72.4	78.1	75.7	75.4	74.4	73.6	73.8	75.8	73.3
630	79.4	74.4	76.7	68.0	75.7	71.3	73.1	70.1	71.4	69.6	73.3	68.8
1,000	76.8	69.7	74.1	63.4	73.0	66.7	70.7	65.7	69.0	65.2	70.4	63.9
2,000	72.3	62.3	69.6	55.9	68.5	59.1	66.6	58.6	65.1	58.3	65.4	55.9
4,000	66.9	53.9	64.3	47.6	62.9	50.5	61.8	50.8	60.6	50.8	59.4	46.9
6,300	62.7	47.7	60.2	41.5	58.4	44.1	58.2	45.2	57.1	45.3	54.8	40.3
10,000	57.8	40.8	55.5	34.7	53.2	36.8	54.0	39.0	52.9	39.1	49.6	33.1
16,000	52.1	33.0	49.9	27.1	47.3	28.9	49.2	32.1	47.9	32.0	44.1	25.5
25,000	45.8	24.8	43.8	19.1	41.5	21.1	44.1	25.2	42.3	24.5	38.5	18.0

Note: Sound levels in decibels re: 20 μ Pa. Reference speed = 160 knots.

6. Aircraft Speeds

Individual aircraft speeds were determined by Volpe by computing the elapsed flying time between the source site and passing abeam site 5A. Table 9 reports the Volpe findings by aircraft type. Speeds were reported by Volpe to the nearest whole knot. Translations to miles per hour and feet per second were carried to one decimal place to preserve computational equivalency of the numbers.

Due to the limited number of C182 flights during the measurement period, no speed observations were made for this aircraft. For modeling purposes the speed determined for the C207 will be used for the C182.

Table 9. Aircraft Speeds for Modeling

Aircraft Type	Number of Observations	Average Speed (knots)	Average Speed (mph)	Average Speed (feet/sec)
AS350	9	87	100.1	146.7
B206B	6	100	115.0	168.7
B206L	26	94	108.1	158.5
C182 *	0	115	132.3	194.0
C207	23	115	132.3	194.0
DHC6	19	104	119.6	175.4

* Note: C182 speed assumed to be the same as C207.

7. Sound Propagation Conditions

For the purposes of this investigation, the average temperature and relative humidity during the measurement period will be used to compute sound propagation variables such as the speed of sound and atmospheric absorption. The values are 71 degrees Fahrenheit and 38 percent relative humidity, respectively.

8. Ambient Sound Levels

For the first round of modeling, ambient sound levels at the observer sites will be assigned by the water-affected and vegetation zones identified in the document "Environmental Assessment of Special Flight Rules in the Vicinity of Grand Canyon National Park." The three vegetation zones are: 1)Desert Scrub (DS) 2) Sparse Coniferous Forest (SC) 3)Pinon / Juniper Forest (PJ).

The noise-generating mechanism is assumed to be wind interaction with the vegetation. The four water-affected zones vary in sound level depending on their proximity to the Colorado River.

8.1 Observer Site Water / Vegetation Zones

Table 9 lists the observer sites and assigned vegetation zones. Zone assignments were determined using a thematic mapping layer that is currently part of the NODSS database. Personnel who staffed each site were asked to confirm the assigned zone. The contents of Table 10 may be found on the accompanying floppy disk in the file AMB_ZON1.CSV. A listing of the file is attached at the end of this memo. The file format is as follows:

- Line 1 is a text description of the file contents.
- Line 2 provides the number of sites (39) in the file.
- Line 3 identifies the data fields in the file.
- Line 4 identifies the units for each data field.
- Succeeding Lines tabulate the site and ambient zone designator.
 - Field 1 contains the 2-character site designator (e.g. "1A").
 - Field 2 contains the ambient zone designator (DS = Desert Scrub, CF = Coniferous Forest, PJ = Pinon / Juniper, or one of four water/rapids-affected zones, WR1, WR2, WR3, or WR4).

Table 10. Observer Site Ambient Sound Level Zones

Site	Zone	Site	Zone	Site	Zone	Site	Zone
1A	DS	3J	WR3	6C	PJ	8C	PJ
1B	DS	3K	DS	6D	PJ	8D	PJ
2A	WR3	4A	DS	7A	DS	8E	PJ
2B	WR2	4B	DS	7B	PJ	9A	DS
2C	WR4	4C	PJ	7C	PJ	9B	DS
2D	WR4	4D	PJ	7E	DS	9C	WR1
3A	WR4	4E	PJ	7G	PJ	9D	DS
3B	WR2	5A	CF	7H	PJ	9E	DS
3D	DS	5B	CF	8A	PJ	9F	WR1
3H	WR3	6A	CF	8B	PJ		

Note: DS = Desert Scrub, CF = Coniferous Forest, PJ = Pinon / Juniper, WR = Water/Rapids.

8.2 Assumed Ambient Sound Levels by Water-Related and Vegetation Zone

Each water-related and vegetation zone has an assumed ambient one-third octave band spectrum and A-weighted sound level. These sound levels are tabulated in Table 11. The contents of Table 11 may be found on the accompanying floppy disk in the file AMB_SPC1.CSV. A listing of the file is attached at the end of this memo. The file format is as follows:

- Line 1 is a text description of the file contents.
- Line 2 provides the number of zones (7) in the file.
- Line 3 identifies the data fields in the file.
- Line 4 identifies the units for each data field.
- Succeeding Lines tabulate the one-third octave band sound levels and the A-weighted sound level for each zone.

Field 1 contains the zone designator (e.g. "DS").

Fields 2 thru 26 contain one-third octave band sound levels, in dB, for the 40 through 10,000Hz bands, inclusive.

Field 27 contains the A-weighted sound level in dB.

Table 11. Ambient One-Third Octave Band Sound Levels by Zone

1/3 OB Center Frequency (Hz)	Water / Vegetation Zone						
	Desert Scrub	Sparse Conifer	Pinon / Juniper	Water/ Rapids 1	Water/ Rapids 2	Water/ Rapids 3	Water/ Rapids 4
40	25.8	34.8	20.6	29.6	32.3	34.6	39.5
50	26.8	35.4	22.4	27.6	30.3	32.6	37.5
63	27.1	34.7	22.9	23.6	26.3	28.6	33.5
80	26.6	33.9	21.7	22.6	25.3	27.6	32.5
100	23.7	31.2	19.9	23.6	26.3	28.6	33.5
125	23.7	29.2	18.7	24.6	27.3	29.6	34.5
160	22.1	26.9	14.7	25.6	28.3	30.6	35.5
200	20.4	25.0	13.3	25.6	28.3	30.6	35.5
250	18.2	27.8	13.1	23.6	26.3	28.6	33.5
315	15.9	26.4	12.3	22.6	25.3	27.6	32.5
400	13.2	26.3	10.6	21.6	24.3	26.6	31.5
500	12.3	25.1	10.1	20.6	23.3	25.6	30.5
630	10.8	24.0	8.8	19.6	22.3	24.6	29.5
800	9.6	22.8	9.4	18.6	21.3	23.6	28.5
1,000	7.8	20.0	11.5	17.6	20.3	22.6	27.5
1,250	6.6	17.2	10.9	16.6	19.3	21.6	26.5
1,600	4.9	17.1	10.7	15.6	18.3	20.6	25.5
2,000	3.1	15.5	8.9	14.6	17.3	19.6	24.5
2,500	1.2	14.1	4.6	12.6	15.3	17.6	22.5
3,150	-0.6	12.5	4.9	10.6	13.3	15.6	20.5
4,000	-1.6	7.4	-0.1	8.6	11.3	13.6	18.5
5,000	-2.7	4.5	-2.0	6.6	9.3	11.6	16.5
6,300	-3.5	1.9	-3.9	4.6	7.3	9.6	14.5
8,000	-3.9	0.6	-5.5	2.6	5.3	7.6	12.5
10,000	-4.0	-0.4	-4.6	0.6	3.3	5.6	10.5
A-level	20.0	31.0	20.0	27.8	30.5	32.8	37.7

Note: Sound levels in decibels re: 20 µPa.

9. Audibility Log Intervals

The data provided in Table 3 tabulate the numbers of aircraft passing abeam the source site during hourly intervals that begin and end exactly on the hour. However, the sound from these aircraft may not reach any particular site until some time later due to:

- (1) *aircraft transit time* - the time required for the aircraft to travel from the source site to a position abeam the observer site, and
- (2) *sound propagation time* - the time required for sound to travel from the abeam point on the flight track to the observer site.

For the purposes of this study the transit latency was calculated by determining the flight track distance between the source site and the point abeam the observer site and dividing that distance by the average aircraft speed of 101.7 knots (171.53 feet/sec). For example, the track distance from the source site to site 5A on the North Rim is 38,811 feet. Dividing this distance by 168.67 feet/second equals a transit time of 226 seconds.

The sound propagation time was calculated by determining the slant distance from the aircraft (at the abeam point) to the observer site, and then dividing that distance by the speed of sound (considered to be 1130 feet/sec at 71 degrees Fahrenheit). Continuing with the example of site 5A, the slant range was determined to be 19,663 feet, so the propagation time would be 17 seconds. Adding the transit and propagation times together, the total latency is computed as 243 seconds (or 4 minutes 3 seconds). Therefore, in comparing the observed minutes of tour aircraft audibility with that predicted by the models, the observer log would be entered by shifting the beginning and end times of the hour by the computed sound latency. At site 5A, for example, the modeled air traffic passing the source site between 8 and 9 am would be compared with observed aircraft audibility between 8:04:03 and 9:04:03.

In the modeling process, the sound arrival latency is not an issue with either NODSS or INM. It is an issue with NMSIM because of the manner in which that model flies individual aircraft in pseudo real time. To address the NMSIM requirement, all of the observer logs were examined and the periods when observers were present tabulated. These periods were then divided into one-hour intervals using the previously described latency calculations beginning and end times. In some instances intervals of less than a whole hour were available at one end or the other of the total observation period. So long as this interval exceeded 30 minutes it was included for calculations. Table 12 identifies all of the nominal one-hour intervals to be computed by NMSIM at each site. This data is also included on the accompanying floppy disk as AUD_INT1.CSV. A listing of the file is attached at the end of this memo. The file format is as follows:

- Line 1 is a text description of the file contents.
- Line 2 provides the number of site-interval records (311) in the file.
- Line 3 identifies the data fields in the file.
- Line 4 identifies the units for each data field.
- Succeeding Lines tabulate the data for each site-interval.

Field 1 contains the 3-character site designator (e.g. "1Ah"). The first two characters identify the site, and the last character ("h," "n," or "v") identifies the organization with which the observer was associated. This is necessary because there are occasions when two observers were at the same site simultaneously and their logs may have begun and ended at different times.

Fields 2 thru 4 contain the month, day and year.

Fields 5 thru 7 contain the interval start time (hours, minutes, seconds)

Fields 8 thru 10 contain the interval end time (hours, minutes, seconds)

Fields 11 contains interval duration, in minutes.

[In the original memorandum, Table 12 follows providing the start and end times for each site, for each hour period. The table is approximately 11 pages long, containing times for some 311 “site hours.”]

Page Intentionally Blank

APPENDIX H. MODEL SENSITIVITY TO AMBIENT SOUND LEVELS

This appendix discusses model sensitivity to ambient sound levels that are entered as input. Model computations were also made with ambient sound levels boosted by 10 decibels. Figure 93 shows the results of these computations, compared with measurements.

Comparison of this figure with Figure 34, page 85 in the main body of this report, indicates the sensitivity of the computation to ambient input. As this comparison shows, a 10-decibel boost of ambient sound levels decreases the computed audibilities, as would be expected, and causes very large negative biases.

Overall, this ambient boost significantly increases overall model error. For NODSS, however, this ambient boost happened to improve model accuracy, because NODSS had significantly over-computed audibility with measured-ambient input. Even though the ambient boost decreases NODSS error, it is not a proper physical way to compute audibility. In effect, the (incorrect) boosted ambient compensated for something else computed inaccurately by NODSS.

In all, these boosted-ambient computations show the computer models to be highly sensitive to their ambient-level input. Because this high sensitivity was expected, the “measured ambient” sound levels have been generalized to the Canyon’s vegetation zones to increase the precision of vegetation-zone ambients in the future (see APPENDIX F).

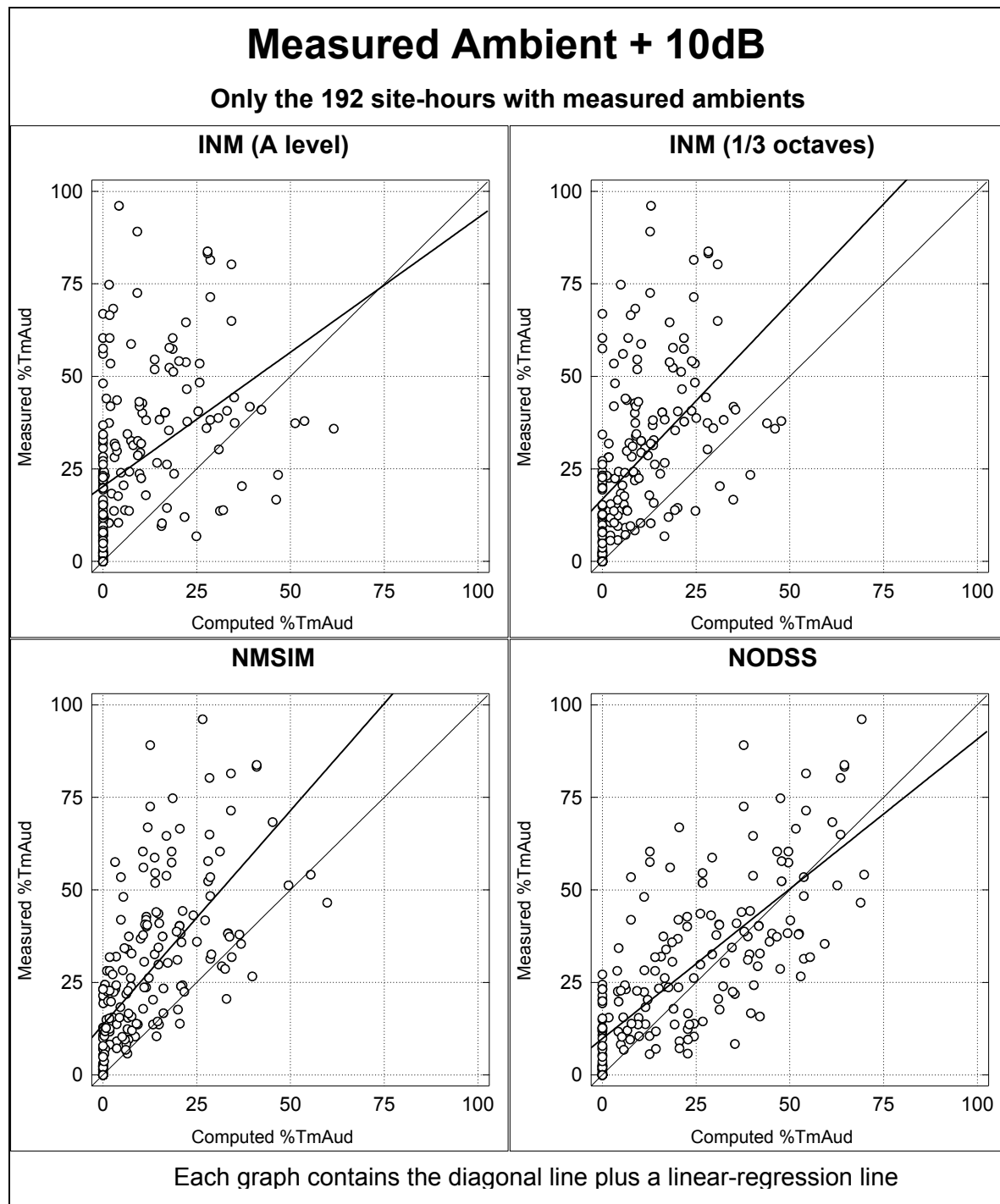


Figure 93. Measured versus computed: Audibility, Using Measured Ambient Plus 10 dB

APPENDIX I. FURTHER DETAILS ABOUT MODEL VALIDATION: MEASURED VERSUS COMPUTED

I.1 Additional Graphical Comparisons of Computed and Measured Tour-Aircraft Sound Metrics

Section 8.4 contains many plots of “measured versus computed” sound values from this study. Figure 94 through Figure 97 show an alternative comparison of these same values—the first two for audibility, the second two for equivalent level (L_{eq}). Site designations are listed in Table 11, page 55.

Instead of plotting “measured versus computed,” these figures show computed separately from measured—both plotted against date-time and against site number. For example, the upper-left frame of the first figure shows how INM-A computations of audibility varied from hour to hour. The “box shapes” for each hour show the variability over all sites.

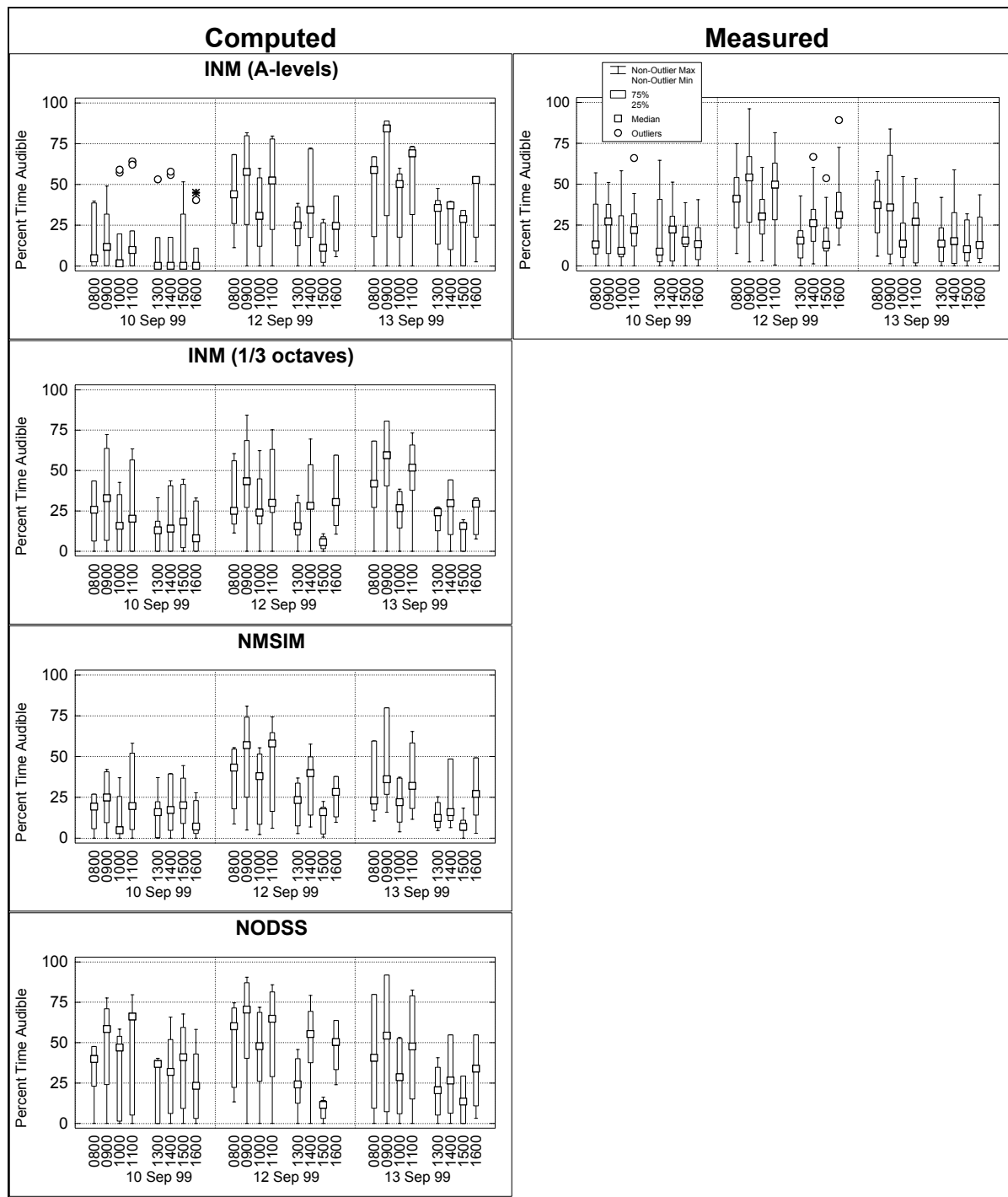


Figure 94. Audibility by Date and Time of Day



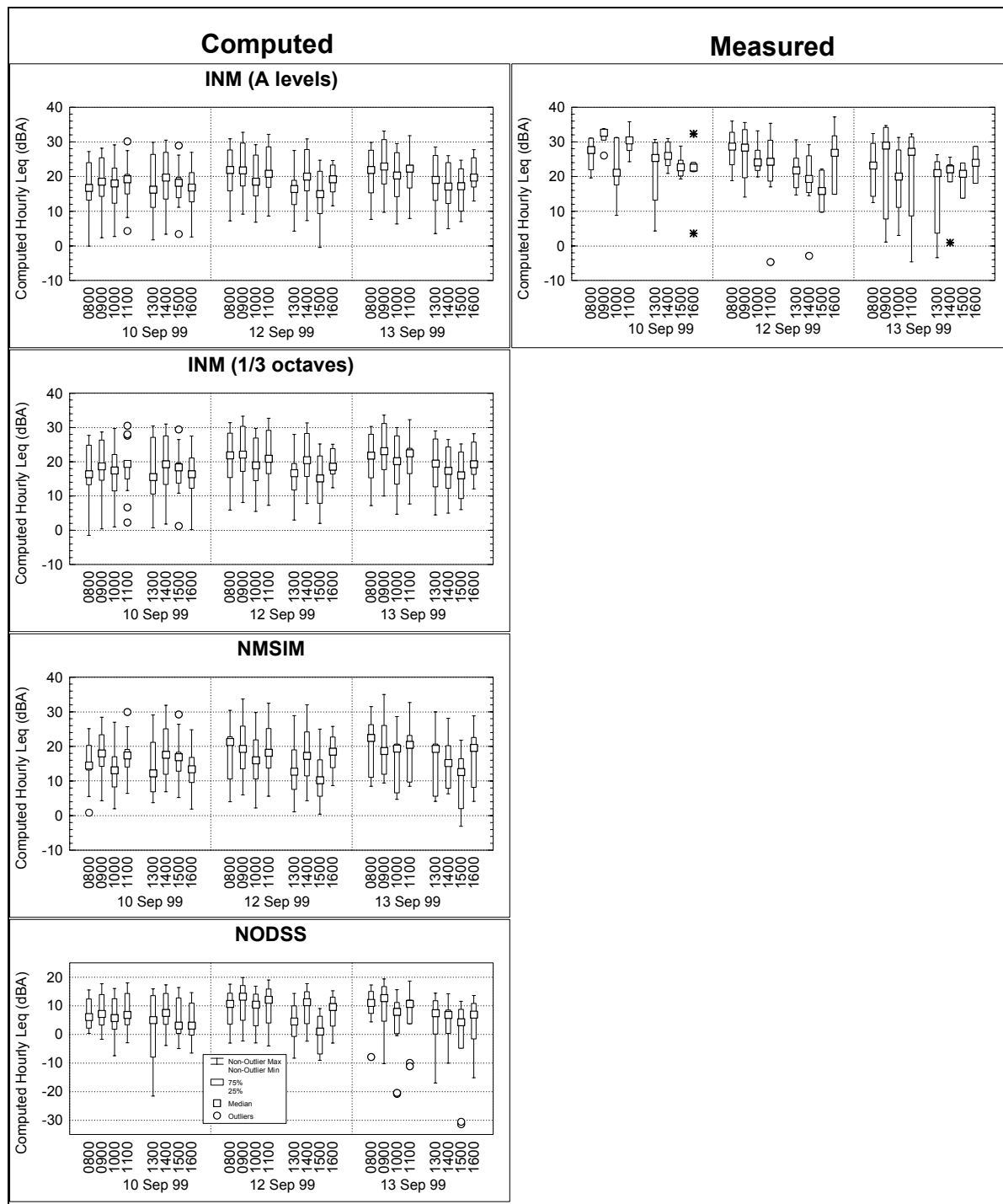


Figure 96. Equivalent Level (L_{eq}) by Date and Time of Day

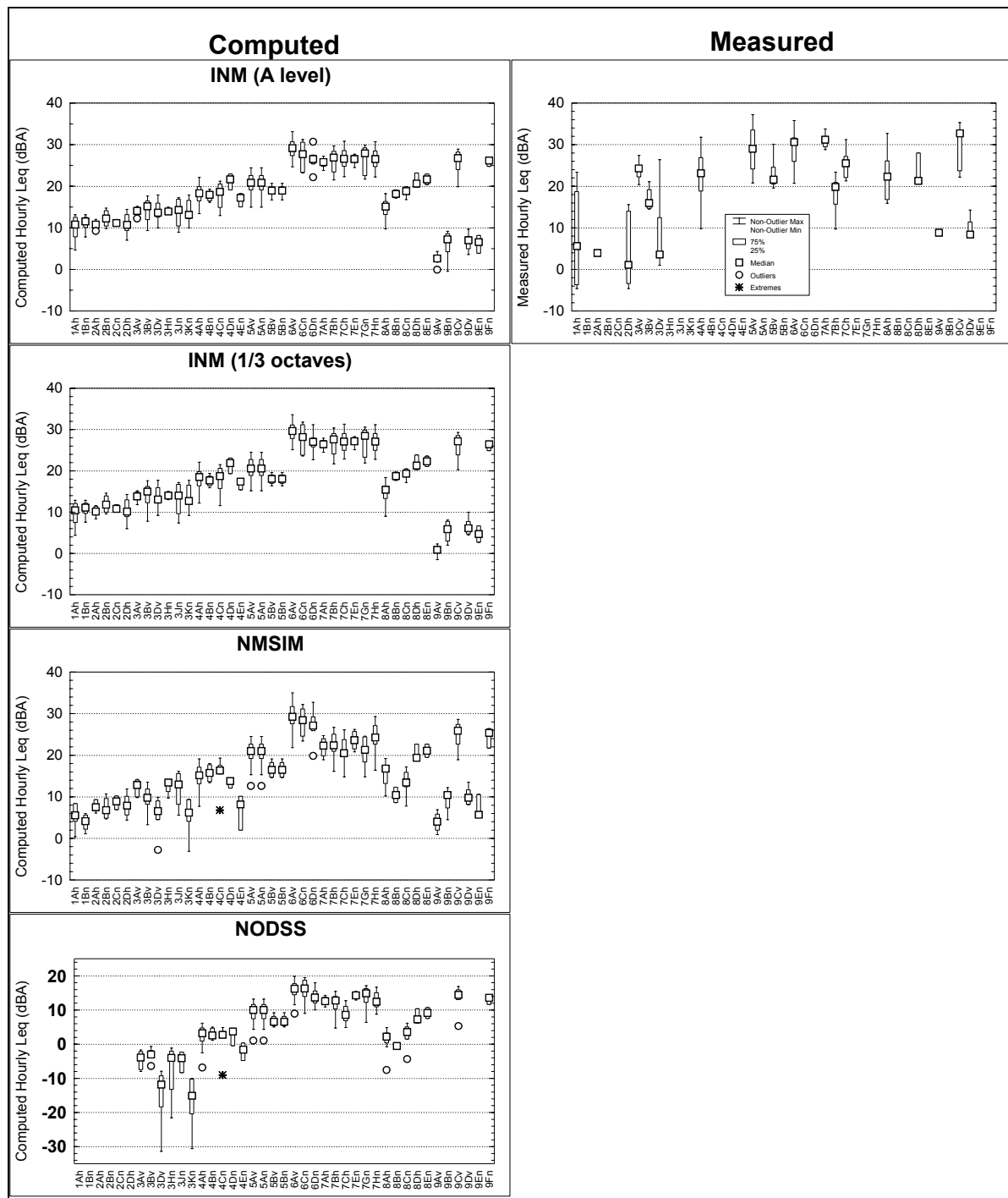


Figure 97. Equivalent Level (L_{eq}) by Site

I.2 Graphical Evidence for the Validity of Hourly Averaging

Section 8.4, above, discusses hourly averaging as necessary to improve the precision of model computations. Figure 98 contains graphical evidence that such averaging actually improves model precision.

The first column of panels in the figure illustrates the inherent hourly scatter in “measured versus computed,” which form the basis of the single-hour precision computations.⁷⁷ The central and right columns show “measured versus computed” for two-hour and four-hour averaging periods, respectively. As is obvious, hourly averaging greatly reduces the point scatter and therefore greatly increases computation precision.

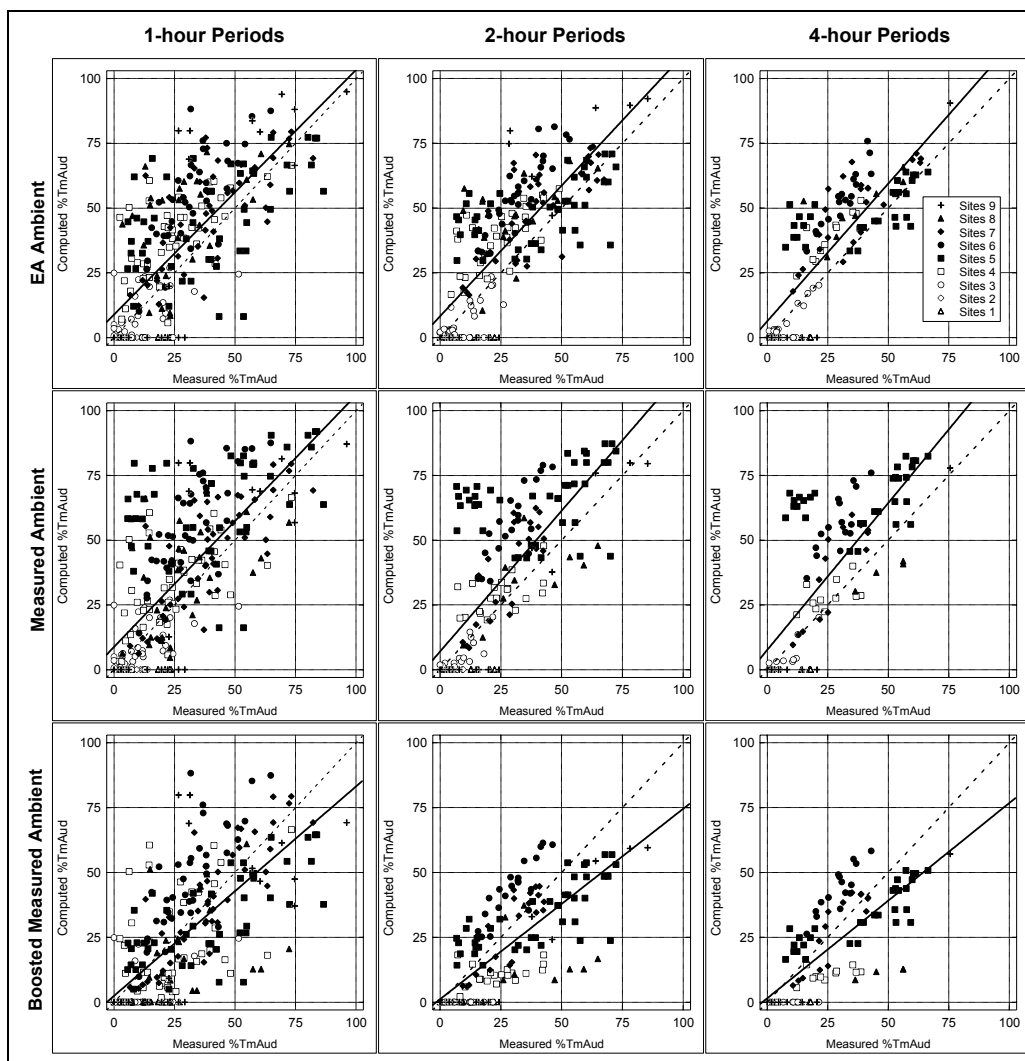


Figure 98. Example of Averaging Several Hours: NODSS

⁷⁷ These plots are similar to the NODSS plots on Figure 34 and Figure 35. However, the axes here are reversed, all 301 site-hours are plotted, and plot symbols vary by site. In addition, the positions of some points have shifted, because these values were computed prior to finalization of computer input.

1.3 Contour error: Computation of Multipliers, Plus 95-percent confidence limits for L_{eq} and for audibility

Figure 56, Figure 57 and Figure 59 above, contain graphs for contour error. This appendix section documents two of the steps in their derivation.

1.3.1 Multipliers

The multiplier inset graphs in these figures were computed from the following equations:

$$\begin{aligned} \text{Variance multiplier for \%TmAud} &= \frac{\left(\frac{V_{\text{Site-to-site}}}{V_{\text{Total}}} \right) + \frac{1}{N} \left(\frac{V_{\text{hour-to-hour}}}{V_{\text{Total}}} \right)}{\left(\frac{V_{\text{Site-to-site}}}{V_{\text{Total}}} \right) + \frac{1}{100} \left(\frac{V_{\text{hour-to-hour}}}{V_{\text{Total}}} \right)} \\ 95\text{-conf-limit multiplier for equivalent level} &= \sqrt{\frac{\left(\frac{V_{\text{Site-to-site}}}{V_{\text{Total}}} \right) + \frac{1}{N} \left(\frac{V_{\text{hour-to-hour}}}{V_{\text{Total}}} \right)}{\left(\frac{V_{\text{Site-to-site}}}{V_{\text{Total}}} \right) + \frac{1}{100} \left(\frac{V_{\text{hour-to-hour}}}{V_{\text{Total}}} \right)}} \end{aligned} \quad (8)$$

where V are the total variances, partitioned by MLwiN into a site-to-site portion and an hour-to-hour portion.

1.3.295-percent confidence limits

1.3.2.1 Equivalent level (L_{eq})

The upper and lower 95-percent confidence limits on the computed L_{eq} follow directly from the variances:

$$(L_{eq})_{95\% \text{ upper lower}} = \pm 1.96 \sqrt{V(d)}, \quad (9)$$

where $V(d)$ is the variance as a function of site-track distance, d . These confidence limits appear in Figure 59. Note in Eq.(9) that variance is not divided by the number of site-hour samples, because the confidence limits are sought for individual hourly measurements, not for their average.⁷⁸

⁷⁸ In Eq.(9), the factor 1.96 is the multiplier that is needed to convert “standard error” (the square-root term) to 95-percent confidence limits. For example, see Section 9.3 of Guttman, Wilks and Hunter, *Introductory Engineering Statistics, 3rd Edition*, John Wiley & Sons, New York, 1982.

1.3.2.2 Audibility

The mathematical relationship between variance and 95-percent confidence limits is more complicated for audibility than for L_{eq} , because audibility values are constrained to lie between 0 and 100 percent. Assuming an underlying binomial distribution, this relationship is computed from:⁷⁹

$$\begin{aligned}
 n &= \frac{p_{cal}(100 - p_{cal})}{V(d)} \\
 a &= n + (1.96)^2 \\
 b &= -\left[\frac{2p_{cal}n}{100} + (1.96)^2 \right] \\
 c &= n \left(\frac{p_{cal}}{100} \right)^2 \\
 (p)_{95\% \text{ upper}} &= 100 \left[\frac{-b + \sqrt{b^2 - 4ac}}{2a} \right] \\
 (p)_{95\% \text{ lower}} &= 100 \left[\frac{-b - \sqrt{b^2 - 4ac}}{2a} \right],
 \end{aligned} \tag{10}$$

where p_{cal} is the calibrated computation of %TmAud and $V(d)$ is the variance as a function of site-track distance, d . These equations are plotted in the bottom frames of Figure 56 and Figure 57, above.

⁷⁹ Guttman, Irwin, Wilks, S.S. and Hunter, J. Stuart. *Introductory Engineering Statistics, 3rd Edition*. New York, John Wiley & Sons, 1982, pp.176-178.

APPENDIX J. FURTHER DETAILS ABOUT MEASURED AUDIBILITY VERSUS PHYSICAL FACTORS

J.1 Compression of Over-100 Percent Audibilities

Three of the computer models (all except NMSIM) simply add together the times of audibility for each aircraft, as if the audibility time periods were end to end. As a result, the computed audibility time can exceed 3600 seconds per hour—that is, the computer can calculate more than 100 %TmAud. In truth, these segments can overlap one another, especially for many aircraft per hour or very far from the flight track.

To compensate, NODSS contains a compression algorithm that reduces large audibilities, to restrain them below 100 percent. This algorithm appears in Figure 99. This same “compression” was applied to INM computations before they were analyzed in this study.

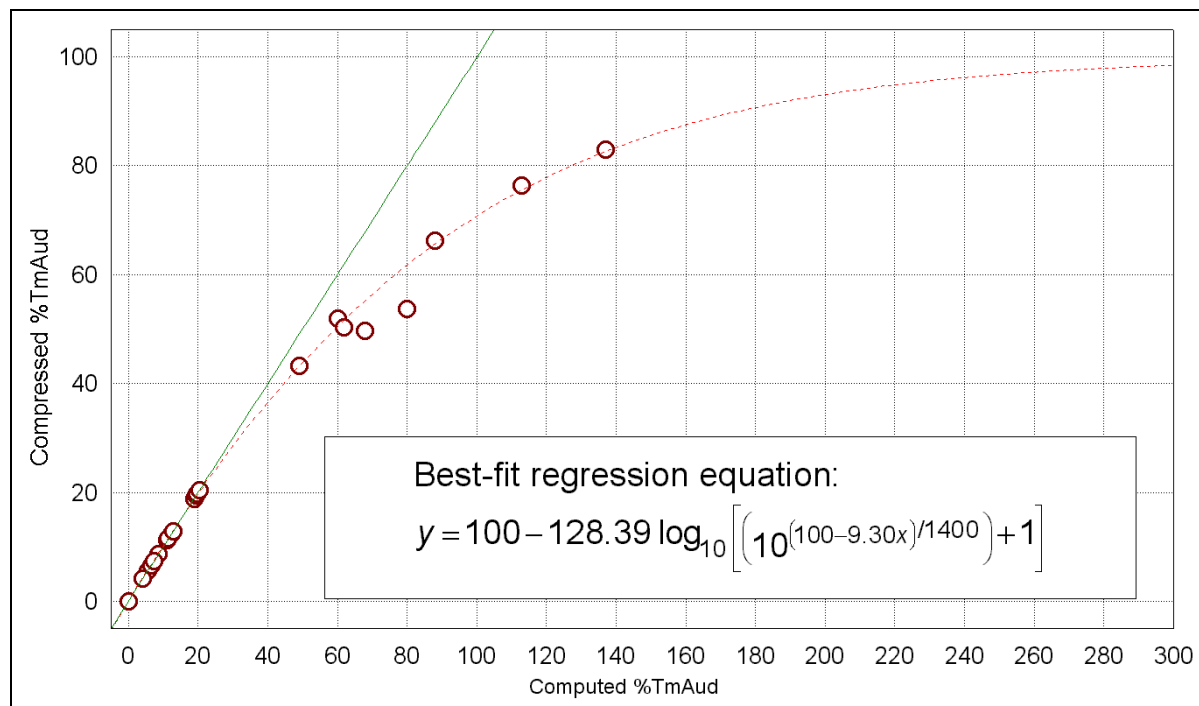


Figure 99. Compression of Over-100% Audibilities

J.2 Some Plots of Measured Audibility versus Individual Physical Factors

Section 9.3 mentions that measured %TmAud was plotted against many individual physical factors, to visualize its dependence upon these factors. Figure 100 contains some of these plots.

Each plot contains only one factor; the other factors are excluded. The missing factors in each plot can change the “shape” of the resulting relationships and thereby distort the view of reality that such plots seem to show. The non-linear regression of measured %TmAud against all these factors, simultaneously, overcomes this difficulty.

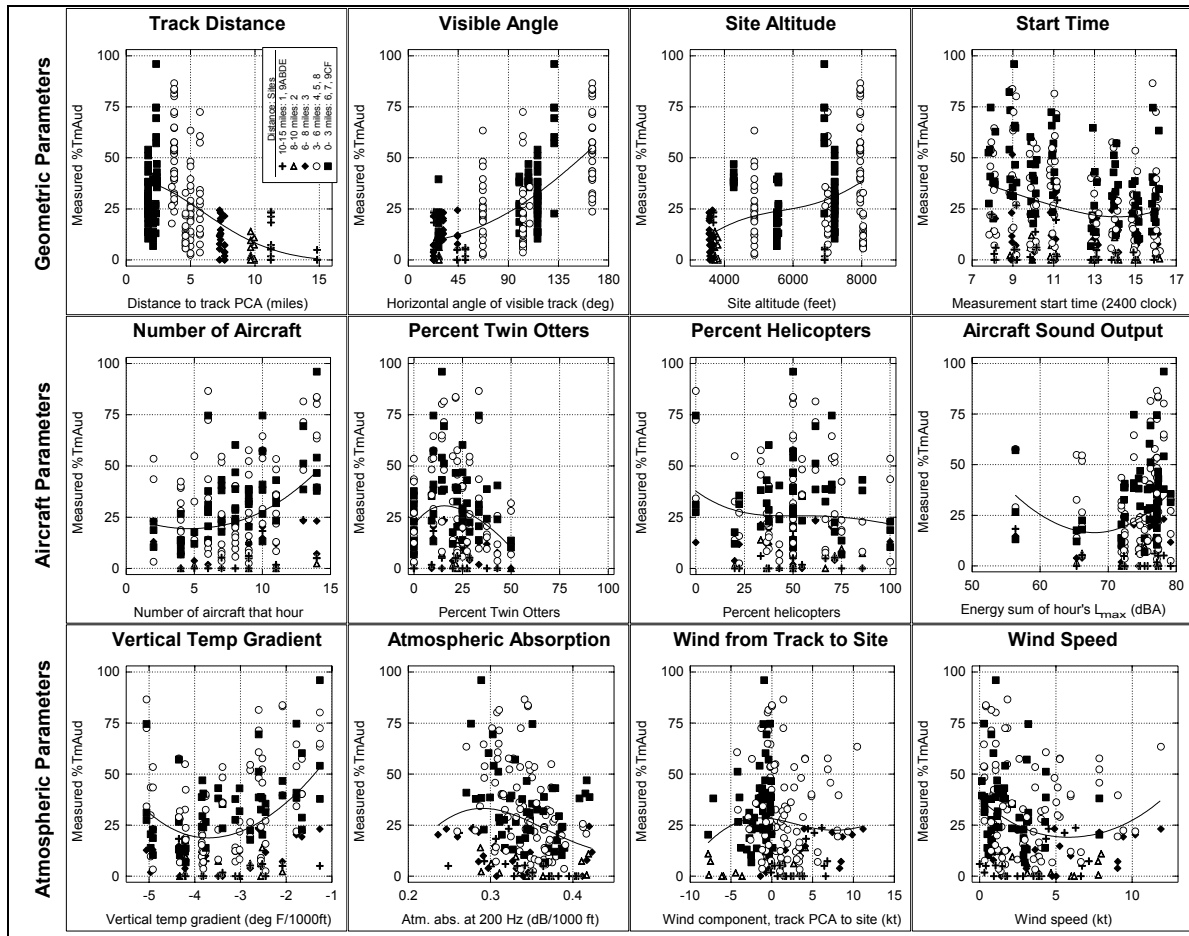


Figure 100. Measured Audibility versus Many Physical Factors, One at a Time

APPENDIX K. INPUT TO THE NON-LINEAR REGRESSION

The figures in this appendix document all the measured input to the non-linear regression in Section 9.3.

Figure 101 documents the meteorology at each of the study's met stations:

- Wind. Wind at each site was adopted from the nearest met station.
- Vertical temperature gradients. Temperature and relative humidity at each met tower were first plotted for each time of day, as a function of met-station elevation above sea level (Figure 102). Then regressions through these points (also shown in the figure) determined that hour's vertical temperature gradient for all site.
- Atmospheric absorption. This same Figure 102 determined temperature and relative humidity as a function of altitude. These values were then adopted for each measurement site, depending on the site's altitude. In turn, temperature and relative humidity were used to compute that site-hour's atmospheric absorption at several frequencies, for use in the regression.

Figure 103 and Figure 104 are examples of NMSIM output that was used to determine visibility angle at each site. These figures show the results for Sites 1B and 7H, respectively. The symbols show what portions of the flight track can be directly seen from each site. These figures show the entire track, though only a portion was used in the modeling, see Section 7.1.1, page 73.

Figure 105 through Figure 108 document all variables by site and over time. The figure panels are arranged to facilitate comparison among the figures. Figure 105 and Figure 106 plot the data by site designation, while Figure 107 and Figure 108 show the variables by hour, by day.

Finally, Figure 109 plots all variables against each other, to show their correlation graphically. This inter-factor correlation was taken into account during regression.

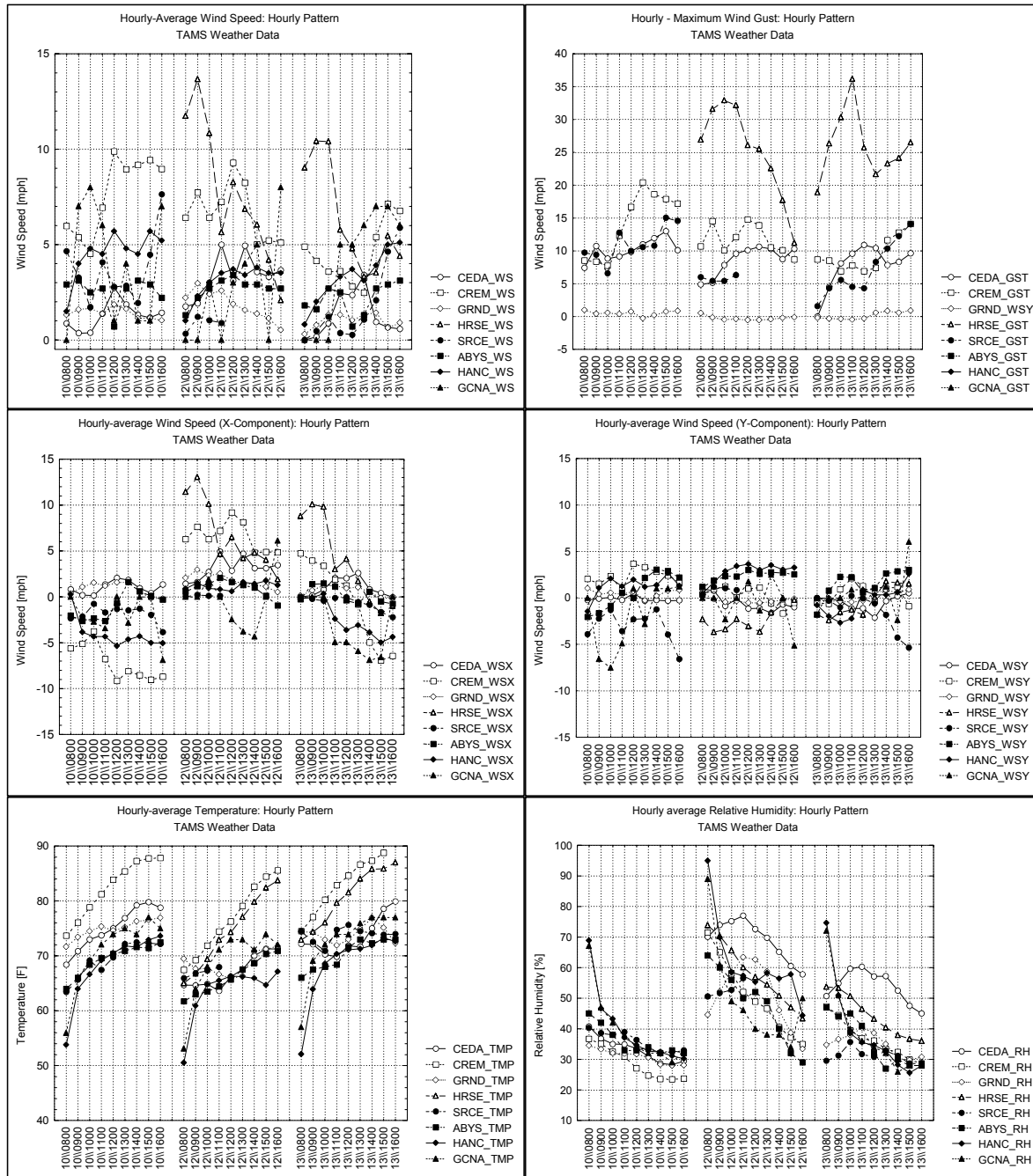
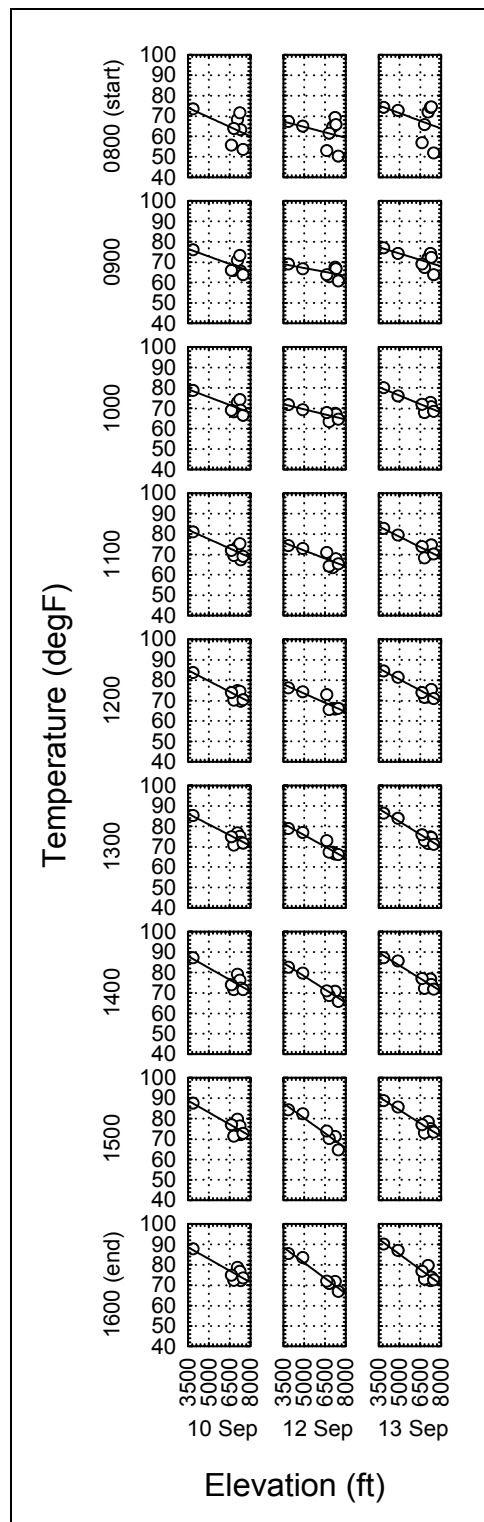


Figure 101. Meteorological Data: Project Towers



**Figure 102. Temperature Gradients:
Project Towers**

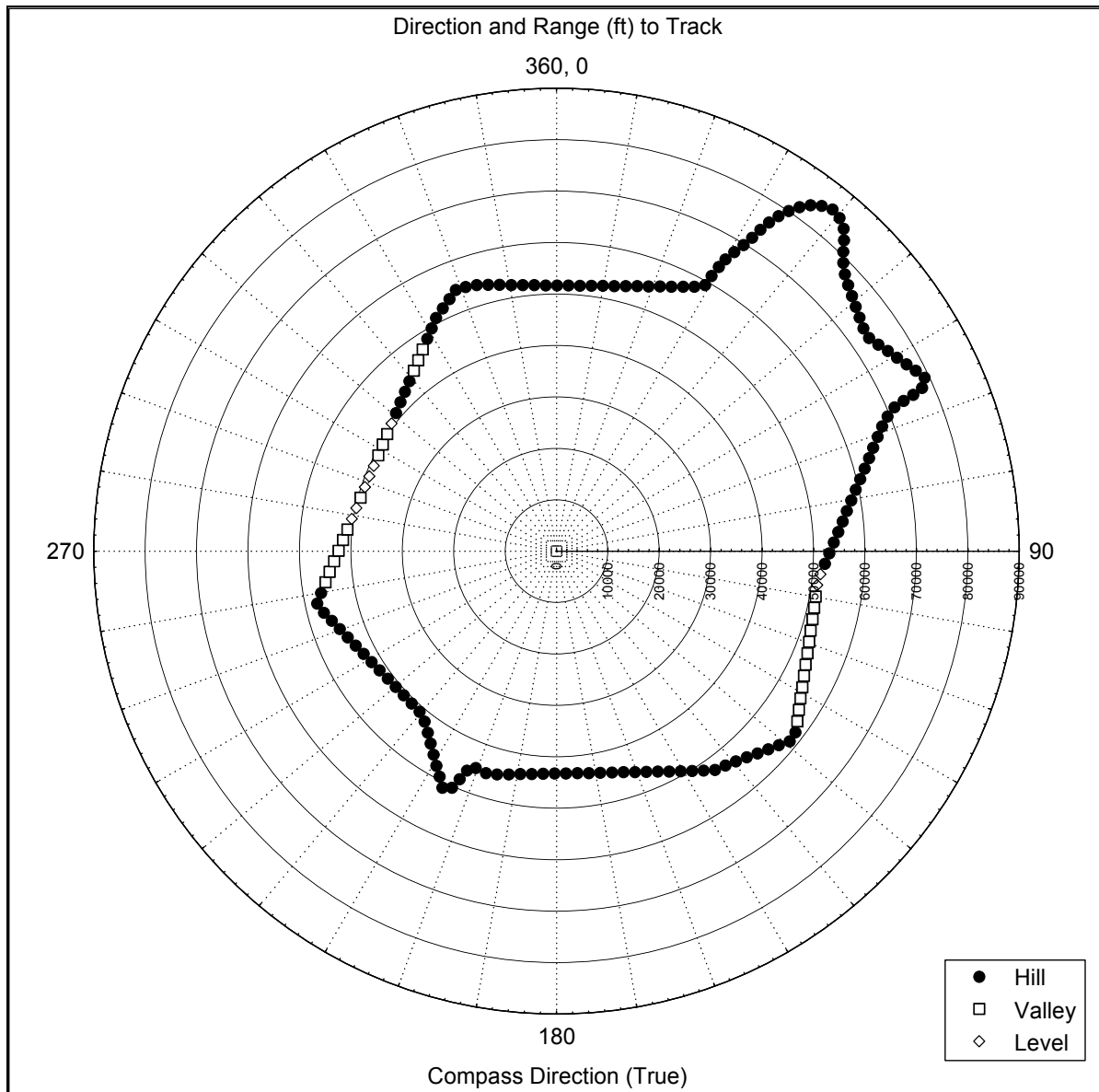


Figure 103. Line-of-sight Example: Site 1B

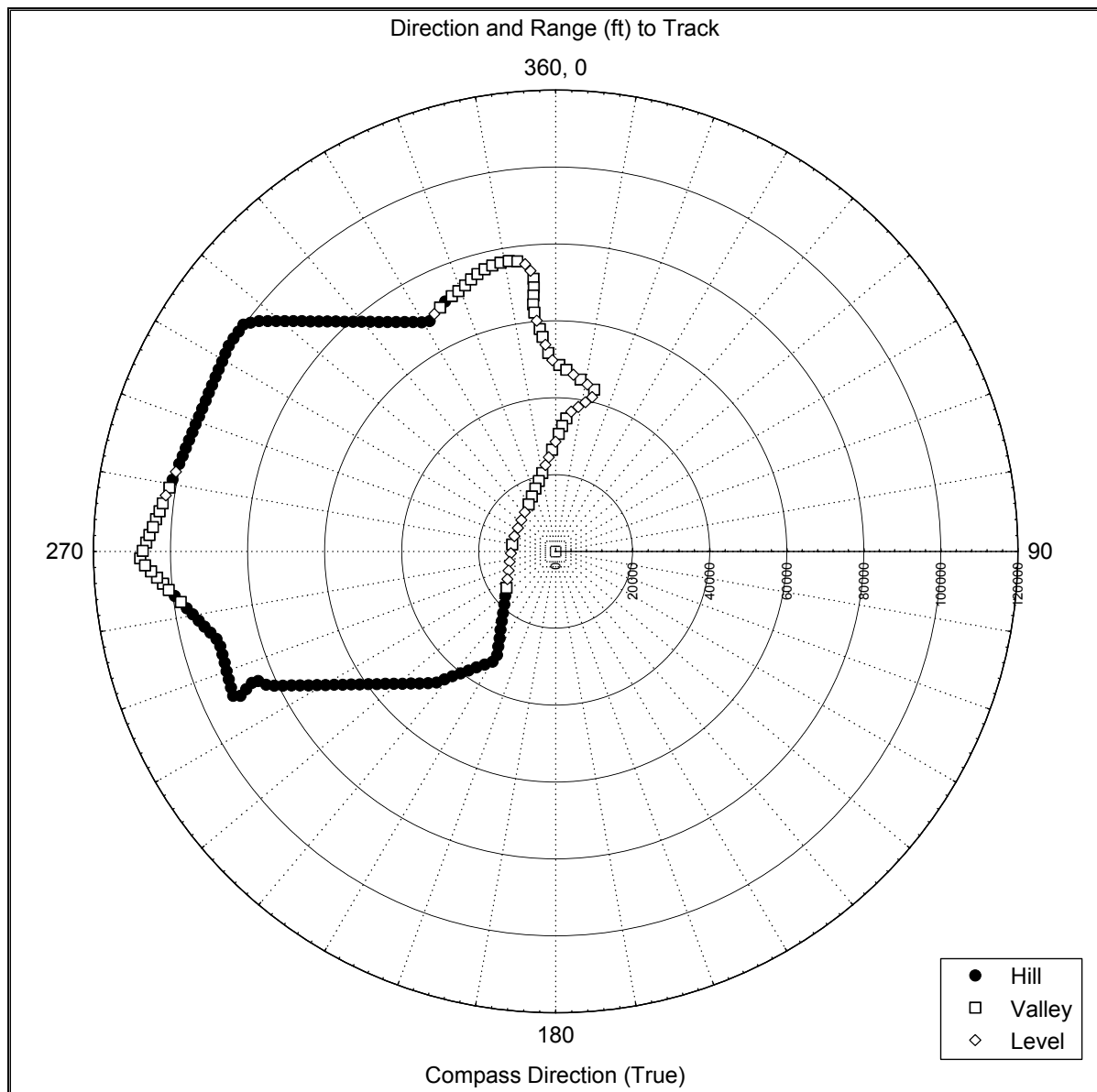


Figure 104. Line-of-sight Example: Site 7H

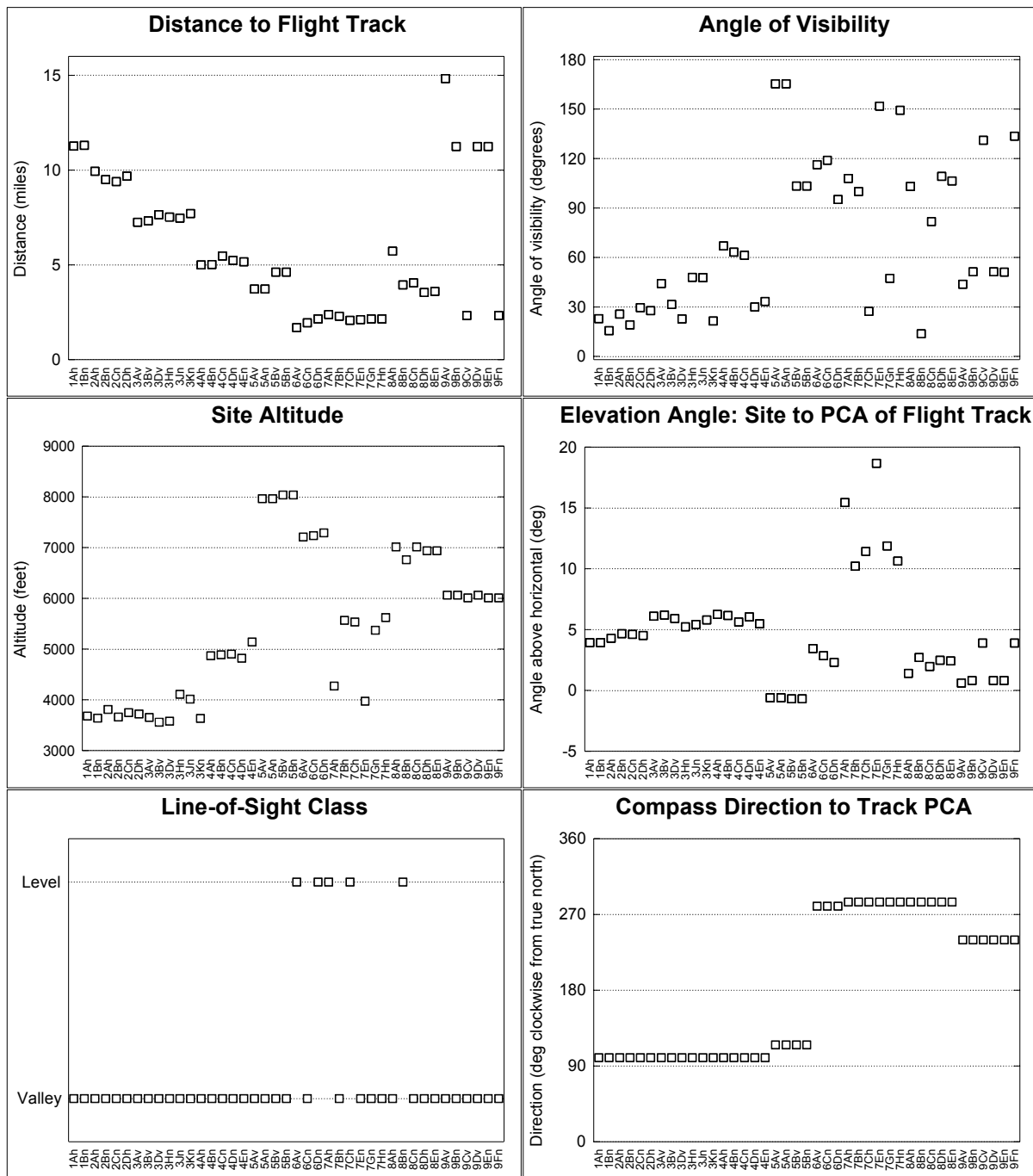


Figure 105. Input Variables by Site

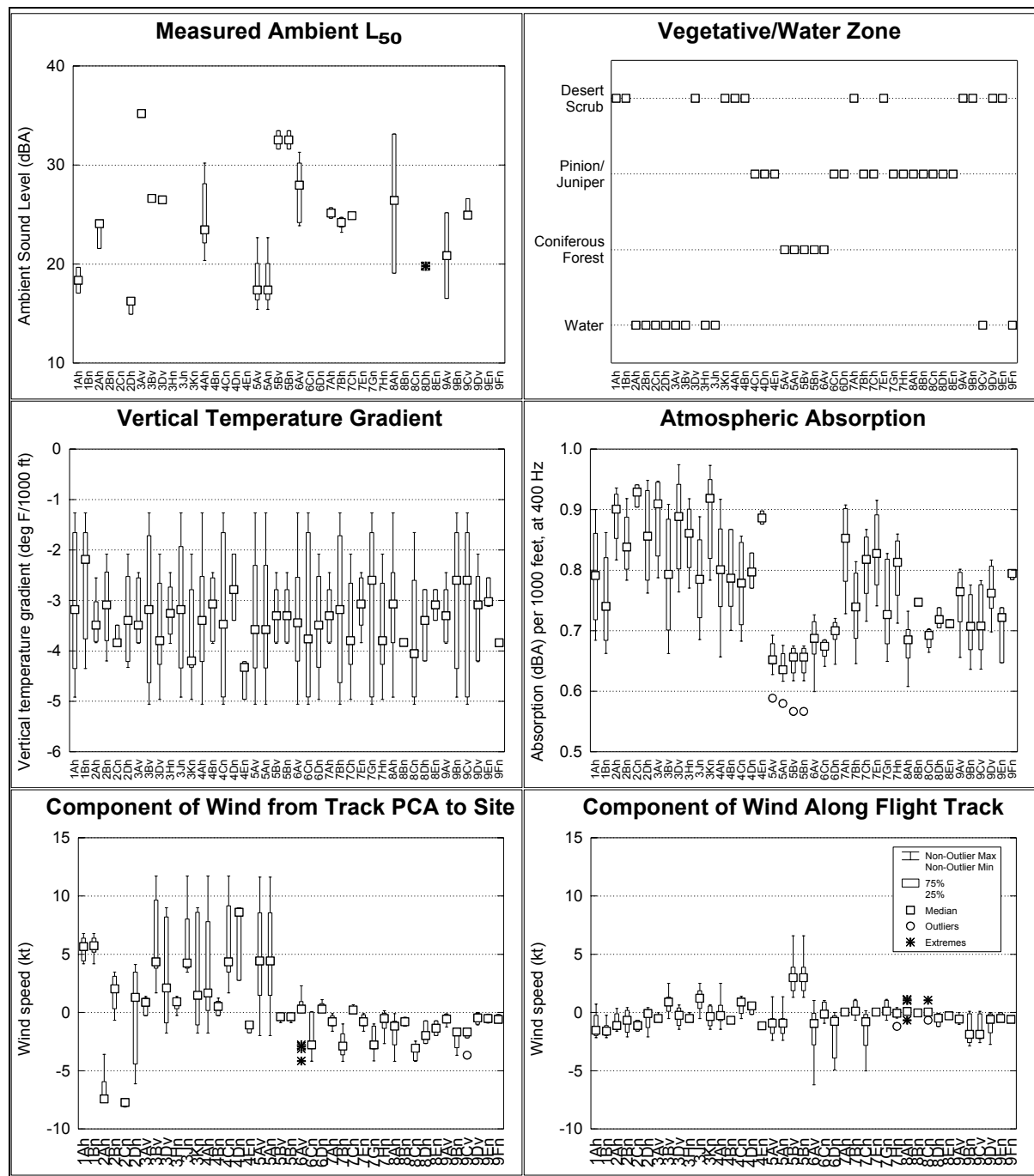


Figure 106. Input Variables by Site (continued)

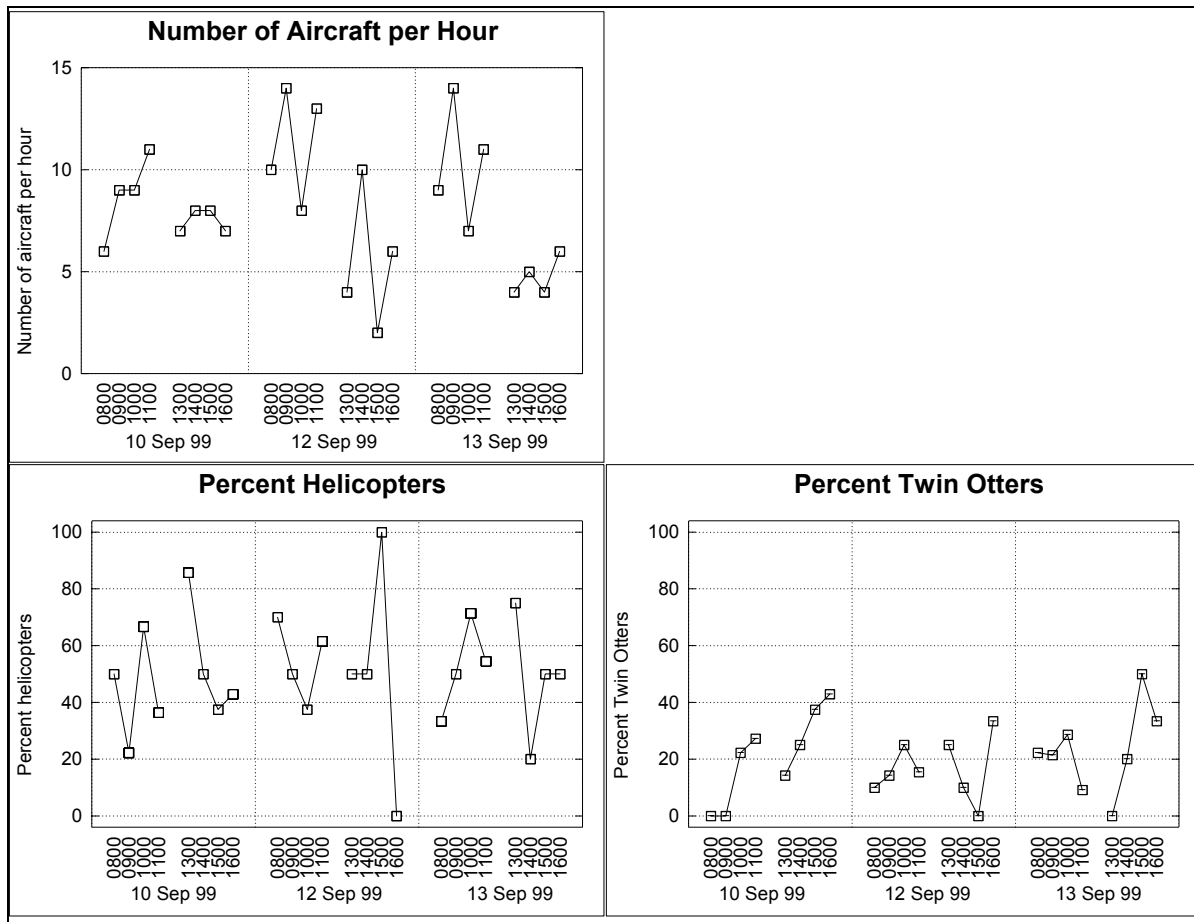


Figure 107. Input Variables over Time

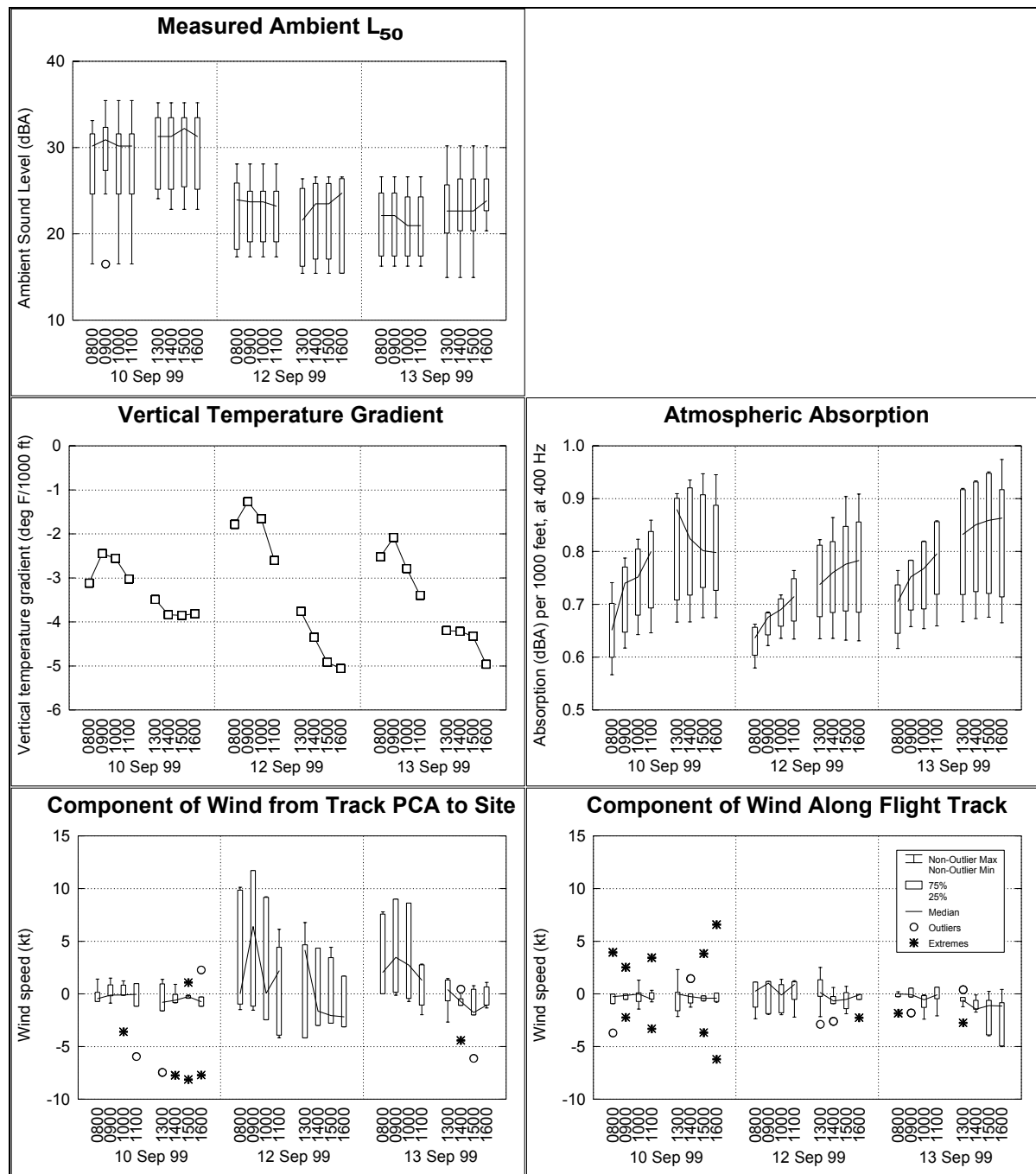


Figure 108. Input Variables over Time (continued)

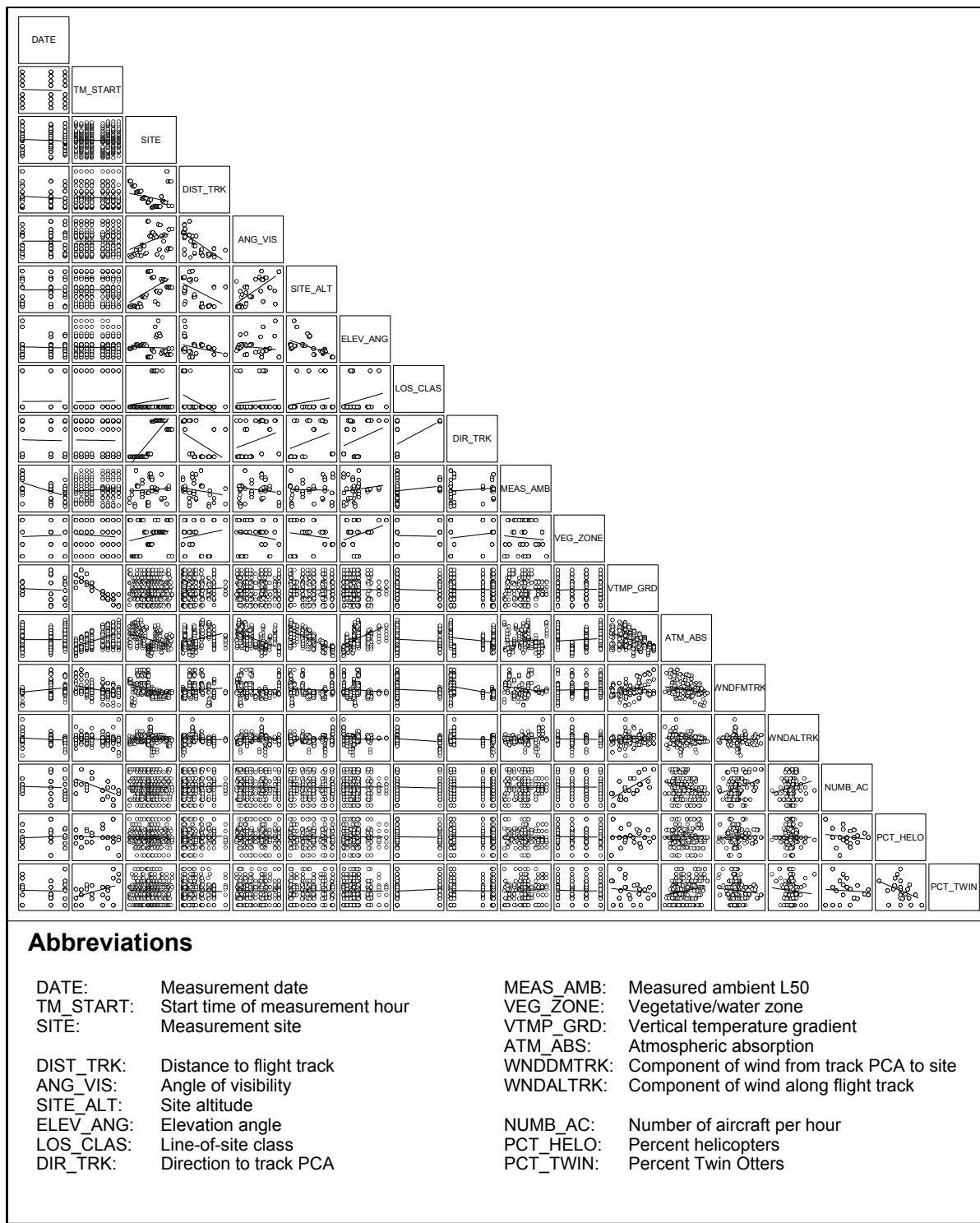


Figure 109. Interdependence of All Variables

APPENDIX L. THE FULL NON-LINEAR REGRESSION EQUATION

L.1 Overview

In this appendix, we develop the non-linear regression equation used in Section 9.31, above. We use Statistica for this development, though any other non-linear regression program would do, as well. This regression equation relates measured audibility to various factors measured simultaneously with audibility. This equation supports Figure 61 above.

We develop this equation piecemeal in this appendix, to separately explain each of its constituent pieces. The reconnection of all these pieces, from their constituent equations, constitutes the full regression equation. It is too long to include here in its fully combined form.

L.2 Sketch of Geometry

We begin with Figure 110, a sketch that looks down from above at a measurement site and several flight tracks. This sketch underlies all the mathematics in this appendix. The central point in the sketch is the measurement site, while the straight lines are flight tracks at various possible distances from that site. Four flight tracks are needed in the figure, to include all possible site-track distances and all possible relationships with the other geometric elements of the sketch. Obviously, only one flight track applies to any given measurement site.

Although this sketch is oriented with flight tracks east of the site (and headed due north), the regression mathematics is independent of this orientation.

In the sketch, the angle extending eastward from the measurement site shows the portion of the track in direct view from the site. The large arc shows the maximum distance of audibility for an aircraft that is in direct view. For this reason, this arc appears only within the angle of direct visibility. The small arc shows the maximum distance of audibility, but for aircraft that are shielded from view. Because sound must diffract over intervening terrain from shielded aircraft, the shielded arc is smaller than the direct-view one.

By drawing these arcs as circles, we ignore tour-aircraft directivity. In fact, fixed-wind tour aircraft direct more acoustic energy to the side than they do fore and aft. The opposite is true for tour helicopters. To a first approximation, these two directivity patterns average out at least to the precision we need in this regression.

As each aircraft flies south to north, it is audible between the points A and B on its particular track:

- Along track 1, the limits of audibility (A and B) occur when the aircraft is out of view, as shown.
- Along track 2, the limits of audibility occur just when the aircraft comes into view and then disappears from view.
- Along track 3, the aircraft cannot be heard for part of the time it is in direct view.
- Along track 4, the aircraft is never heard.

In the remainder of this appendix, we build the regression equation upon this sketch in Figure 110.

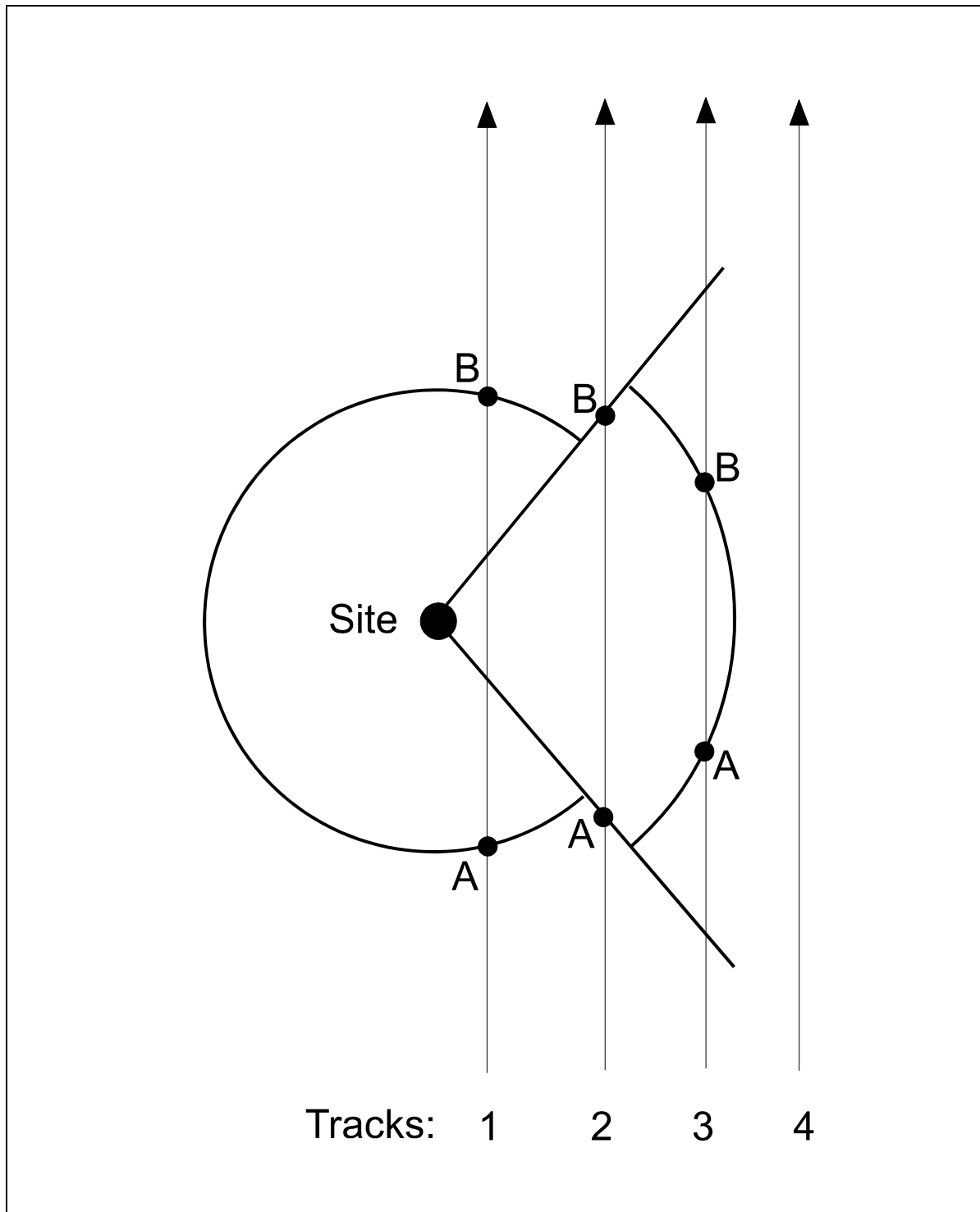


Figure 110. Site Sketch for the Non-Linear Regression

L.3 Definitions Needed in the Final Regression Equation

L.3.1 Dependent Variable

P_{Aud} is the audibility (%TmAud) for that site-hour (%).

Measured audibility is used to determine regression coefficients. Once these are determined, then the resulting regression equation computes this audibility from the various factors measured simultaneously with audibility each site-hour.

L.3.2 Independent Variables (Factors) for Each Site-Hour

d_{Trk} is the distance to the track from the site (miles).

F_{Local} is the local-shielding category for the site: yes or no.

F_{LOS} is the line-of-sight category for the site: valley or level.

L_{Amb} is the L_{50} ambient sound level that site-hour (dBA).

m_{DnWnd} is the downwind (track PCA to site) magnitude of the wind velocity that site-hour (kt).

m_{CrsWnd} is the crosswind (in direction of aircraft travel) magnitude of the wind velocity that site-hour (kt).

n_{AC} is the number of aircraft that pass that hour.

p_{Helo} is the percentage of helicopters that hour (%).

p_{Vista} is the percentage of Vistaliners that hour (%).

s_{AC} is aircraft speed (ft/sec), which averages 173 ft/sec.

T_{Grad} is the vertical temperature gradient that hour (degF/1000ft).

α_{200} is the atmospheric absorption at 200 Hz that site-hour (dB/1000ft).

α_{400} is the atmospheric absorption at 400 Hz that site-hour (dB/1000ft).

θ_{Trk} is the compass direction from the site to the track PCA (deg CW from true north).

ϕ_{Vis} is the horizontal angle subtended by the visible portion of the flight track at the site (deg).

L.3.3 Regression Coefficients

C_{CrsWnd} determines—through Eq.(22)—the sound-level effects of the wind component along the flight track.

C_{DnWnd} determines—through Eq.(22)—the sound-level effects of the wind component from track PCA to site.

C_{EF} is the effective frequency for broadband (A level) atmospheric absorption (Hz).

C_{Local} determines—through Eq.(25)—the sound-level effects of local shielding.

C_{LOS} determines—through Eq.(24)—the sound-level effects of “level” propagation, compared to “valley” propagation, when aircraft are in direct view.

C_{TempGrad} determines—through Eq.(21)—the sound-level effects of vertical temperature gradients.

C_{Terrain} determines—through Eq.(23)—the sound-level effects of intervening terrain.

C_{Vista} determines—through Eq.(3)—how much audibility time is contributed by Vistaliners, compared to non-Vistaliners.

L.4 Definitions Needed Only for Derivation of the Regression Equation

L.4.1 Dependent variable

P_{AudRaw} is the measured audibility (%TmAud), but before compression below 100 percent.

L.4.2 Independent variables

A, B, C, D and E are regression coefficients for a supplemental regression within this derivation.

$L_{AC,FFAud}$ is the free-field aircraft sound level, just at the threshold of audibility (dBA).

$L_{AC,FF}$ is the free-field sound level of a single aircraft (dBA).

L_{maxRef} is the average tour-aircraft L_{max} at a reference slant distance of 1000 feet (dBA).

$n_{NonVistaAC}$ is the number of non-Vistaliners that pass in one hour.

$n_{VistaAC}$ is the number of Vistaliners that pass in one hour.

$p_{NonVista}$ is the percentage of non-Vistaliners that hour (%).

r is radial distance from aircraft to site (ft).

r_{Aud} is the radius of audibility, either shielded or in direct view (ft).

r_{Shield} is the audibility radius for aircraft when shielded from direct view (ft).

r_{Vis} is the audibility radius for aircraft when in direct view (ft).

t_{1AC} is the audibility time for a single aircraft (sec).

$t_{1ACNonVista}$ is the audibility time for a single non-Vistaliner (sec).

$t_{1ACTrk1}$ (or 2 or 3) is the time duration of audibility for a single aircraft flying along track 1 (or 2 or 3) in Figure 110 (sec).

$t_{1ACVista}$ is the audibility time for a single Vistaliner (sec).

t_{Total} is the total audibility time of all aircraft, before compression (sec).

$t_{TotalNonVista}$ is the total audibility time of all non-Vistaliners, before compression (sec).

$t_{TotalVista}$ is the total audibility time of all Vistaliners, before compression (sec).

α_{Ef} is atmospheric absorption per 1000 feet, at an unspecified “effective frequency” (dB).

$\Delta L = L_{AC,FF} - 66$.

$\Delta L_{AudCrit}$ is the broadband (A-level) audibility criterion (dB).

ΔL_{CrSWnd} is the change in aircraft sound level due to the cross-wind component of the wind velocity (in the aircraft flight direction) (dB).

ΔL_{DnWnd} is the change in aircraft sound level due to the down-wind component of the wind velocity (from track PCA to site) (dB).

ΔL_{Local} is the change in aircraft sound level due to local shielding (dB).

ΔL_{LOS} is the change in aircraft sound level due to “level” propagation, instead of “valley” propagation when aircraft is in direct view (dB).

ΔL_{Other} are all other sound-level changes that occur along the path from aircraft to site (dB).

$\Delta L_{Terrain}$ is the change in aircraft sound level due to intervening terrain (dB).

$\Delta L_{TempGrad}$ is the change in aircraft sound level due to vertical temperature gradients (dB).

L.5 Percent Time Audible

L.5.1 Basic Equation

We begin with this basic equation for P_{Aud} :⁸⁰

$$P_{Aud} = 100 - 128.4 \log_{10} \left(10^{(100 - 9.30 P_{AudRaw}) / 128.4} + 1 \right). \quad (1)$$

This equation compresses the raw audibility, P_{AudRaw} (computed next), to a value never greater than 100 percent. This is the same compression equation used by three of the computer models in this study (see Appendix I.1).

L.5.2 Relation to Total Audibility Time and Aircraft Traffic

We next relate P_{AudRaw} to the total audibility time and aircraft traffic (number per hour and percentage of each type):

⁸⁰ Initially, the constants in this equation were to remain unspecified (as regression coefficients), so that Statistica could determine a modified compression algorithm from the measured audibilities. However, the non-linear regression would not converge when these regression coefficients were included. Therefore, they were taken out and the prior constants substituted, as shown in this equation.

$$\begin{aligned}
 P_{\text{AudRaw}} &= 100 \left(\frac{t_{\text{Total}}}{3600} \right) \\
 &= 100 \left(\frac{t_{\text{TotalVista}} + t_{\text{TotalNonVista}}}{3600} \right) \\
 &= 100 \left(\frac{n_{\text{VistaAC}} t_{1\text{ACVista}} + n_{\text{NonVistaAC}} t_{1\text{ACNonVista}}}{3600} \right) \\
 &= 100 n_{\text{AC}} \left(\frac{\left(\frac{p_{\text{Vista}}}{100} \right) t_{1\text{ACVista}} + \left(\frac{p_{\text{NonVista}}}{100} \right) t_{1\text{ACNonVista}}}{3600} \right) \\
 &= 100 n_{\text{AC}} \left(\frac{\left(\frac{p_{\text{Vista}}}{100} \right) t_{1\text{ACVista}} + \left(\frac{100 - p_{\text{Vista}}}{100} \right) t_{1\text{ACNonVista}}}{3600} \right) \\
 &= n_{\text{AC}} \left(\frac{p_{\text{Vista}} t_{1\text{ACVista}} + (100 - p_{\text{Vista}}) t_{1\text{ACNonVista}}}{3600} \right).
 \end{aligned} \tag{2}$$

L.5.3 Effect of Vistaliners: First Regression Coefficient

We next introduce our first regression coefficient, C_{Vista} , to relate the audibility times for Vistaliners and non-Vistaliners:⁸¹

$$t_{1\text{ACVista}} = \left(\frac{1}{1 + (1.1)^{-C_{\text{Vista}}}} \right) t_{1\text{ACNonVista}}. \tag{3}$$

The expression in parenthesis can only take on values between zero and unity. For $C_{\text{Twin}} = -\infty$, the expression equals zero; for $C_{\text{Vista}} = +\infty$, it equals unity. We have used an expression of this type (similar to the logistic function) to restrict $t_{1\text{ACVista}} \leq t_{1\text{ACNonVista}}$ in the regression. The best-fit value for C_{Vista} will tell us directly how much audibility time is contributed by Vistaliners, compared to non-Vistaliners.

For conciseness, we now leave off “NonVista” from the subscript of t —that is, we define:

$$t_{1\text{AC}} \equiv t_{1\text{ACNonVista}}. \tag{4}$$

Combining equations to this point, we have P_{Aud} as a function of several site-hour factors, one regression coefficient, and $t_{1\text{AC}}$. To finish, we must develop equations for $t_{1\text{AC}}$, as a function of the parameters in Figure 110 and the site-hour factors that influence them.

⁸¹ Initially, we set the “base” in this equation equal to e , the base of the natural logarithms. However, the resulting expressing varied so quickly with C_{Twin} that the regression equations would not converge.

L.6 Audibility Time for One Aircraft

From Figure 110, the audibility time for one aircraft, t_{1AC} , is the time it takes that aircraft to fly from point A to point B:

$$t_{1AC} = \frac{\min \left[\max \left[t_{1ACTrk1}, t_{1ACTrk2} \right], t_{1ACTrk3} \right]}{S_{AC}}. \quad (5)$$

The audibility times in this equation depend upon which track is relevant for that site-hour, depending upon the site's visibility angle and the hour's meteorology (which effects the radii in Figure 110).

From straightforward geometry:

$$\begin{aligned} t_{1ACTrk1} &= 2\sqrt{\max \left[r_{\text{Shield}}^2 - d_{\text{Trk}}^2, 0 \right]} \\ t_{1ACTrk2} &= 2d_{\text{Trk}} \tan \left(\frac{\phi_{\text{Vis}}}{2} \cdot \frac{\pi}{180} \right) \\ t_{1ACTrk3} &= 2\sqrt{\max \left[r_{\text{Vis}}^2 - d_{\text{Trk}}^2, 0 \right]}. \end{aligned} \quad (6)$$

The factor $\pi/180$ is needed in this equation because Statistica requires all angles to be in radians, rather than in degrees. The “max” functions are needed to force the expression to zero when required (and prevent square roots of negative numbers).

Combining equations to this point, we have P_{Aud} as a function of several site-hour factors, one regression coefficient, and r_{Shield} and r_{Vis} —the two audibility radii in Figure 110. To finish, we must develop equations for these two radii.

L.7 Audibility Radii

The audibility radii are the most complicated part of the regression equation. We develop expressions for these two radii in these steps:

- Aircraft level as function of distance, free field. First, we develop an equation for aircraft sound level as a function of distance, assuming only spherical divergence and atmospheric absorption.
- Distance as function of aircraft level, free field. Next, we “invert” this equation, to solve it backwards for distance as a function of aircraft level.
- Conditions for audibility. Next, we determine audibility by introducing ambient sound level.
- Other sound-level changes (attenuations). Finally, we introduce other factors into the equation, to account for terrain shielding and meteorological effects.

L.7.1 Aircraft Level as Function of Distance, Free Field

Consistent with aircraft sound-level emissions that were used as computer input in this study, we start with measured aircraft reference levels at a slant distance of 1000 feet, to the side of the tour-aircraft flight path:

$$L_{maxRef} = 66 \text{ dBA}, \quad (7)$$

which is the average value for all types of aircraft in this study.

With 1000 feet as our initial distance, we then reduce this aircraft level by spherical divergence and atmospheric absorption, to obtain the aircraft free-field sound level at distance r :

$$\begin{aligned} L_{AC,FF} &= L_{maxRef} - 20 \log_{10} \left(\frac{r}{1000} \right) - \alpha_{Ef} \left(\frac{r-1000}{1000} \right) \\ &= 66 - 20 \log_{10} \left(\frac{r}{1000} \right) - \alpha_{Ef} \left(\frac{r-1000}{1000} \right) \\ L_{AC,FF} - 66 &= -20 \log_{10} \left(\frac{r}{1000} \right) - \alpha_{Ef} \left(\frac{r-1000}{1000} \right) \\ \Delta L &= -20 \log_{10} \left(\frac{r}{1000} \right) - \alpha_{Ef} \left(\frac{r-1000}{1000} \right). \end{aligned} \quad (8)$$

In this equation, α_{Ef} is the atmospheric absorption per 1000 feet, at an unspecified “effective frequency” that we will later make more specific.

L.7.2 Distance as Function of Aircraft Level, Free Field

L.7.2.1 Substitution of functional form through a supplemental regression

Eq. (8), just above, involves both the distance r and its logarithm, so cannot be directly solved backwards (inverted) to obtain distance, r , as a function of aircraft level. To overcome this difficulty, we must change the functional form of Eq. (8). Previous work indicates that the following functional form might closely fit:

$$\Delta L = A + B(\log_{10} r) + C(\log_{10} r)^2 + D(\log_{10} r)^3, \quad (9)$$

where A, B, C and D are constants we must determine from a supplemental regression. To constrain this functional form, we impose the following requirements on these coefficients:

- The regression curve must pass through $\Delta L = 0$ at $r = 1000$.
- The curve's slope must equal -20dB/decade at $r = 1000$.
- The curve's inflection point must occur at $r = 1000$.
- The coefficient D must be positive, to force a downward curve.

With these constraints:

$$\Delta L = (60 + 27E^2) + (-20 - 27E^2)(\log_{10} r) + (9E^2)(\log_{10} r)^2 + (-E^2)(\log_{10} r)^3, \quad (10)$$

where E^2 has been substituted for D.

We then use Eq.(8) to compute ΔL over the distance range $1000\text{ft} < r < 100,000\text{ft}$, and for absorption coefficients between 0.1 and 2.4. We then regress the results of these computations to the functional form in Eq.(10), separately for each α_{Ef} , to obtain that α_{Ef} 's best-fit value of E^2 .

Next, we plot these values of E^2 against α_{Ef} and find the plot to be highly linear. So we linearly regress E^2 against α_{Ef} to obtain:

$$E^2 = 10 \alpha_{\text{Ef}}, \quad (11)$$

($R^2 = 0.99999997$). With this substitution, Eq.(10) then becomes:

$$\Delta L = (60 + 270\alpha_{\text{Ef}}) + (-20 - 270\alpha_{\text{Ef}})(\log r) + (90\alpha_{\text{Ef}})(\log r)^2 - 10\alpha_{\text{Ef}}(\log r)^3. \quad (12)$$

Eq.(12) is the substituted functional form for Eq.(8).

L.7.2.2 Inversion of this functional form

Unlike Eq.(8), Eq.(12) can be mathematically inverted—that is, it can be solved backwards for r as a function of ΔL . We use the computer program Derive to accomplish this. Since Eq.(12) is a cubic equation in $(\log_{10} r)$, the inversion will yield three roots, only one of which will be real (free of the square root of -1):

$$\log_{10} r = 3 - \frac{2\sqrt{6} \sinh \left(\frac{\frac{7 \ln 2}{2} - \ln \left(\frac{\sqrt{27\alpha_{\text{Ef}} (\Delta L)^2 + 3200} - 3\sqrt{3\alpha_{\text{Ef}} \Delta L}}{5} \right)}{3} \right)}{3\sqrt{\alpha_{\text{Ef}}}} \quad (13)$$

$$\log_{10} r = 3 - \frac{2\sqrt{6} \sinh \left(\frac{\frac{7 \ln 2}{2} - \ln \left(\frac{\sqrt{27\alpha_{\text{Ef}} (L_{\text{AC,FF}} - 66)^2 + 3200} - 3\sqrt{3\alpha_{\text{Ef}} (L_{\text{AC,FF}} - 66)}}{5} \right)}{3} \right)}{3\sqrt{\alpha_{\text{Ef}}}}.$$

By this equation, we have distance from the aircraft, r , as a function of an effective absorption coefficient, α_{Ef} , and the tour-aircraft's free-field sound level, $L_{\text{AC,FF}}$, at the site.

L.7.2.3 Effective absorption frequency: second regression coefficient

From analysis results of Appendix C.4.3, page 176, it appears that the controlling frequencies for tour-aircraft audibility, are between 100 and 500 Hz. For this reason, we compute pure-tone absorption (per 1000 feet), using the relevant ANSI standard, for all site-hours in the study.⁸²

⁸² American National Standards Institute, "Method for the Calculation of the Absorption of Sound by the Atmosphere," American National Standard ANSI S1.26-1978, Acoustical Society of America, New York, 1978.

$$\begin{aligned} 0.24 \text{ dB/1000ft} < \alpha_{200} < 0.42, \text{ and} \\ 0.56 \text{ dB/1000ft} < \alpha_{400} < 0.97. \end{aligned} \quad (14)$$

Plots of atmospheric absorption as a function of frequency, within the range of the study's meteorology, are highly linear. This allows us to express α_{Ef} as a linear function of α_{200} and α_{400} :

$$\alpha_{Ef} = \alpha_{200} + (0.005 C_{Ef} - 1)(\alpha_{200} - \alpha_{400}). \quad (15)$$

In this equation, we introduce our second regression coefficient, C_{Ef} , the effective frequency for broadband (A level) atmospheric absorption. The best-fit value of this coefficient will tell us what single frequency can best be used to compute the net atmospheric absorption of A-weighted sound level. In this equation, both α_{200} and α_{400} are computed for each measured site-hour from that site-hour's temperature and relative humidity.

L.7.3 Conditions for Audibility

We next need to convert Eq.(13) from r as a function of aircraft level, $L_{AC,FrFld}$, to r when the aircraft is at the threshold of audibility. To do that, we express the broadband (A-level) audibility criterion, $\Delta L_{AudCrit}$, in the standard manner as:

$$\Delta L_{AudCrit} = (L_{AC,FFAud} + \Delta L_{Other}) - L_{Amb}, \quad (16)$$

where ΔL_{Other} are all other sound-level changes (mostly attenuations) that occur along the path from aircraft to site—as discussed in the next section.

We initially planned to use this broadband criterion, $\Delta L_{AudCrit}$, as a regression coefficient—and thereby solve for it by regression. Unfortunately, it confounded too severely with various attenuation regression coefficients (introduced below) and therefore had to be set equal to its currently accepted value:

$$\Delta L_{AudCrit} = -8 \text{ dB}. \quad (17)$$

With this substitution:

$$\begin{aligned} -8 &= (L_{AC,FFAud} + \Delta L_{Changes}) - L_{Amb} \\ L_{AC,FFAud} &= L_{Amb} + 8 - \Delta L_{Other}. \end{aligned} \quad (18)$$

This value of $L_{AC,FFAud}$ is the free-field aircraft sound level just at the limit of audibility—that is, at a distance of r_{Aud} . For this reason, we substitute from Eq.(18) into Eq.(13) to obtain the distance of audibility:

$$\log_{10} r_{\text{Aud}} = 3 - \frac{2\sqrt{6} \sinh \left(\frac{\frac{7 \ln 2}{2} - \ln \left(\frac{\sqrt{27\alpha_{\text{Ef}} (L_{\text{AC,FFAud}} - 66)^2 + 3200} - 3\sqrt{3\alpha_{\text{Ef}} (L_{\text{AC,FFAud}} - 66)} \right)}{5} \right)}{3\sqrt{\alpha_{\text{Ef}}}} \right)}{3} \quad (19)$$

where:

$$L_{\text{AC,FFAud}} = L_{\text{Amb}} + 8 - \Delta L_{\text{Other}} \quad (20)$$

We have now completed our expression for the audibility radii, r_{Aud} . Two such radii are needed: r_{Shield} and r_{Vis} —corresponding to whether or not the aircraft is shielded by the terrain or in direct view. The various terms within ΔL_{Other} will differ for these two conditions.

L.7.4 Other Sound-Level Changes

The only undefined term in the combined Eq.(19) and Eq.(20) is ΔL_{Other} , which accounts for all other sound-level changes along the path from aircraft to site. Such changes are caused by upward refraction due to vertical temperature gradients, upward and downward refraction due to wind, terrain shielding, differences between “level” terrain and “valley” terrain along non-shielded paths, and shielding due to site peculiarities such as large boulders.

L.7.4.1 Upward refraction due to vertical temperature gradients: third regression coefficient

Vertical temperature gradients refract sound either upward or downward and thereby can effect aircraft sound levels at the site. To account for this effect, we set:

$$\Delta L_{\text{TempGrad}} = (C_{\text{TempGrad}})^2 T_{\text{Grad}}, \quad (21)$$

where C_{TempGrad} is our third regression coefficient. By squaring the multiplicative term in this way, we force $\Delta L_{\text{TempGrad}}$ to be negative when T_{Grad} is negative, and vice versa. During Canyon measurements, all temperature gradients were negative (temperature lapses), and so this mechanism will always reduce sound levels, never increase them.

Vertical gradients that cause refraction will produce the most effect for sound paths that diffract over intervening terrain. For this reason, we include this term only in r_{Shield} , below.

L.7.4.2 Refraction due to wind: fourth and fifth regression coefficients

Wind speeds always increase with increasing height above the ground. As a result, sound traveling downwind is refracted downward, while sound traveling upwind is refracted upward. To account for this effect, we set:

$$\begin{aligned} \Delta L_{\text{DnWnd}} &= (C_{\text{DnWnd}})^2 m_{\text{DnWnd}} \quad \text{and} \\ \Delta L_{\text{CrSWnd}} &= (C_{\text{CrSWnd}})^2 m_{\text{CrSWnd}}, \end{aligned} \quad (22)$$

where C_{DnWnd} and C_{CrSWnd} are our fourth and fifth regression coefficients. By squaring the multiplicative terms in this way, we force each Δ term to be negative when its corresponding wind parameter (magnitude, m) is negative, and vice versa. In this equation, the wind-magnitude terms are components of the wind from track PCA to site (downwind component) and along the track (crosswind component), respectively.

Vertical gradients that cause refraction will produce the most effect for sound paths that diffract over intervening terrain. For this reason, we include this term only in r_{Shield} , below.

L.7.4.3 Terrain shielding: sixth regression coefficient

Sound diffracting over intervening terrain is attenuated. To account for this, we set:

$$\Delta L_{Terrain} = -(C_{Terrain})^2, \quad (23)$$

where $C_{Terrain}$ is our sixth regression coefficient. This coefficient is squared to force $\Delta L_{Terrain}$ to be negative (attenuation). Obviously, we include this term only in r_{Shield} , below.

L.7.4.4 Line-of-sight effect: seventh regression coefficient

When aircraft are in direct view, sometimes the terrain under the propagation path is level, and sometimes it dips sharply down into a valley. These two conditions may cause differences in sound propagation along such paths. To account for this possibility, we set:

$$\Delta L_{LOS} = (C_{LOS})^2 F_{LOS}, \quad (24)$$

where C_{LOS} is our seventh regression coefficient and F_{LOS} is the dummy line-of-sight variable that equals unity for “level” propagation, zero for “valley” propagation. This coefficient is squared to force a positive ΔL_{LOS} for “level” propagation, compared to zero effect for “valley” propagation. Obviously, we include this term only in r_{Vis} , below.

L.7.4.5 Site peculiarities: eighth regression coefficient

Local site peculiarities can cause local shielding. To account for this possibility, we set:

$$\Delta L_{Local} = (C_{Local})^2 F_{Local}, \quad (25)$$

where C_{Local} is our eighth regression coefficient and F_{Local} is the dummy local-shielding variable that equals unity for sites expected of local shielding, zero otherwise. This coefficient is squared to force a positive ΔL_{Local} for local-shielding sites. We include this term in both r_{Vis} and r_{Shield} , below.

L.7.4.6 Combined effect

The combined effect of all these mechanisms is:

$$\begin{aligned}\Delta L_{\text{Other}} &= \max[\Delta L_{\text{TempGrad}} + \Delta L_{\text{DnWnd}} + \Delta L_{\text{CrsWnd}} + \Delta L_{\text{Terrain}}, \Delta L_{\text{LOS}}] + \Delta L_{\text{Local}} \text{ for } r_{\text{View}}, \text{ and} \\ &= \Delta L_{\text{LOS}} + \Delta L_{\text{Local}} \text{ for } r_{\text{Shield}}.\end{aligned}\quad (26)$$

The max[] term in this equation is needed to prevent r_{Shield} from being larger than r_{Shield} due to downward refraction over intervening terrain.

L.8 Summary

This completes the regression equation. The full equation consists of Eq.(2) above, with subsequent equations substituted into it, as needed. The final equation relates the measured P_{Aud} for each site-hour to the factors measured simultaneously at each site-hour. It employs a total of eight regression coefficients, for which Statistica's non-linear regression math provides best-fit values. Table 39 contains the values of these regression coefficients.

Table 39. Resulting Values of Non-linear Regression Coefficients

Symbol	Value	Use in regression equation	Explanation
C_{CrsWnd}	0.0025	$\Delta L_{\text{CrsWnd}} = (C_{\text{CrsWnd}})^2 m_{\text{CrsWnd}}$	ΔL is the change in aircraft sound level due to the crosswind component of the wind velocity (in the aircraft flight direction).
C_{DnWnd}	1.215	$\Delta L_{\text{DnWnd}} = (C_{\text{DnWnd}})^2 m_{\text{DnWnd}}$	ΔL is the change in aircraft sound level due to the down-wind component of the wind (from track PCA to site).
C_{Ef}	356	$\alpha_{\text{Ef}} = \alpha_{200} + (0.005 C_{\text{Ef}} - 1)(\alpha_{200} - \alpha_{400})$	C_{Ef} is the effective frequency for broadband (A-level) atmospheric absorption.
C_{Local}	-0.108	$\Delta L_{\text{Local}} = (C_{\text{Local}})^2 F_{\text{Local}}$	ΔL is the change in aircraft sound level due to local shielding.
C_{LOS}	-0.256	$\Delta L_{\text{LOS}} = (C_{\text{LOS}})^2 F_{\text{LOS}}$	ΔL is the change in aircraft sound level due to "level" propagation, instead of "valley" propagation when aircraft is in direct view.
C_{TempGrad}	-0.922	$\Delta L_{\text{TempGrad}} = (C_{\text{TempGrad}})^2 T_{\text{Grad}}$	ΔL is the change in aircraft sound level due to vertical temperature gradients.
C_{Terrain}	3.546	$\Delta L_{\text{Terrain}} = -(C_{\text{Terrain}})^2$	ΔL is the change in aircraft sound level due to intervening terrain.
C_{Vista}	9.22	$t_{1\text{ACVista}} = \left(\frac{1}{1 + (1.1)^{-C_{\text{Vista}}}} \right) t_{1\text{ACNonVista}}$	$t_{1\text{ACVista}}$ is the audibility time for a single Vistaliner (compared to a non-Vistaliner).

Page Intentionally Blank